

# STUDY OF THE EARTH'S DYNAMICS BY MEANS OF SATELLITE LASER RANGING TECHNIQUES

Minoru Sasaki

## CONTENTS

### ABSTRACT

#### I. INTRODUCTION

#### II. DEVELOPMENT OF SLR SYSTEMS, SPECIFICATIONS OF SLR SATELLITES AND SLR OBSERVATIONS

1. SLR System Installed at the Kanozan Geodetic Observatory
2. SLR System Installed at the Simosato Hydrographic Observatory
  - (1) Hardware and software of the system
  - (2) Improvements of the system
3. Hydrographic Department Transportable Laser Ranging Station (HTLRS)
  - (1) Mount and transmitting/receiving optical subsystems
  - (2) Laser subsystem and electronics
  - (3) Other specifications and software
4. Specifications of SLR Satellites
5. Observations Made by the Fixed SLR System at the Simosato Hydrographic Observatory
  - (1) Operation
  - (2) Calibration
  - (3) Data preprocessing
6. Observations Made by the HTLRS
  - (1) Test and collocation at Simosato
  - (2) Operations at isolated islands

#### III. DEVELOPMENT OF AN ORBITAL PROCESSOR/ANALYZER

1. Algorithm of Data Processing and Analysis
  - (1) Basic relation
  - (2) Linearlization
  - (3) Minimum variance estimate
  - (4) Extention to the sequential estimation algorithm
  - (5) Estimation of precision of a baseline length
2. Dynamical Models and Their Formulation
  - (1) Time systems
  - (2) Coordinate systems
  - (3) Acceleration due to the perturbation force
  - (4) Expression of A-matrix
  - (5) Formulation of observational variables
3. Programing
  - (1) Formation

- (2) Capability and computation

#### IV. RESULTS OF DATA PROCESSING AND ANALYSIS

##### 1. Short Arc Solutions

- (1) Successive Passes Orbit Revising Technique (SPORT)
- (2) Station coordinates and baseline determination

##### 2. Global Solutions

- (1) Geophysical parameters
- (2) Earth rotation parameters
- (3) Station coordinates
- (4) Changes of baseline lengths and plate motions

##### 3. Discussions on Solutions

- (1) On the short arc solutions
- (2) On the treatment of the permanent tide
- (3) On the geophysical parameters
- (4) On the earth rotation parameters
- (5) On the station coordinates
- (6) On the changes of baseline lengths and plate motions

#### V. SUMMARY AND CONCLUSIONS

##### ACKNOWLEDGMENTS

##### REFERENCES

#### Abstract

Since mid-1970's three Satellite Laser Ranging (SLR) systems were completed in Japan. An experimental system was developed by the Hydrographic Department of Japan (JHD) and the Geographical Survey Institute (GSI) in cooperation and was installed at an observatory of GSI. Another SLR system was installed at the Simosato Hydrographic Observatory and observations have been continued there since 1982. A transportable SLR system was also developed by JHD and field observations in isolated islands have been continued since early 1988. The author has been deeply involved in planning, development, observation and data preprocessing for the three systems.

An orbital processor/analyzer based on the linear estimation theory has been developed by the author and was named HYDRANGEA. Applying the HYDRANGEA to SLR data, the earth rotation, coordinates of SLR stations, baseline lengths among SLR stations and some geophysical parameters as GM,  $J_2$ , and so on were determined.

Namely, it is shown that a specific short arc method with use of SLR data obtained simultaneously at plural stations for successive passes of a satellite is extremely effective to determine baseline lengths among SLR stations. The precisions of the resultant lengths of straight baselines of Simosato-Titi Sime (938km) and Simosato-Minamitori Sima (2025km) determined by using the processor/analyzer with use of LAGEOS and AJISAI SLR data attain to 4 mm and 7 mm, respectively.

The semi-long arc method is also applied. By using a number of LAGEOS five-day-arcs and GEM-T1 gravity field, two geophysical parameters are derived as  $GM = 398600.4453 \pm 0.0003 \text{ km}^3/\text{s}^2$  and  $J_2 = (1082.571 \pm 0.015) \times 10^{-6}$ .

The pole position  $(x_p, y_p)$  and excess rotation per day  $(\Delta\omega)$  of the earth in five day intervals from September 1983 to October 1984 are estimated by means of 85 five-day-arcs of LAGEOS SLR data. The mean systematic difference of this result from a result of ERP (CSR) 85L07 derived by the Center for Space Research (CSR) of the University of Texas at Austin is  $(\delta x_p, \delta y_p, \delta\omega) = (-0.51 \text{ milliarcseconds (mas)}, -0.13 \text{ mas}, -0.87 \text{ ms/d})$  and the standard deviation of each five-day-result is  $(\Delta x_p, \Delta y_p, \Delta\omega) = (\pm 1.1 \text{ mas}, \pm 1.4 \text{ mas}, \pm 0.42 \text{ ms/d})$ .

The coordinates of worldwide SLR stations at epochs of 1984.80, 1986.76 and 1988.11 are derived from LAGEOS SLR data. The internal errors of three dimensional rectangular coordinates determined for positions of 14 stations at 1984.80 are (2.6 cm, 2.4 cm, 2.9 cm) and the systematic difference of the result from the set of CSR coordinates of LSC 85L07 and mean individual difference between the result and the CSR result are (+0.5 cm, +0.5 cm, +3.1 cm) and (3.4 cm, 3.1 cm, 5.1 cm), respectively.

From the differences of each corresponding baseline arc lengths on the earth's surface between several SLR stations for three epochs above, plate motions among Simosato, Hawaii, Monument Peak (California) and so on are derived as Simosato-Hawaii :  $-11.9 \text{ cm/y}$ , Simosato-Mon. Peak :  $-5.7 \text{ cm/y}$ , Simosato-Quincy :  $-1.1 \text{ cm/y}$ , Simosato-Wetzell :  $-3.1 \text{ cm/y}$ , Simosato-Yaragadee :  $-6.2 \text{ cm/y}$ , Hawaii-Mon. Peak :  $+1.3 \text{ cm/y}$ , Hawaii-Quincy :  $+0.6 \text{ cm/y}$ , Hawaii-Wetzell :  $-7.0 \text{ cm/y}$ , Hawaii-Yaragadee :  $-10.9 \text{ cm/y}$ , Mon. Peak-Wetzell :  $0.0 \text{ cm/y}$  and Mon. Peak-Yaragadee :  $-9.6 \text{ cm}$ .

Almost all the results except for the baseline between Simosato and Wetzell well coincide with the estimation of AM0-2model given by Minster/Jordan [1978].

The change of arc length between Simosato and Wetzell is estimated as  $-3.1 \text{ cm}$  (contraction) despite of the both stations being believed on the same Eurasian plate. This phenomenon is considered to be the result of the movement of the Philippine Sea plate which is underthrusting the Japanese Islands.

## I. INTRODUCTION

In order to establish the origin of the Geodetic Coordinate System of Japan (Tokyo Datum), astronomical observations were started in 1874 at an observatory of the former Hydrographic Department of Japan (JHD) in Tokyo.

The Japanese geodetic triangulation network was extended from the origin to almost all over Japan in the late 1800's and early 1900's. However the network could not reach many isolated islands around the mainland of Japan. Therefore astronomical measurements to determine latitude and longitude were made on those isolated islands, but the results obtained usually included errors of several hundred meters [Takemura and Kanazawa 1983, Takemura and Kanazawa 1984, Takemura 1985, Takemura 1986] because of observation error and the deflection of the vertical at each observation point.

As for the effect of the deflection of the vertical, the situation is the same for the datum origin. In most countries the definitions of latitude and longitude for datum origins of the geodetic reference coordinates were determined by means of astronomical method and there were also local errors caused by the effect of the deflection of the vertical at each origin. For the case of Japan, such an error at the datum origin was not small because the origin at the central part of Tokyo is located at an area of large deflection of the vertical between both of the specific edges of mountainous district and of deep trench. Even if except such an effect of the deflection of the vertical at the origin, it is also known today that there are systematic distortion of more than 10 m at the north and south edges of the triangulation

network in Japan [Takemura and Kanazawa 1983, Takemura and Kanazawa 1984].

There had been no effective way to correct these kinds of discrepancy of definitions of datum origins, nor local errors before the first launch of an artificial satellite in 1957. The geodetic surveys using satellites were started after the launch and many other research works of orbital determination, estimation of geodetic values of the radius, flattening and dynamical form factor,  $J_2$ , of the earth and global geocentric coordinate systems were continued by using observation data of satellites in the world [e.g. Lundquist and Veis 1966, Veis 1967, Lundquist 1967].

On the early stage of the "Satellite Geodesy" in 1960's the relative positions of the distant observation points were measured mainly by using a geometrical method of simultaneous photographing of a satellite rather than the dynamical method because of lower accuracy of satellite dynamics than geometrical method in those days. In Japan some U.S. balloon satellites of diameters from 30 m to 40 m were used for determination of the position of isolated islands [Yamazaki 1971]. The discrepancies for the positions of some isolated islands on nautical charts were discovered and corrected by such satellite observations [Yamazaki *et al.* 1967, Yamazaki *et al.* 1972, Sasaki 1980].

The LASER (Light Amplification by Stimulated Emission of Radiation) technique was discovered in 1960. A set of retroreflectors for laser light reflection was installed on BEACON-B satellite at first soon after the discovery and launched in 1964. The retro-reflectors were equipped on geodetic satellites consequently launched as BEACON-C, GEOS-A, DIADEM-C, DIADEM-D and GEOS-B. The Satellite Laser Ranging (SLR), namely, the round trip time of laser pulse between the ground and a satellite is measured and converted to distance by multiplying the velocity of light, was started and continued after the installation of laser reflectors in some satellite observatories which belong to the Smithsonian Astrophysical Observatory (SAO), the Goddard Space Flight Center (GSFC) and the Centre National d'Etudes Spatiales (CNES) [Gaposchkin and Lambeck 1970]. In Japan the SLR observation was originated by the Tokyo Astronomical Observatory (TAO) in late 1960's. A SLR system of TAO has been located at the Dodaira Observatory and the system was improved several times [Kozai *et al.* 1973].

The analysis of satellite dynamics was originated and developed by Kozai [e.g. Kozai 1962] in Japan just after the first launch of a satellite, and Kinoshita [1976] completed the 3rd-order-theory of analytical expansion for satellite dynamics. Applications of satellite dynamics to geodetic researches have been made and a datum correction between the Tokyo Datum and a global geodetic coordinate system was estimated [Kozai 1981].

In 1969, the Space Activities Commission of Japan decided to start a basic research of the Japanese Geodetic Satellite which has functions to be optically observed from the ground both by photographing for direction determination and by laser ranging. There was no such a kind of satellite in the world before.

At the early stage of the basic research for the Japanese Geodetic Satellite, the original design of the satellite was a balloon type of 10 m diameter of which surface reflects solar light for direction observation by photographing at the ground sites and also reflects laser light back toward the incident direction to each ground laser site for ranging. Small glass beads stuck on all the balloon surface of thin film were considered as the laser reflector. However because of a large diffraction effect by such small glass beads [Sasaki 1975] the design of the reflector was changed to the corner cube reflector (CCR)'s. The feasibility of this type of satellite was investigated.

The next stage of research work for development of the satellite was started by the National

Space Development Agency of Japan (NASDA) in 1977 and the formal name of the satellite as "Geodetic Satellite-one (GS-1)" was given. The evaluations for specifications of laser reflectivity and solar light reflectivity and for launch orbit of the satellite were made. The outline of resultant optimum orbit was given as circular, 1500 km of altitude and 50 degrees of inclination by applying simulations for observation opportunity in the Japanese territory [Sasaki 1979]. The body of the balloon was planned to be made of aluminum-coated polyethylene film. However the thin film was too weak to support such CCR reflectors on the surface certainly without damaging the film, especially at the instant of expansion of the balloon into space from the rocket. Although the trials and tests to make thick and strengthen the balloon surface using firm materials and multi-layers were practiced, the sufficient reliability at the expansion to space with many CCR's on its surface could not be obtained. This problem was remained.

Following the long term SLR observation at the Dodaira Observatory of the Tokyo Astronomical Observatory a development of a satellite laser ranging system was started under cooperation with the Hydrographic Department of Japan (JHD) and the Geographical Survey Institute (GSI) of Japan in 1973. The system was intended to track the first Japanese Geodetic Satellite which would be launched later and be named "AJISAI".

In mid-1970's a new era for satellite geodesy came. A French satellite, STARLETTE, to use exclusively for laser ranging was launched in 1975 and a U.S. Laser Geodynamics Satellite, LAGEOS, was also launched in 1976. According to advance of electronics, the high precision measurement of time interval and the very narrow laser pulse were realized as SLR techniques. The numerical technique was started to be used well for the satellite dynamics instead of analytical method in the past owing to rising up of computation speed and size of memory and to decreasing cost of computation. The SLR work was to be advanced and its accuracy was raised up after the ages of the new era.

In the following Chapters the subjects on SLR work made mainly by the author after mid-1970's to solve the earth's dynamics as developments of SLR systems, SLR observations, development of an orbital processor/analyzer and results of processing and analysis of SLR data by using the developed processor/analyzer are presented.

## II. DEVELOPMENT OF SLR SYSTEMS, SPECIFICATIONS OF SLR SATELLITES AND SLR OBSERVATIONS

### 1. SLR System Installed at the Kanozan Geodetic Observatory

The development of a satellite laser ranging system started in 1973 and the developed system was installed at the Kanozan Geodetic Observatory of GSI in 1976. The new trial of the development are as follows [Sasaki 1977] :

- i) An electro-optical shutter is attached to the laser transmitter to make the width of the output laser pulse narrow;
- ii) A high resolution oscilloscope is linked to investigate the forms and patterns of transmitted and received laser pulse;
- iii) An electro-optical equipment for automatic satellite tracking is attached to track bright satellites such as a balloon type.

The system is composed of a mount, transmitting and receiving telescopes, a laser transmitter, receiving electronics, a mount controller, clock and a data processor. The mount of the system has three

axes of the satellite tracking axis, the elevation axis for pointing the maximum elevation of a satellite path, and the azimuth axis on which other two axes are installed.

The receiving telescope of the system is of a Cassegrain with 40 cm diameter set on the tracking axis. The laser transmitter assembly having transmitter telescope of 7.6 cm diameter on the top is mounted on the same frame of the receiving telescope with another telescope of 12.5 cm diameter for TV tracking.

The rotation of each axis of the mount is given by a pulse motor and an encoder. The system is driven in any of three modes. The tracking velocity is controlled using a key board of a hand box in the manual mode. In the computer mode, numerical input from a computer can be accepted. In the automatic mode a satellite image brighter than seven star magnitude can be tracked by the TV camera with an image intensifier and an X-Y analyzer. Once the satellite image is tracked in the center of a CRT screen, the X-Y analyzer and mount controller keep the image center.

The receiving electro-optical subsystem consisting of ND filters, a rotating shutter, an iris, an interference filter, a PMT with 2.1 ns rise time in a Peltier cooler and a pre-amplifier, is involved in the backside of the receiver telescope. The height of the mount with telesopes is 2.3 m high and the mount weighs 2 tons.

The laser transmitter transmits pulses of 3.3 Joules of 21 ns width in the repetition rate of once per 5 seconds. An electro-optical shutter can be applicable to make the pulse width narrow to 6 ns. In this case the output energy decreases to 0.2 Joules. The system has a 500MHz oscilloscope with a camera remotely controlled. The set of oscilloscope and camera make it possible to analyze the wave forms of transmitted laser pulse and the received wave forms in order to realize a higher range precision. A Loran C receiver was manufactured for the time comparison.

A computer (Data General Nova 01) was prepared. However, because of insufficient memory in comparison with larger operating system for data I/O, the computer control could not be realized at the first duration of the development.

The block diagram of the system is shown in Figure II-1.

A typical range test for long range calibration by using a target installed at 18.511 km ahead gives an result as

$$18522.44 \text{ m} \pm 0.1 \text{ m}.$$

The value includes the internal delay time of the system. The amount is 78 ns. [Mori *et al.* 1977].

The staff of the Kanozan Geodetic Observatory started to range a satellite, BEACON-C, after some improvements of the computer and control subsystems. The observations were succeeded in late 1982 and early 1983. Total passes and shots observed in the duration are 10 and 66, respectively. The mean residual for polynomial fitting is around 3.5 m [Hosono 1983]. After several ranging observations were made by using this system, no more ranging activities were realized.

## 2. SLR System Installed at the Simosato Hydrographic Observatory

### (1) Hardware and software of the system

In 1980 the Hydrographic Department of Japan (JHD) started a project to determine the location of the mainland referred to a global geocentric coordinate system by using SLR technique, and to expand a geodetic control network to major isolated islands around the Japanese mainland by means of SLR technique employing a transporatable SLR station and the satellite Doppler technique. Eventually all the mainland and islands within Japanese territory are to be determined referring to a global

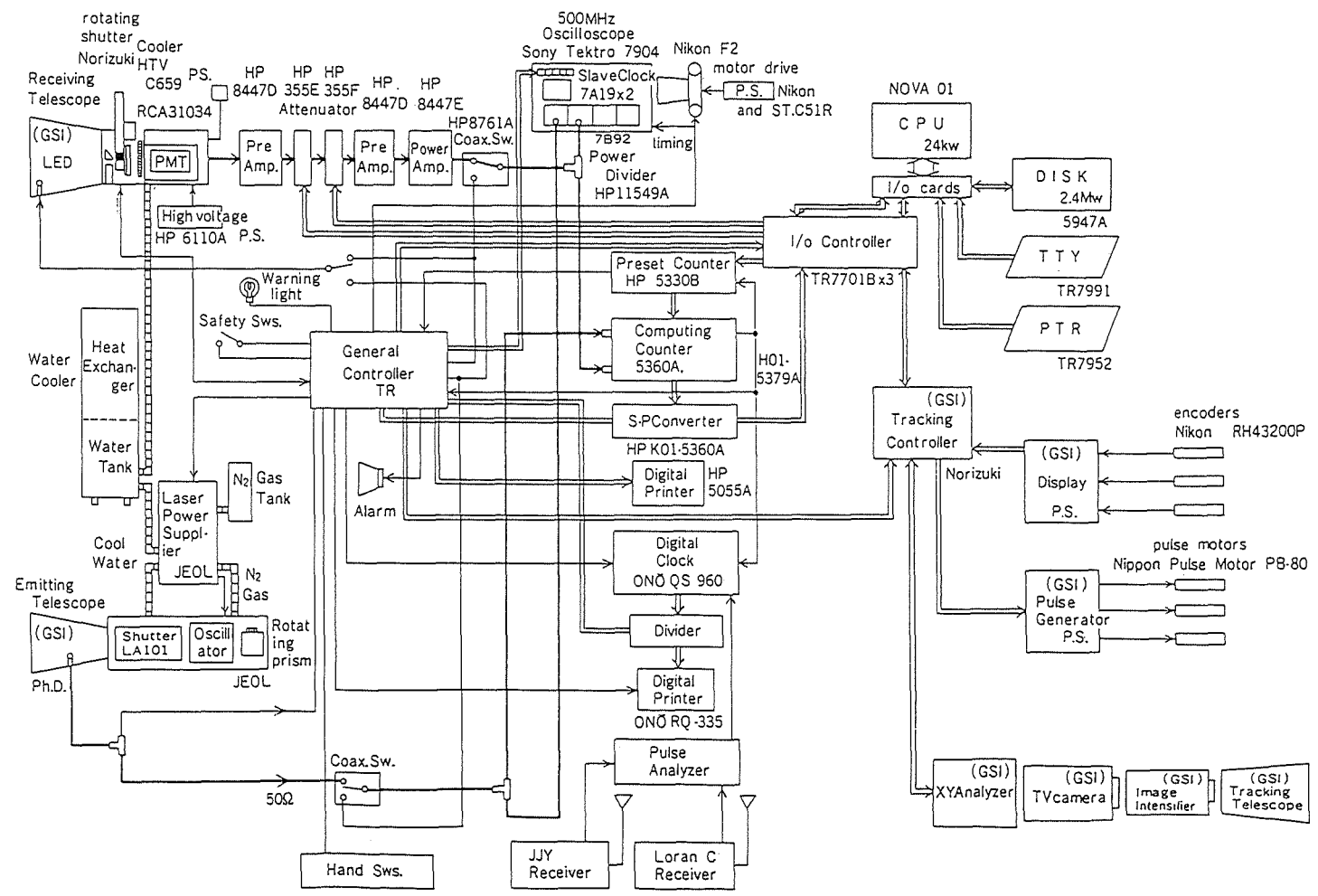


Figure II - 1. Block diagram of the experimental satellite laser ranging system installed at the Kanozan Geodetic Observatory in 1976.

geocentric coordinate system [Yamazaki and Mori 1983 ; Sasaki 1987].

As a major subject of the project, a satellite laser ranging system was installed at the Simosato Hydrographic Observatory (Nachi-Katsuura Cho, Wakayama Prefecture) in March 1982 by JHD [Sasaki *et al.* 1983]. The mount of the system is a type of gimballed elevation over azimuth. Each axis is controlled by a DC-torque motor, a tachometer and a 20 bits encoder. A Galilean transmitter telescope of 17 cm diameter and a Cassegrain receiver telescope of 60 cm are on the elevation axis. The output laser pulse is transmitted through Coudé path from the laser transmitter set up under the mount.

The laser subsystem is a type of Neodymium YAG (Nd : YAG) frequency doubled and mode locked type which transmits pulses of 150 mJ energy and 0.2 ns width each. The repetition rate of laser output is 4 pps. The transmitter assembly is located on the laser table in a clean booth area. The laser subsystem has a continuous wave oscillator and four amplifiers. An initial mode-locked pulse of the energy of around 6 nJ grows to 0.5 J at the wavelength of 1064 nm going through the amplifiers and the final output energy for green light after a second harmonic generator is 0.15 J. All the optical block diagram except the laser assembly is given in Figure II-2.

The receiving electronics attached behind the receiving telescope consist of a sun shutter, a computer controlled field of view adjustment and optical attenuator, a temperature controlled spectral filter and a photo-multiplier-tube (PMT) with the quantum efficiency of 29% and the rise time of 0.14 ns. The range counter has the resolution of 20 ps. As for the control subsystem, the manual operation adding to the computer control for tracking is capable with a joystick. The I/O rate from the computer to the mount controller is 30 Hz. The divergence control, start and stop threshold change, range gate position and width control, and offset time change to the orbital prediction are remotely controlled.

A clock integrating Rubidium frequency standard is monitored by receiving four Loran C waves of the North West Pacific Chain within the precision of 1  $\mu$ s. The delay time in the Loran C receiver is monitored by receiving the self transmitted simulation signal. A computer, PDP 11/60, with 64 kW memory, having peripheral equipments of two 5 Mbyte disks, a MT drive, a PTR/PTP and a CRT console is prepared. The ground targets for range calibration were set up. The transmitted laser output power to a ground target is decreased to the energy level from  $10^{-5}$  to  $10^{-11}$  by using an attenuator adaptor.

The total system except the clock subsystem was manufactured by G.T.E. Sylvania, California and the clock subsystem was made by Hitachi Ltd. The installation was made by G.T.E. Sylvania and Hitachi.

The basic software was prepared with the hardware at first. However a number of programs were additionally developed. The computer programs of the SLR system are divided into three groups as

- i) ephemeris calculation, preset of the initial status of the system, ranging operation, range calibration, tests and diagnostics;
- ii) preprocessing procedure for SLR data obtained;
- iii) star tracking and correction of the pointing error of the mount.

The first group of the software is made to have a tree structure unifying many small programs [Sasaki 1983]. The ephemeris calculation and satellite tracking are made by means of analytical method using the SAO formatted orbital elements. The corrections for distortion of the mount are added to original azimuth and elevation file of the satellite ephemeris.

As the second group, programs for a scheduling of monthly observation, a daily pass table plan



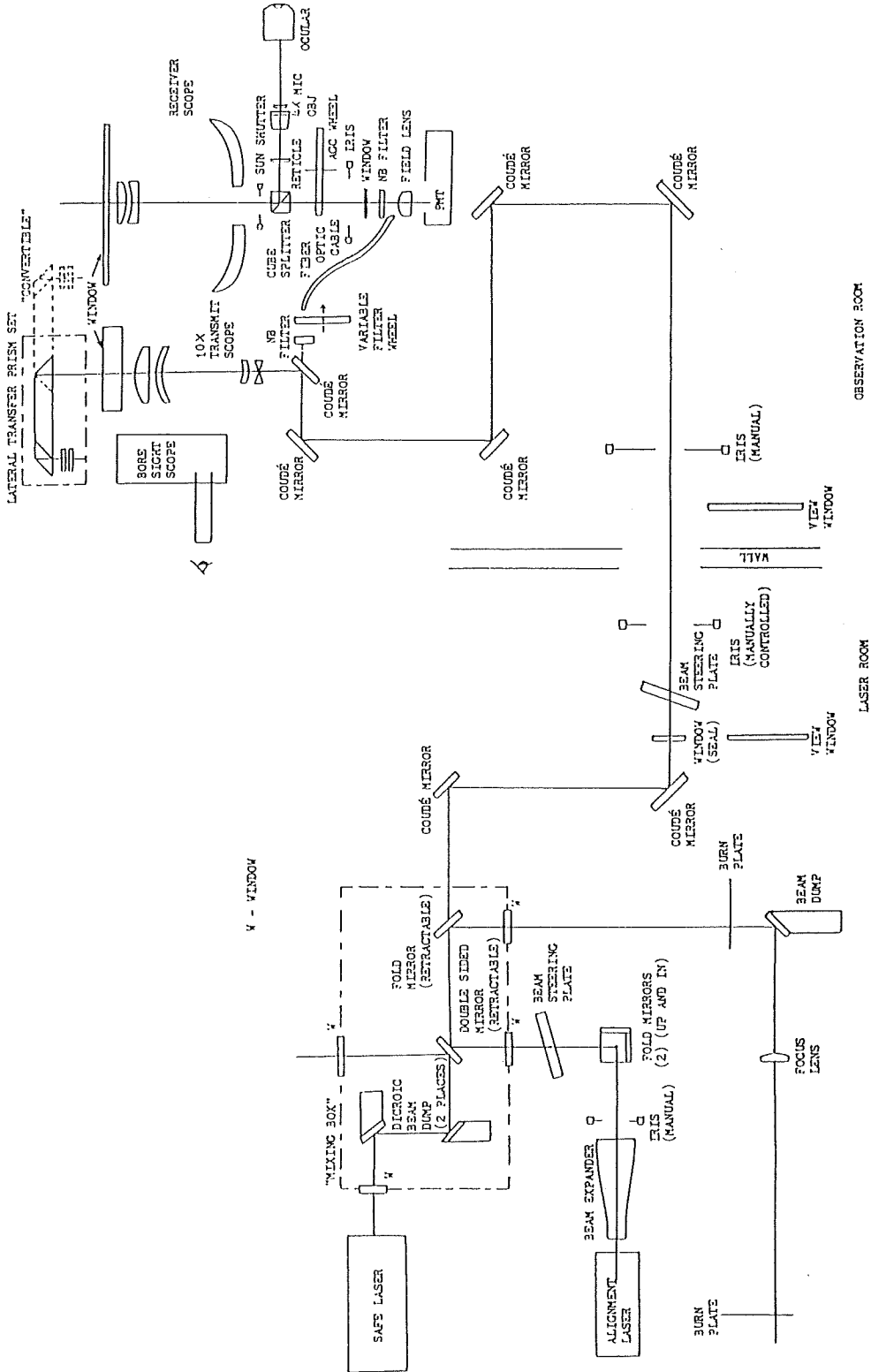


Figure II - 2. Block diagram of the optical subsystems of the Simosato fixed SLR system installed in 1982.

with route chart on the hemisphere, an atmospheric correction to observed SLR data, a rough noise rejection on CRT screen, a polynomial fitting to range residuals for precise noise rejection, a graphic display of range residuals, a quick-look data selection, telex data output to PTP, a full rate data output to MT, were made.

The third group includes an apparent place calculation for fixed star, an azimuth elevation pointing direction, a real time star tracking and an estimation of pointing error. The pointing error of the mount of the SLR system can be detected by tracking fixed stars, and by applying a least squares method to all the measured angle to the fixed stars.

## (2) Improvements of the system

The efforts of several improvements for the system as follows have been made since 1983 [Sasaki and Suzaki 1986]. After the use of the photo-multiplier-tube (PMT, Varian VPM 154s) for one and a half years, measurements of the sensitivity and gain of the PMT gave the values of 16% of quantum efficiency and  $10^3$  of gain. As the gain had decreased much from the nominal gain of  $10^5$ , the trial use of another micro-channel-plate PMT (Hamamatsu R-2024U) was started.

The existence of pointing error of the mount in a low atmospheric temperature was supposed in winter. The collimation procedures by star tracking, ground target aiming and laser light transmissions toward stars were repeated and it became clear that the distortion of the bore sight scope, caused by the combined part of iron of primary mirror tube and aluminum of its holder, was over 2 minutes of arc at maximum at temperature under 3—5 degrees of Centigrade. After that, the collimation procedure of the optical axis of the telescope and beam direction of laser transmission was made not by using the cross hair of the bore sight scope but by using the centering of tracking star of main telescope and laser transmission directing to the same star.

An analytical program was used for calculation of satellite ephemeris. To verify the availability of the program, another tracking program using numerical integration was developed and was compared with. The results show that the analytical ephemeris deflects from numerical ephemeris. Checking of the analytical program was made and an insufficient treatment of acceleration caused by solar force was found. After that, however, the new numerical program was only used when the SAO orbital elements became old and the hitting rate decreased because of longer calculation time than analytical one and complicated procedure to use the numerical program.

In order to increase the reliability of a system clock, an additional atomic frequency standard (NEATOMIC Rb-3100E) was added as the second clock. Recently a GPS receiver/timer of Trimble 5000A was also adopted as another time comparison system.

In late 1987, an additional telescope with 20 cm diameter was attached on the 60 cm telescope to measure the timing of flickering of the Japanese Geodetic Satellite, AJISAI. The timing data are used for the photographing of AJISAI, which will be made near the SLR system to determine the direction of satellite from the ground simultaneously. Behind the new telescope a photo detector was involved and timing of the rising and falling of AJISAI's flickerings were measured with a precision of 0.1 ms.

The electronic circuits of the fixed SLR system were checked and around one twentyth of signal loss at a discriminator (Motolola MC1651) inserted after the PMT output was found. The loss is caused by lower band width of the integrated circuit than the pulse width of the PMT output. Two amplifiers (B & H DC-3002A) with the bandpass from DC to 3.15 GHz and the gain of 23.5 dB were added. Much improvement for only faint return light signals was recognized owing to a smallness of maximum input limit of the amplifiers. To improve the still lower sensitivity of the system for return

signal and to increase range precision from current 10 cm level to a few centimeters level, the testing of constant fraction discriminators (CFD-Tennelec TC453 and TC454) has been trying to use at the Simosato Hydrographic Observatory since early 1989.

The maintenance of the system has been made by the staff of the Simosato Hydrographic Observatory and also the staff of Hitachi Ltd. according to a contract with the observatory. The efforts above were made by both the staff and the author.

### 3. Hydrographic Department Transportable Laser Ranging Station (HTLRS)

#### (1) Mount and transmitting/receiving optical subsystems

A transportable laser ranging system of JHD named the Hydrographic Department Transportable Laser Ranging Station (HTLRS) was completed in late 1987 [Sasaki 1988a]. The mount of the system has a specific feature as shown in Figure II-3. The elevation axis control is fully on a bench in a horizontal plane which rotates around the azimuth axis.



Figure II — 3. Overview of the Hydrographic Department Transportable Laser Ranging Station(HTLRS). (in late 1987 at the yard of the Simosato.)

A large mirror measuring 50 cm x 35 cm is rotated around the elevation axis and is used both for reflecting the output laser beam from the Coudé path to a satellite and for reflecting the return signal from the satellite to a receiver telescope. The optical block diagram of the system is shown in Figure II-4. The output laser beam propagates going up through the Coudé path along the azimuth axis. The beam is reflected by a small azimuth control mirror and goes in a horizontal plane to the central part of the large mirror. The beam is also reflected by the large mirror toward a satellite. The diameter of the transmitting beam is around 10 cm. The return signal from the satellite comes to the whole part of the same large mirror and goes to a receiver telescope with 35 cm diameter set up at the other side

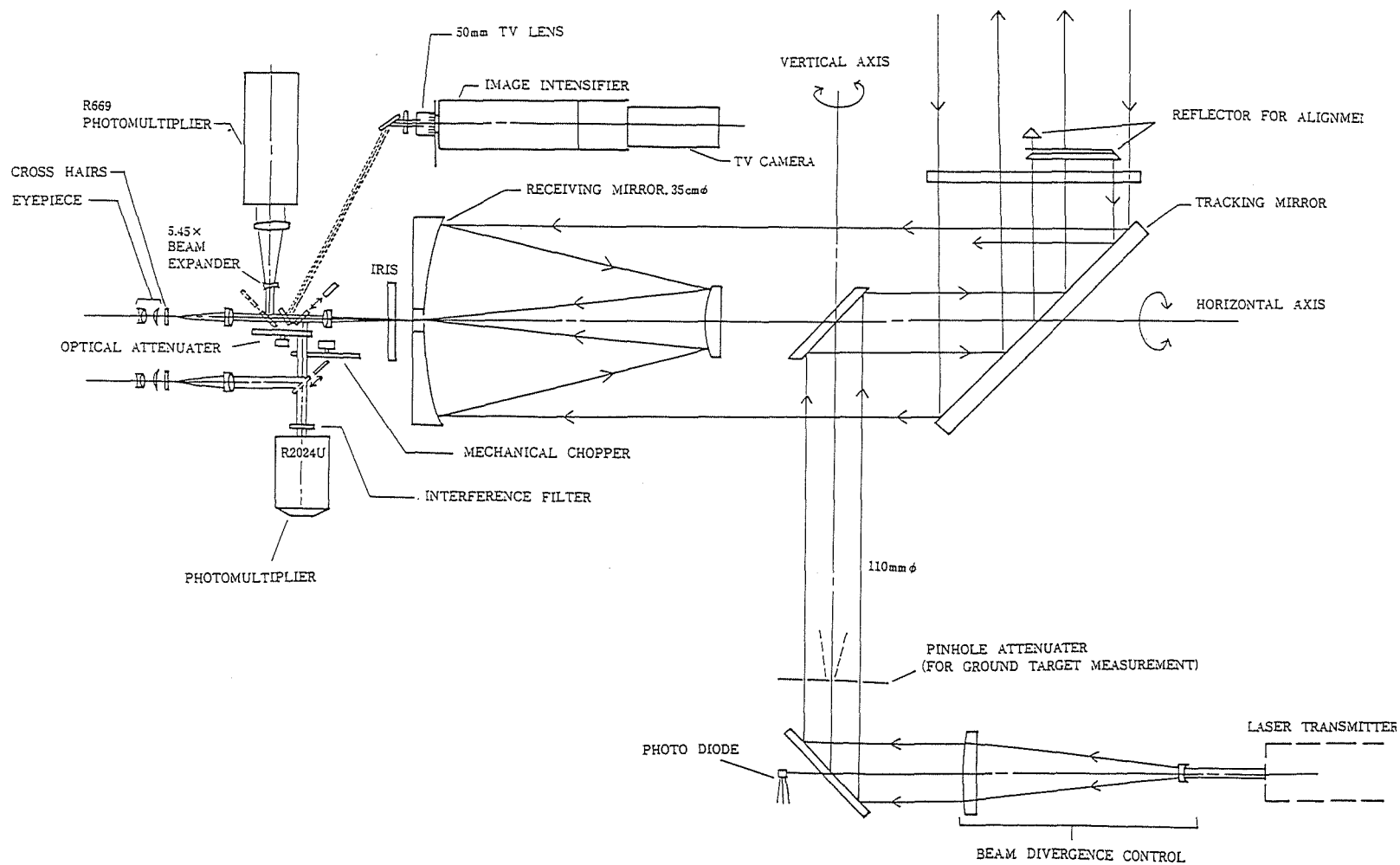


Figure II - 4. Block diagram of the transmitting and receiving optical subsystems of the HTLRS.

on the bench. The receiver telescope is originally an ordinary telescope with the diameter of 14 inches, Celestron (C-14), having improved holding part of the primary mirror.

The parallel beam to the optical axis of the telescope makes a point image at the focus, where a remote controlled iris limits the field of view with a range from 100  $\mu$ rad to 5 mrad. The light is splitted into two directions by using a dichroic mirror with 99.5% reflectivity for the wave length of 532 nm. The reflected green light is guided to a micro-channel-plate photo multiplier tube (MCP-PMT) through a remotely controlled optical attenuator with a range from 0 to 40 dB, a mechanical chopper to protect the PMT from the strong scattered transmitting laser light and an interference filter with 1.0 nm bandpass and 45 % transparency. This light is also led to an eyepiece. The path of the remaining splitted light without green spectrum is changable by some mirrors. In one case all the remaining light goes to a television guide having an image intensifier with a tracking capability of upto 6.5 star magnitude. In another case the light goes to a photo-multiplier tube to detect the timing of flickers of reflected solar light from the Japanese Geodetic Satellite, AJISAI.

### (2) Laser subsystem and electronics

The laser is a frequency doubled and mode-locked Neodymium YAG (Nd:YAG) system and transmits laser pulses of 50 mJ energy each and 50-100 ps width with a repetition rate of 5 pps. The transmitter assembly consists of a pumping oscillator followed by a pulse slicer, one stage of a double-passing amplifier and an second-harmonic generator. The oscillator transmits a mode-locked pulse train which includes seven to nine pulses of 7.5 ns interval and the slicer selects one pulse from the pulse train. The selected narrow pulse is amplified by the double-passing amplifier. The diameter of the output laser beam is 7 mm and beam divergence is 0.6 mrad.

The start pulse is detected by a fast photodiode (Hamamatsu S-2381 with 200 ps risetime. The receiving electronics to detect the returned signal and to measure the flight time, consist of a MCP-PMT (Hamamatsu R2024U with gating function), two amplifiers (NEPA 1001AA with 50 MHz - 3 GHz bandpass and 20dB gain, each), a fast dual comparator (Plessey SP9687), a receiver control unit and a time interval counter with 20 ps resolution. The PMT has a gain of  $5 \times 10^5$  and a risetime of 300 ps. The quantum efficiency of the PMT is 6 % at 532 nm of wavelength. The position and width of range gate are controlled within the range from 0.6  $\mu$ s to 0.1 s and from 200 ns to 30 ms, respectively.

The each axis of the mount is driven by a DC-torque motor, a tachometer and a 20 bits encoder. The pointing direction is controlled by a servo controller and an amplifier according to value of computer output at an I/O rate of 20 Hz. The tracking angular velocity for each axis is from sidereal to 13 deg/s. The estimate tracking accuracy is within 10 arcseconds.

Almost the same clock subsystem with that of the fixed SLR system including a Rubidium frequency standard, a Loran C receiver/transmitter is adopted. A Hitachi B16/FX (8087) microcomputer with a 5 inch - and a 3.5 inch-floppy disk drive is used for system control and ephemeris calculation. Another Hitachi B16/FX (8086) is used to record the timing of AJISAI flickers. The rising and falling timing of the AJISAI flickering of the brightness from 4.5 to 1.0 star magnitude can be detected by another PMT, and the timings are recorded independently of laser ranging. The each time of AJISAI flash is observed by a monitor lamp on the console panel with sound and the threshold level for timing can be adjusted by using the monitor functions.

### (3) Other specifications and software

Meteorological equipments of a thermometer, a humidity meter, a pressure meter, a wind direction and speed meter are prepared and these are set up outside of the housing. Most part of the

system is housed in two air-conditioned shelters. The sizes of the shelters are 2.1 m x 2.3 m x 3.3 m for mount/optics/laser subsystems and 2.1 m x 2.3 m x 3.8 m for other control subsystems. The total weight is around 5 tons. The total system housed in the shelters can be transported by a transport plane. The system can be operated by using two power generators on two carts with capability of 20 kW in AC 200V and 50 Hz and 7.5 kW in 100V, 50Hz, respectively. The outline of the specifications of HTLRS are given in Table II-1. The HTLRS was manufactured by Hitachi Ltd. according to the precise specifications of JHD.

The computer programs similar to the fixed SLR system were made as ephemeris calculation, ranging operation, range calibration, preprocessing for obtained SLR data, star tracking and pointing error correction. However much improvements for easy procedure and use by using graphic display function were realized. Especially for tracking and preliminary signal data selection from a number of noises, some programs give good operability on the CRT screen using the joystic like some computer games.

#### 4. Specifications of SLR Satellites

An important new era in satellite geodesy began in February 1975 with the launch of a French satellite in order to use entirely for laser ranging. In 1976 another satellite only for SLR was launched by NASA in an orbit of higher altitude. The specifications of these satellites and others are given in this section.

The French satellite was launched by the Centre National d'Etudes Spatiales (CNES) and named STARLETTE. This satellite was the first satellite specially designed to minimize the effects of non-gravitational forces and to obtain the highest possible accuracy for laser range measurements [Marsh *et al.* 1985]. The satellite has the aspect of a specularly reflecting sphere of diameter of 24 cm. It has a core which is largely uranium 238 covered by an aluminum alloy shell containing 60 corner cube reflectors. The mass of the satellite is 47.3 kg. The orbit has perigee and apogee heights of 810 km and 1105 km, respectively, and inclination of 49.8 degrees.

The NASA satellite named the *L*aser *G*eodynamics *S*atellite (LAGEOS) was launched in May 1976. The satellite is a sphere, 60 cm in diameter, having a mass of around 407 kg (See Figure II-5). The spherical aluminum outer portion of the satellite has a mass of 117 kg. Embedded within it are 422 corner cube reflectors made of fused silica and four reflectors made of germanium. A cylindrical brass inner core of the satellite is 27.5 cm long and 31.8 cm in diameter and has a mass of 175 kg. LAGEOS was launched into a nearly circular orbit at altitude of 5900 km to reduce the effects of atmospheric drag and uncertainties in the orbit due to unmodeled short-wavelength gravity signals. Its spherical shape and high density minimize the sensitivity of the orbit to radiation pressure [Cohen and Smith 1985].

The Japanese Geodetic Satellite, AJISAI, was launched in August 1986 by the National Space Development Agency (NASDA) of Japan. The functions of AJISAI are 1) to reflect input laser light back toward the ground for precise ranging and 2) to reflect solar light to determine the direction to the satellite from an observation site [Sasaki 1986a]. The satellite is a hollow sphere, 2.15 m diameter, and weighs 685 kg (Figure II-6). The surface is covered with corner cube reflectors and separate solar light reflectors. The launch orbit is circular with an inclination of 50 degrees and altitude of 1500 km [Sasaki 1986b]. The center of mass correction of AJISAI which is necessary to process and to analyze AJISAI SLR data, is given as  $1010 \pm 13$  mm by a simulation calculation [Sasaki and Hashimoto 1987]. The major specifications of these three SLR satellites are tabulated in Tables II-2, II-3 and II-4.

Table II — 1. Specifications of the Hydrographic Department Transportable Laser Ranging Station(HTLRS)

Subsystem	Specification
Laser	
Oscillator	mode-locked Nd:YAG with an amplifier
Wavelength	532 nm
Output energy	50 mJ
Pulse width	50 - 100 ps
Repetition rate	5 pps
Mount	
Configuration	elevation over azimuth / Coude path
Angular resolution	20 bits(1.2 arcsec)
Tracking control	computer / TV guide
Tracking rate	from sidereal to 13 deg per second
Tracking accuracy	less than 10 arcsec
Transmitter/receiver	
Type	a common flat plate for elevation control
Telescope	Galilean for transmitter and Coude for receiver
Diameter	10 cm for transmitter and 35 cm for receiver
Beam divergence	80 $\mu$ rad - 2 mrad
Field of view	0.1 - 5 mrad
Spectral filter	1.0 and 3.0 bandpass(changeable)
Optical attenuator	0 - 40 dB
Electronics	
Start pulse detector	photo diode with 200 ps rise time
Receiving detector	Micro-Channel-Plate PMT with 300 ps rise time
Discriminator	fast dual comparator
Flight time counter	20 ps resolution
Gate range	0.6 $\mu$ s - 0.1 s shift with 200 ns - 30 ms width
Control	
Mount control	DC servo using torque motor/tachmeter/encoder
Data flow rate	20 Hz with computer and servo system
Clock	
Frequencu standard	a Rubidium oscillator with $2 \times 10^{**}-11$ rate
Comparison	multi-Loran C wave
Computer	
CPU	two 16 bits micro computer
Peripherals	a hard disk, a 5 inch- and two 3.5 inch-floppy disks, printer/recorder, two CRTs and a modem
Ajisai flash timing recorder	
Detection	rise/fall time measurements by using a PMT
Meteorological sensors	
Functions	temperature, humidity, pressure wind speed and wind direction
Shelters	
Size	2.1 m x 2.3 m x 3.5 m and 2.1 m x 2.3 m x 3.8 m
Weight	5 tons for two shelters including contents
Air condition	two air conditioners for cooling and heating
Power generator	
Output power	20 kw for AC 200 V and 7.5 kw for AC 100 V
Oil consuming	9 liters per hour for two generators

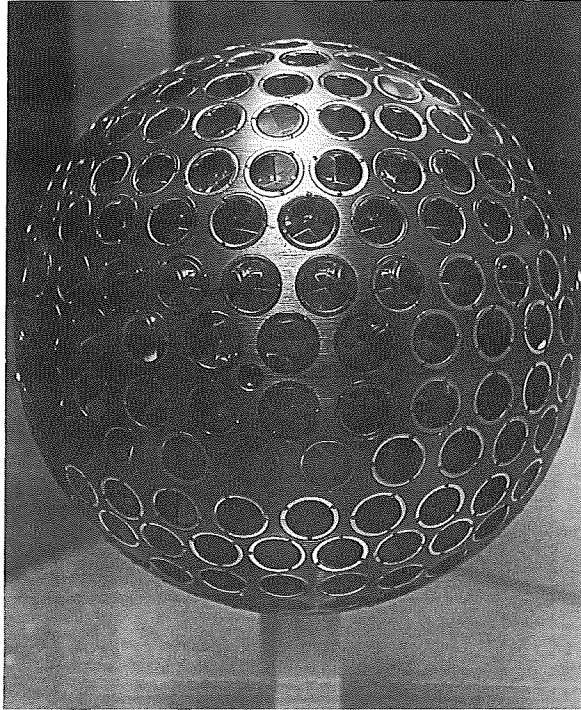


Figure II — 5. Laser Geodynamics  
Satellite(LAGEOS).  
(60cm of diameter and 5900km of orbital height).



Figure II — 6. Japanese Geodetic Satellite, AJISAI.  
(215cm of diameter and 1500km of orbital height).



Table II—2. Major specifications of STARLETTE

Configuration	An aluminum alloy shell with inner core of uranium 238		
Diameter	24 cm		
Weight	47.3 kg		
Laser reflector	60 CCRs		
Orbit	Perigee height	:	810 km
	Apogee height	:	1105 km
	Inclination	:	49.8 deg
Launch	Feb. 1975		

Table II—3. Major specifications of LAGEOS

Configuration	Spherical aluminum outer portion with cylindrical brass inner core		
Diameter	60 cm		
Weight	407 kg		
Laser reflector	422 fused silica CCRs and 4 germanium CCRs		
Orbit	Perigee height	:	5858 km
	Apogee height	:	5958 km
	Inclination	:	109.8 deg
Launch	May 1976		

Table II—4. Major specifications of AJISAI

Configuration	Spherical aluminum outer portion with cylindrical brass inner core		
Configuration	Polyhedron inscribed in a sphere		
Diameter	215 cm		
Weight	685 kg		
Laser reflector	Number of reflectors : 120 sets, 1436 CCR's Effective area : 91.2 cm <sup>2</sup>		
Solar light reflection	Number of mirrors : 318 pieces		
	Curvature of mirrors : 8.4—9.0 m		
	Reflectivity efficiency : 0.85		
	Brightness : approx. 1.5—3.5 star mag.		
	Duration of a flicker : approx. 5 ms		
	Rate of flickers : approx. 2 Hz		
Spin rate	40 rpm		
Launch orbit	Altitude : 1500 km		
	Inclination : 50 deg.		
	Eccentricity : 0.000		
Launch	August 1986		

Table II—5. Geodetic positions of the reference point of the fixed SLR system and the fiducial stone marker at Simosato (Tokyo Datum).  
[after Takemura 1983]

Location	Site ID	Coordinates (Tokyo Datum)
Cross point of Az. and El. axes, the SLR system at Simosato Hydrogr. Obs.	International	33° 34' 27".496N
	7838	135 56 23.537E
	Domestic SHO—L	62.44 m
Cross line, the fiducial stone marker at Simosato Hydrogr. Obs.	Domestic	33° 34' 28".078N
	SHO—HO	135 56 23.236E 58.36 m

In addition to these SLR satellites, BEACON-C had been observed till mid-1986 in the world-wide satellite laser tracking stations. This satellite, launched by NASA in 1965, was a complexed satellite for radiowave and laser ranging. The altitude of its orbit was 1150 km.

## 5. Observations Made by the Fixed SLR System at the Simosato Hydrographic Observatory

### (1) Operation

The installation of the fixed SLR system was started in early February 1982 at the Simosato Hydrographic Observatory. The mount and laser subsystem were placed on a large concrete pier extended over the observation room and the control room. A fiducial stone marker as a reference point and three ground targets for range calibration were set up around the observatory. The distances to three targets from the intersecting point of the axes of elevation and azimuth (the reference point of the system) are 1414.70 m, 1442.37 m and 2359.27 m, respectively. The geodetic positions of the intersection of the azimuth and elevation axes of the SLR system and the cross point of the stone marker, based on nearby reference triangulation stations [Takemura 1983] are given in Table II-5.

The test observation was started just after completion of installation and the first return was obtained soon after the start of observation from STARLETTE on March 8, 1982. The rangings to BEACON-C (BE-C) and LAGEOS were attained within four days after that [Sasaki 1982]. The routine ranging observation was started in April 1982. The target satellites were LAGEOS, STARLETTE and BE-C. The orbital elements of these satellites were supplied for around a year by, at first, Smithsonian Astrophysical Observatory (SAO) and by Goddard Space Flight Center (GSFC) of NASA later.

The observation schedule is made by selecting passes of more than 30 degrees of maximum elevation for daytime and night passes of LAGEOS, and more than 40 degrees of maximum elevation for daytime passes and more than 45 degrees for night passes of other satellites. The precise predictions for observable satellite paths are computed by using the mini-computer of the SLR system and stored on the disk. The atmospheric temperature, pressure and relative humidity are measured just before and after each tracking.

The tracking is carried out for elevation above 20 degrees. The operation is made by at least two persons, one is a console operator in the control room and the other is sky watcher standing near the mount on the top of the building. Sometimes one more operator for laser status control is added in

the control room.

The along-track manual search of a target satellite by using offset value change of prediction time of the current tracking satellite and joystic corrections for azimuth and elevation can be added to the current computer control from console in real time. The measured range (Observed) minus predicted range (Calculated), (O-C), range gate position and width, pointing azimuth and elevation and joystic corrections are also displayed on the CRT screen in real time. The divergence of laser transmission, field of view, start and stop thresholds and receiver attenuation can be remotely controlled by the operator. The transmitted time of laser pulse, measured range, O-C, pointing direction and functions above are recorded on a magnetic tape at every laser transmitting time.

A narrow-band optical filter and suitably selected tracking functions enable daytime observation. The capability largely depends on the condition of transparency of the sky. Usually the beam divergence for observation of LAGEOS, STARLETTE and BE-C are controlled within 0.1-0.2, 0.3-0.7 and 0.4-1.0 milliradians, respectively. The field of view at daytime observation is set to less than 0.3 milliradians to protect the PMT [Sasaki *et al.* 1984].

From just after the launch of AJISAI at early morning on August 13, 1986 (JST) the tracking of AJISAI was started at the Simosato Hydrographic Observatory.

The status of ranging observation at the observatory in 1988 with change of the status from 1982 are listed in Table II-6. The rates of return signals per transmitted shots and the mean numbers of return signals per a successive pass and mean range precision are given in Tables II-7 and II-8, respectively.

## (2) Calibration

Several calibrations are applied to obtain range data properly. The beam divergence is calibrated by illuminating the laser beam on a screen placed some 1 km ahead. The alignment of mirrors in the Coudé path for output laser beam is often regulated by using a lateral transfer prism attached on the top of the transmitter telescope which leads the beam to a bore sight scope. The star-tracking is used for the calibration of pointing direction of the mount and for the collimation of the transmitter telescope, receiver telescope, bore sight scope, the telescope for AJISAI flicker timing and the laser beam. The characteristic errors in the both axes caused by each eccentricity between the center of the encoder and the axis of rotation are obtained in this process. The pointing corrections and the effect of atmospheric refraction are added to the satellite ephemeris file for tracking.

The clock of the system is always monitored by receiving several Loran C waves of the Northwest Pacific Chain. The calibration of the Loran C monitor was made by the comparison with a portable clock traveled from the Tokyo Astronomical Observatory [Ono 1983]. Recently a GPS receiver for time comparison is also used for current time comparison.

To obtain a systematic range correction of the SLR system at a moment, the ground target ranging is carried out. In order to evaluate the system delay included in the electronic circuits the true distance and the atmospheric effect for ground target ranging are necessary. The atmospheric effect is estimated by applying the measured values of the atmospheric temperature, pressure and relative humidity to a formula given by Abshire [1980] as follows :

The group velocity of light in the air is given by

$$v = c (1 + 10^{-6} N)^{-1},$$

were

Table II - 6. Status of ranging observation at Simosato 1982-1988

( ):daytime observation

satellite	operated pass number in 1988	successful pass number in 1988	ratio of successful- per operated passes (%)						
			1988	1987	1986	1985	1984	1983	1982
LAGEOS	167( 44)	102( 2)	61( 5)	78(54)	72(34)	77(57)	54(34)	36(22)	28(18)
AJISAI	311(103)	271(82)	87(80)	86(87)	93(96)	---	---	---	---
STARLETTE	111( 48)	78(37)	70(77)	63(63)	84(84)	82(81)	64(57)	54(49)	42( 5)
BEACON-C	---	---	---	---	67(63)	77(74)	59(56)	62(50)	40(32)

Table II - 7. Ratio of return signals per transmitted shots

(1988)

satellite	return signal (a)	transmitted (b)	ratio (%) (a)/(b)
LAGEOS	40,718	1,048,200	3.9
AJISAI	142,152	838,000	17.0
STARLETTE	14,850	168,100	8.8

Table II - 8. Mean number of return signals in a successful pass and range precision

satellite	number of mean return signal							precision(cm)
	1988	1987	1986	1985	1984	1983	1982	
LAGEOS	399	440	658	815	418	221	221	9.5
AJISAI	525	616	822	--	--	--	--	9.3
STARLETTE	190	240	275	359	320	268	94	10.3
BEACON-C	--	--	274	440	374	454	175	10.3

$$N = 80.343 \left( 0.9650 + \frac{0.0164}{\lambda^2} + \frac{0.00028}{\lambda^4} \right) \frac{P}{T} - 11.3 \frac{e}{T}$$

$$e = 6.11 \frac{Rh}{100} 10^{7.5(T-273.15)/(237.3+(T-273.15))}$$

- $c$  : the vacuum speed of light,
- $P$  : atmospheric pressure (in millibars),
- $T$  : atmospheric temperature (in degrees Kelvin),
- $Rh$  : relative humidity (%),
- $\lambda$  : wavelength of the light (in microns).

The range precision of ground target ranging is a few centimeters level and variation of mean range to the ground target is changed in 10 cm level at maximum according to the change of intensity of output laser and returned signal. Some testings indicate that the variation of range mainly depends on the change of pulse height emitted from PMT and start and stop threshold levels of the discriminator used.

(3) **Data preprocessing**

The range data to a satellite include some false ranges caused by optical noises especially in the case of daytime observation. Such false data are manually rejected consulting a graph of range residuals to prediction ranges on a CRT screen at first. Next, to remove the atmospheric effect from raw range data for filtering process by curve fitting to the range residuals, an atmospheric range correction is applied to range data by using Marini-Murray formula [1973] given as follows :

The range correction to add to the measured range is

$$dR = - \frac{g(\lambda)}{f(\phi, H)} \frac{A+B}{\sin E + \frac{B/(A+B)}{\sin E + 0.01}}$$

where

$$g(\lambda) = 0.9650 + \frac{0.0164}{\lambda^2} + \frac{0.000228}{\lambda^4}$$

$$f(\phi, H) = 1 - 0.0026 \cos 2\phi - 0.00031H,$$

$$A = 0.002357P + 0.000141e,$$

$$B = (1.084 \times 10^{-8}) PTK + (4.734 \times 10^{-8}) \frac{P^2}{T} \frac{2}{(3 - 1/K)},$$

$$K = 1.163 - 0.00968 \cos 2\phi - 0.00104T + 0.00001435P,$$

$$e = 6.11 \frac{Rh}{100} 10^{7.5(T-273.15)/(237.3+(T-273.15))}$$

- $dR$  : range correction (in meters),
- $E$  : true elevation of satellite,
- $P$  : atmospheric pressure at the site (in millibars),
- $T$  : atmospheric temperature at the site (in degrees Kelvin),
- $Rh$  : relative humidity at the site (in %),
- $\lambda$  : wavelength of the laser (in microns),
- $\phi$  : latitude of the site,
- $H$  : altitude of the site (in kilometers).

Polynomials of 1st to 9th order in time expansion are used in the on-site minicomputer for the filtering of noise signal. Waving residuals sometimes appear owing to inaccurate orbital elements used for prediction or owing to the low order of the polynomials. In some cases, the residuals are separated into two or three groups with some one meter difference. Such results may be caused by multi-pulses

of output laser light. The range data whose residuals are larger than three times of the root mean square are rejected as bad data.

Because of insufficient memory of the on-site computer, the maximum order of data fitting is limited within 9th order. However data processing experience gives us that around 25th order polynomials are necessary for a lower satellite at maximum. In order to obtain more accurate range precision a larger computer at the Headquarters of JHD is used for similar polynomial fitting but applicable to higher order. As the example of mean range precision calculated at the JHD Headquarters, range precisions for the data obtained at Simosato in 1987 are 10.0 cm for LAGEOS, 11.5 cm for STARLETTE and 9.5 cm for AJISAI [Kanazawa *et al.* 1989].

A part of range data obtained, named quick-look (QL) data, is sent soon after the preprocessing to the Goddard Laser Network at GSFC through telex or GE MARK III communication line. The LAGEOS QL data are transferred to the Center for Space Research at the University of Texas at Austin and are used for estimation of the earth rotation parameters as the IERS activity. The full rate data on magnetic tapes are also sent to GSFC. The data are stored in the Crustal Dynamics Database and are used to detect plate motions and crustal movements. The range data of all the SLR stations are also derived to each SLR station.

## 6. Observations Made by the HTLRS

### (1) Test and collocation at Simosato

The Hydrographic Department Transportable Laser Ranging Station (HTLRS) was installed on a concrete base prepared at the front yard of the Simosato Hydrographic Observatory in September 1987. The positions of the center of the reference marker on the center of the concrete base almost just under the station, the brass marker on the east side of the base and the intersection of the azimuth and elevation axes of the HTLRS at the moment of December 1987 were measured based on the nearby fiducial stone marker and the brass marker on the roof of the office. The locations referred to the Tokyo Datum are (33° 34' 26".2895N, 135° 56' 23".5855E, 57.587 m H) [Sasaki 1988a], (33° 34' 26".296N, 135° 56' 23".655, 57.59 m H) and (33° 34' 26".290N, 135° 56' 23".586E, 59.52 m H) [Sengoku 1989]. Two ground targets were prepared for range calibration. An example of the precision of ranging to the ground target installed 2.3 km ahead is 2.4 cm (rms) for 188 return signals (Figure II-7). The range test to satellites was started after installation of the HTLRS and return signals from AJISAI, LAGEOS, and STARLETTE were obtained. The mean range precision was 3-5 cm level. An example of the range residuals of LAGEOS to raw range minus range fitted by polynomials is given in Figure II-8.

After finalizing total tuning up of the HTLRS, the first collocation observation of the station with the fixed SLR system at the Simosato Hydrographic Observatory was made from December 13 to December 18, 1987 and the SLR data of six passes of LAGEOS and three passes of AJISAI were obtained. According to an analysis of Sengoku [1989], who used both geometrical method using polynomial fitting and dynamical method using the orbital processor/analyzer, HYDRANGEA, developed by the author, the resultant systematic range difference between the fixed SLR system and the HTLRS was 1.1 cm and the range data of the fixed SLR system is larger than those of the HTLRS. He says more data are necessary for precise analysis.

### (2) Operations at isolated islands

After the collocation, the HTLRS was shipped to Titi Sima island of Ogasawara (Bonnin) Islands, in early January 1988. The HTLRS was installed at a yard of a facility of the Nippon Telephone

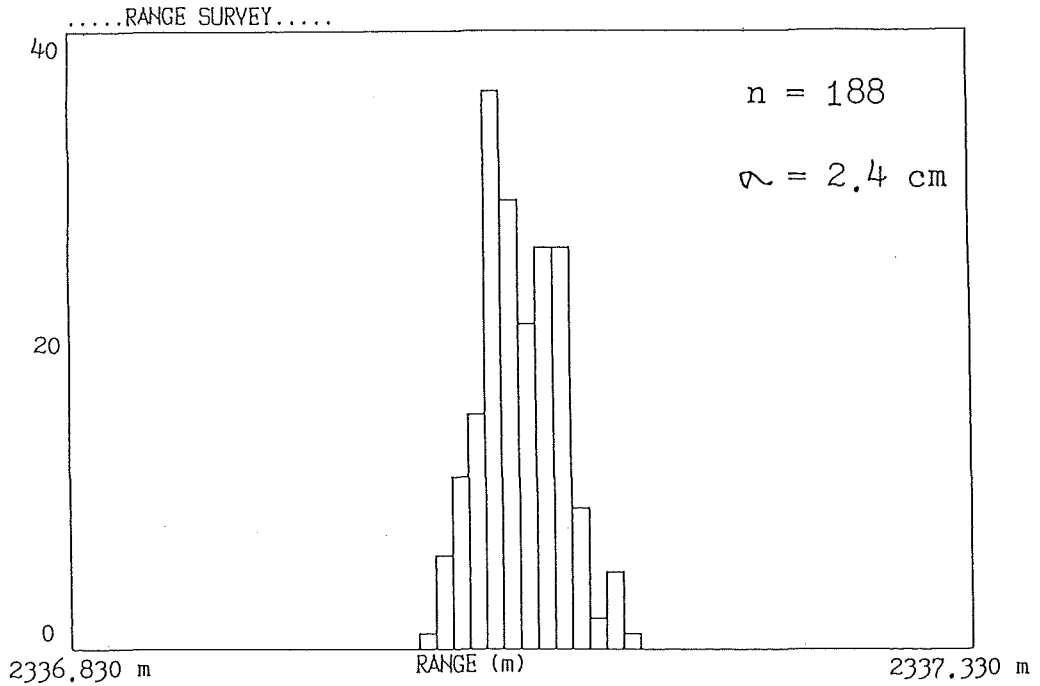


Figure II — 7. A histogram of ground target ranging made by the HTLRS.

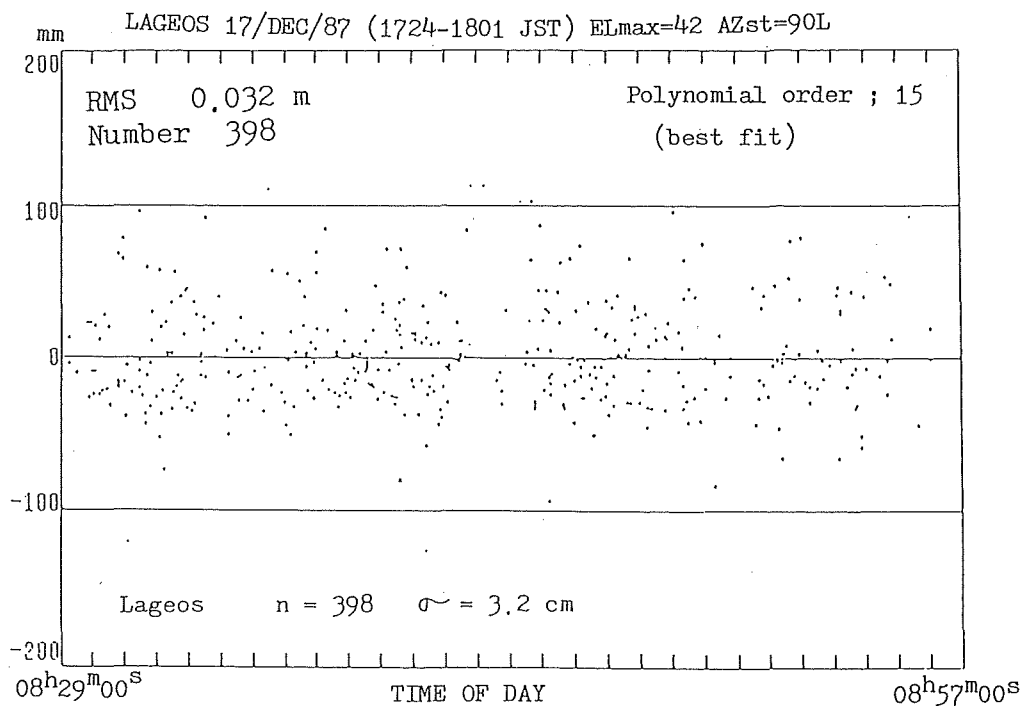


Figure II — 8. An example of LAGEOS SLR data residuals after polynomial fitting(HTLRS).

Table II—9. Range data obtained in the first field work of HTLRS at Titi Sima  
(Jan. —Mar. 1988)

satellites	Titi—sima (HTLRS)		Simosato (fixed—SLR system)	
	passes	shots	passes	shots
AJISAI	38	19,700	94	36,400
LAGEOS	11	5,500	22	1,500
STARLETTE	4	600	22	2,900
mean precision	3.6 cm		9 cm	

Table II—10. Range data obtained at the second field work of HTLRS at Isigaki Sima  
(Jul. —Sep. 1988)

satellite	Isigaki—sima (HTLRS)		Simosato (fixed—SLR system)	
	passes	shots	passes	shots
AJISAI	28	17,400	36	21,800
LAGEOS	22	15,700	16	6,000
STARLETTE	2	500	9	1,900
mean precision	4 cm		10 cm	

Table II—11. SLR data acquisition table  
Hydrographic Department 1982—1988

Simosato fixed SLR station (passes/shots)				
	LAGEOS	AJISAI	STARLETTE	BEACON—C
1982	47/11,000	—	36/4,700	59/11,900
1983	137/29,900	—	116/29,400	199/92,200
1984	223/93,300	—	118/37,800	150/56,100
1985	297/242,200	—	108/38,900	155/68,300
1986	224/147,500	169/139,000	92/25,300	56/15,400
1987	162/71,300	277/170,700	77/18,500	—
1988	102/40,700	271/142,000	78/14,900	—
Transportable SLR station (passes/shots)				
		LAGEOS	AJISAI	STARLETTE
1988	Titi—sima isl.	11/5,500	38/19,700	4/600
1988	Isigaki—sima isl.	22/15,700	28/17,400	2/500
1989	Minamitori—sima isl.	31/12,800	46/16,400	0/0



and Telegram (NTT) company near Yoake-yama mountain. The observation was continued from mid-January to mid-March and range data of 19,700 shots in 38 passes of AJISAI, 5,500 shots in 11 passes of LAGEOS and 600 shots in 4 passes of STARLETTE were obtained at the temporary station. The mean range precision of these data is 3.6 cm. These numbers and the SLR data obtained by the fixed SLR system at the Simosato in the same duration are given in Table II-9. After the HTLRS was returned to Simosato from the island and was tuned up again at Simosato, the collocation observation was made there again. In late-July 1988, the HTLRS was shipped to Isigaki Sima (island) in the Nansei Islands and SLR observation was made till late-September 1988. The data obtained are shown in Table II-10.

In early January 1989, the HTLRS was transported with four crews to Minamitori Sima (Marcus) island by two transport air planes and all the transportation, installation and observation was completed well by mid-March 1989. The total range data obtained at Simosato from 1982 to 1988 and obtained by the three field works at the isolated islands are given in Table II-11.

The method and procedure of data preprocessing of the HTLRS are almost the same for the case of the fixed SLR system. The similar process to make SLR data file in floppy base is made by using the on-site microcomputer.

### III. DEVELOPMENT OF AN ORBITAL PROCESSOR/ANALYZER

#### 1. Algorithm of Data Processing and Analysis

To process and analyze SLR data, several orbital processors were developed as, e.g. UTOPIA [McMillan 1983], GEODYN [Martin *et al.* 1976] or KOSMOS [Murata 1978]. Early versions of these processors had no new astro-geodetic constants and dynamical models, e.g. IAU (1976) System of Astronomical Constants [JHD 1984] and the first draft of the MERIT STANDARDS [Melbourne *et al.* 1980] in the days of 1980. So, the author started to make an orbital processor/analyzer in early 1981 [Sasaki 1981] based on a linear estimation theory [Tapley 1973] with the new constants and dynamical models to estimate satellite orbits, station coordinates and geophysical parameters. The processor/analyzer has been revised several times [Sasaki 1984a; Sasaki 1984b; Sasaki 1988b] after that to obtain more geophysical parameters and precise results. A set of station coordinates, named JHDSC-1 later in e.g. the Japanese Ephemeris for 1988, were obtained [Sasaki 1984b]. Though the precision (range residuals) of early versions of this orbital processor was 40 to 50 cm level, recent precision reaches 5 cm level.

In this chapter, the algorithm for estimation of a satellite orbit and geophysical parameters is summarized.

#### (1) Basic relation

The equations of motion of a satellite around the earth expressed in an inertial and non-rotating coordinate system are given by two first order differential equations as

$$\dot{\mathbf{r}} = \mathbf{v}, \quad \dot{\mathbf{v}} = -\mu \frac{\mathbf{r}}{r^3} + \mathbf{R}(\mathbf{r}, \mathbf{v}, \boldsymbol{\alpha}, t) \quad (1)$$

where  $\mathbf{r}$ : position vector of the satellite,  $\mathbf{v}$ : velocity vector,  $\mu$ : geocentric constant of gravitation (=  $GM$ ),  $\mathbf{R}$ : perturbation acceleration which is a function of  $\mathbf{r}$ ,  $\mathbf{v}$ , a set of model parameters  $\boldsymbol{\alpha}$  and time  $t$ . If the unmodeled error can be ignored,  $\mathbf{R}$  can be expressed explicitly. When some constant

parameters as constant part of station coordinates, earth rotation parameters,  $GM$ , earth gravity coefficients and so on whose values should be estimated in the estimation procedure are denoted by a vector  $\beta$ , the equation of motion is given as

$$\dot{\beta} = 0. \quad (2)$$

Equations (1) and (2) can be rewritten as following using an  $n$ -dimensional state vector  $X$ , which denotes all the unknown parameters of number of  $n$  to be estimated as the position and velocity of the satellite and geophysical parameters:

$$\dot{X} = F(X, t), \quad \text{initially } X(t_0) = X_0. \quad (3)$$

Usually the state vector is related to observed values non-linearly. The observations are also influenced by random observation errors. In order to estimate the state vector, observations are made. If observations of  $m$ -kinds are made at an instant of time,  $t_i$ , the  $m$ -dimensional  $i$ -th vector of observation values,  $Y_i$ , is expressed with an error vector,  $\varepsilon_i$ , as

$$Y_i = G(X_i, t_i) + \varepsilon_i, \quad i = 1, 2, \dots, \ell, \quad (4)$$

where  $G(X_i, t_i)$  is a  $m$ -vector of a non-linear function relating the state and the observation.

## (2) Linearization

To estimate the state of a non-linear dynamical system the linearization is one of the most effective method. In such a linearization method it is necessary to find a good approximation and to consider errors due to the linearization assumption.

If the difference between (true)  $X(t)$  and a reference trajectory (approximation)  $X^*(t)$  is sufficiently small in the duration  $t_0 < t < t_{max}$ , equations (3) and (4) can be expanded around the reference trajectory as

$$\begin{aligned} \dot{X} &= \dot{X}^* + [\partial F / \partial X]^*(X - X^*) + \dots, \\ Y_i &= G(X_i^*, t_i) + [\partial G / \partial X]_{i^*}^*(X_i - X_i^*) + \dots + \varepsilon_i. \end{aligned} \quad (5)$$

If the terms of  $(X - X^*)^2$  are neglected and the definitions

$$\begin{aligned} x(t) &= X(t) - X^*(t), & A(t) &= [\partial F / \partial X]^*, \\ y_i &= Y_i - G(X_i^*, t_i), & \tilde{H}_i(t_i) &= [\partial G / \partial X]_{i^*}^*, \end{aligned} \quad (6)$$

are used, equations (3) and (4) can be rewritten as

$$\dot{x} = A(t)x, \quad \text{initially } x(t_0) = x_0, \quad t_0 < t < t_{max} \quad (7)$$

and

$$y_i = \tilde{H}_i(t_i)x_i + \varepsilon_i, \quad i = 1, 2, \dots, \ell. \quad (8)$$

If a state transition matrix,  $\Phi(t_i, t_k)$ , is introduced into the linear estimation theory, the equation

$$x_i = \Phi(t_i, t_0)x_0 \quad (9)$$

is the solution of equation (7), and equation (8) becomes

$$y_i = \tilde{H}_i(t_i)\Phi(t_i, t_0)x_0 + \varepsilon_i. \quad (10)$$

The state transition matrix satisfies the following relations [e.g. Liebelt 1967] :

$$\begin{aligned} \text{a) } \Phi(t_i, t_k) &= \frac{\partial x(t_i)}{\partial x(t_k)}, \\ \text{b) } \Phi(t_i, t_i) &= I = \Phi(t_k, t_k), \\ \text{c) } \Phi(t_i, t_k) &= \Phi(t_i, t_j)\Phi(t_j, t_k), \\ \text{d) } \Phi(t_i, t_k) &= \Phi^{-1}(t_k, t_i), \\ \text{e) } \dot{\Phi}(t, t_k) &= A(t)\Phi(t, t_k), \end{aligned} \quad (11)$$

If definitions,

$$y = \begin{bmatrix} y_1 \\ y_2 \\ \vdots \\ y_l \end{bmatrix}, \quad H = \begin{bmatrix} \tilde{H}_1 \Phi(t_1, t_0) \\ \tilde{H}_2 \Phi(t_2, t_0) \\ \vdots \\ \tilde{H}_l \Phi(t_l, t_0) \end{bmatrix}, \quad \varepsilon = \begin{bmatrix} \varepsilon_1 \\ \varepsilon_2 \\ \vdots \\ \varepsilon_l \end{bmatrix},$$

are used, all the observation equations can be expressed as

$$y = Hx_0 + \varepsilon. \tag{12}$$

**(3) Minimum variance estimate**

To solve  $n$ -unknowns,  $x_0$ , and  $(l \times m)$ -unknowns,  $\varepsilon$ , from  $(l \times m)$ -observations,  $y$ , in equation (12), is the proposition of this problem. As the number of unknowns is greater than the number of observations, some constraint condition is necessary. In this estimation, to minimize the diagonal elements of the covariance matrix,

$$P = E[(\hat{x} - E[\hat{x}])(\hat{x} - E[\hat{x}])^T], \tag{13}$$

is adopted as the constraint condition, where  $E$  means to take expecting value and  $\hat{x}$  denotes the solution of this static process. It is assumed that the observation error  $\varepsilon_i$  satisfies the a priori statistics as

$$E[\varepsilon_i] = 0, \quad E[\varepsilon_i \varepsilon_j^T] = R_i \delta_{ij}, \tag{14}$$

where  $\delta_{ij}$  is the Kronecker delta and  $R_i$  is an element of a positive definit matrix,  $R$ .  $R$  can be given depending on the characteristics of error structure. If the diagonal elements of the expectation value of  $\varepsilon_i \varepsilon_j^T$ ,  $R_i$ , can be given by the standard deviation associated with the  $i$ -th observation, namely,  $R_i = \sigma_i^2$ , the following procedure reduces to the least square method.

As the solution of equations (7), (9) and (12), the best linear unbiased minimum variance estimate,  $\hat{x}_0$ , of state  $x_0$  is obtained by satisfying the conditions described above, namely :

- a) linearity expressed as  $x = My$ ,
- b) unbiased  $E[\hat{x}] = x$ ,
- c) minimum variance  $\partial P_{ii} / \partial x = 0$ .

The expression of the solution is given [e.g. Liebelt 1967] as

$$\hat{x}_0 = (H^T R^{-1} H)^{-1} H^T R^{-1} y. \tag{15}$$

The solution  $\hat{x}_0$  is best estimate for unknown  $x$  at initial time  $t = t_0$ .

The best estimate  $\hat{x}_0$  of  $x$  at  $t = t_0$  obtained from the observations  $y_1, y_2, \dots, y_l$  at  $t = t_1, t_2, \dots, t_l$  is also expressed as

$$\hat{x}_0 = E[x_0 | y_1, y_2, \dots, y_l]. \tag{16}$$

The expression of the covariance matrix of  $\hat{x}_0$  is rewritten using equations (13), (12) and (14) as

$$\begin{aligned} P_0 &= E[(\hat{x}_0 - x_0)(\hat{x}_0 - x_0)^T] \\ &= E[((H^T R^{-1} H)^{-1} H^T R^{-1} (Hx_0 + \varepsilon) - x_0)((H^T R^{-1} H)^{-1} H^T R^{-1} (Hx_0 + \varepsilon) - x_0)^T] \\ &= ((H^T R^{-1} H)^{-1} H^T R^{-1}) E[\varepsilon \varepsilon^T] ((H^T R^{-1} H)^{-1} H^T R^{-1})^T \\ &= (H^T R^{-1} H)^{-1}, \end{aligned} \tag{17}$$

namely

$$\hat{x}_0 = P_0 H^T R^{-1} y. \tag{18}$$

Next, let us consider as follows ; after we obtained the initial values for unknowns like above, if we observe one more observation, what kind of new result can be obtained?

So, we add one observation,  $Y_{t+1}$  for the time,  $t_{t+1} > t$  as,

$$y_{t+1} = \tilde{H}_{t+1}(t_{t+1}) x_{t+1} + \varepsilon_{t+1}. \tag{19}$$

Using similar relation with equation (9), equation (19) can be written as

$$y_{t+1} = \tilde{H}_{t+1}(t_{t+1}) \Phi(t_{t+1}, t_0) x_0 + \varepsilon_{t+1},$$

or using new definition,  $H_{t+1} = \tilde{H}_{t+1} \Phi(t_{t+1}, t_0)$ ,

$$y_{t+1} = H_{t+1}x_0 + \varepsilon_{t+1}.$$

If we write this equation in matrix form using equation (12) of old observation set, the new expression for all the observations is

$$\begin{bmatrix} \dots \\ y_{t+1} \\ \dots \end{bmatrix} = \begin{bmatrix} \dots \\ H_{t+1} \\ \dots \end{bmatrix} x_0 + \begin{bmatrix} \dots \\ \varepsilon_{t+1} \\ \dots \end{bmatrix}. \quad (20)$$

If we write equation (20) with primes as  $y' = H'x_0' + \varepsilon'$ , the solution and the new best estimate of  $x_0$  can be expressed similarly to equation (15) using definition  $r_{t+1} = E[\varepsilon_{t+1}, \varepsilon_{t+1}^T]$  as

$$\begin{aligned} \hat{x}'_0 &= (H'^T R'^{-1} H')^{-1} H'^T R'^{-1} y' \\ &= \left\{ (H^T \mid H_{t+1}^T) \begin{pmatrix} R^{-1} & \dots \\ O & r_{t+1}^{-1} \end{pmatrix} \begin{pmatrix} \dots \\ H_{t+1} \end{pmatrix} \right\}^{-1} (H^T \mid H_{t+1}^T) \begin{pmatrix} R^{-1} & \dots \\ O & r_{t+1}^{-1} \end{pmatrix} \begin{pmatrix} \dots \\ y_{t+1} \end{pmatrix} \\ &= (H^T R^{-1} H + H_{t+1}^T r_{t+1}^{-1} H_{t+1})^{-1} (H^T R^{-1} y + H_{t+1}^T r_{t+1}^{-1} y_{t+1}) \\ &= (H_{t+1}^T r_{t+1}^{-1} H_{t+1} + P_0^{-1})^{-1} (H_{t+1}^T r_{t+1}^{-1} y_{t+1} + P_0^{-1} \hat{x}_0). \end{aligned} \quad (21)$$

If equation (15) is used for computation of the best estimate at an initial time of  $t_0$ ,  $\hat{x}_0$  can be obtained through one inverting process of an  $n \times n$  matrix. However if equation (21) is used for estimation  $\hat{x}_0$ , sequential procedure to make  $P_0^{-1}$  and  $P_0^{-1} \hat{x}_0$  and to add one more observation can be realized.

The solution given by equation (15) or (21) will agree with the weighted least square solution if the weighting matrix,  $W$ , equals to the inverse of observation noise covariance matrix,  $R$ , namely,  $W = R^{-1}$ . Actually the precision of range data or weight for each observation can not be clear and usually we can use mean (root mean square) values of the range residuals for the case of final convergence. In such a case the diagonal elements of the covariance matrix,  $P$ , reduce to close values of true standard deviation (variance) of each unknown parameter.

It has been considered to estimate the unknowns at an initial instant of time  $t = t_0$ . However we can estimate a status at some time,  $t = t_k > t_0$ , just after the end of the last observation,  $y_{t_0}$ , in subsequent observations,  $y_1, y_2, \dots, y_l$ . In this case we can use  $x_k$  at  $t = t_k > t_0$  instead of  $x_0$  at  $t = t_0 < t_l$  through the procedure after equation (9). Namely,

$$\begin{aligned} x_i &= \Phi(t_i, t_k) x_k, \\ H &= \begin{bmatrix} \tilde{H}_1 \Phi(t_1, t_k) \\ \tilde{H}_2 \Phi(t_2, t_k) \\ \vdots \\ \tilde{H}_l \Phi(t_l, t_k) \end{bmatrix} \\ P_k &= (H^T R^{-1} H)^{-1} \end{aligned}$$

and

$$\hat{x}_k = P_k H^T R^{-1} y. \quad (22)$$

If  $\bar{x}_k$  denotes a future prediction of  $x$  at  $t = t_k$ ,

$$\bar{x}_k = E[x_k \mid y_1, y_2, \dots, y_l].$$

The similar relation of equation (9) to the best estimate  $x_j$  at a past time  $t = t_j < t_k$  follows that

$$E[x_k \mid y_1, y_2, \dots, y_l] = \Phi(t_k, t_j) E[x_j \mid y_1, y_2, \dots, y_l],$$

and the prediction  $\bar{x}_k$  of  $x$  at  $t = t_k$  is given by the equation,

$$\bar{x}_k = \Phi(t_k, t_j) \hat{x}_j, \quad (23)$$

or for the case to estimate  $x$  at the initial time,  $t_0$ , from the estimated  $x_k$  at  $t = t_k > t_0$  using equation (22),

$$\begin{aligned} \bar{x}_0 &= \Phi(t_0, t_k) \hat{x}_k \\ &= \Phi^{-1}(t_k, t_0) \hat{x}_k. \end{aligned} \quad (24)$$

If a future prediction of the covariance matrix at  $t = t_k$  is defined by

$$\bar{P}_k = E[(x_k - \bar{x}_k)(x_k - \bar{x}_k)^T \mid y_1, y_2, \dots, y_l], \quad (25)$$

this equation can be rewritten as followings using a determined - or a priori covariance matrix  $P_j$  at a past time,

$$\begin{aligned}\bar{P}_k &= E[\Phi(t_k, t_j)(x_j - \hat{x}_j)(x_j - \hat{x}_j)^T \Phi^T(t_k, t_j) | y_1, y_2, \dots, y_l] \\ &= \Phi(t_k, t_j) P_j \Phi^T(t_k, t_j).\end{aligned}\quad (25)$$

(4) **Extention to the sequential estimation algorithm**

It is also expected to estimate unknown parameters just after each observation sequentially instead of the estimation procedure made once after gathering all the observation date like the batch estimation method described in the previous section.

The next problem is, when an estimate of  $x_j$ ,  $\hat{x}_j$ , and covariance matrix,  $P_j$ , for the time at  $t_j$  were already obtained, how to estimate the  $\hat{x}_k$  and  $P_k$  after an observation,  $Y_k$ , at  $t = t_k$ .

The best estimate  $\hat{x}_j$  and  $P_j$  can be propagated as equations (23) and (26).

The problem can be solved similarly to the end of the previous section. Considering that if  $\hat{x}_j$  is unbiased,  $\bar{x}_j$  will also be unbiased since  $E[\bar{x}_k] = \Phi E[\hat{x}_j]$ , Hence,  $\bar{x}_k$  can be interpreted as an observation and following relations will hold

$$\begin{aligned}y_k &= H_k x_k + \varepsilon_k \\ \bar{x}_k &= x_k + \eta_k\end{aligned}\quad (27)$$

were  $E[\varepsilon_k] = 0$ ,  $E[\varepsilon_k \varepsilon_k^T] = R_k$ ,  $E[\eta_k] = 0$  and  $E[\eta_k \eta_k^T] = \bar{P}_k$ .

Using following definitions,

$$y = \begin{bmatrix} \bar{x}_k \\ y_k \end{bmatrix}, H = \begin{bmatrix} I \\ \bar{H}_k \end{bmatrix}, \varepsilon = \begin{bmatrix} \eta_k \\ \varepsilon_k \end{bmatrix}, R = \begin{bmatrix} \bar{P}_k & | & O \\ O & | & R_k \end{bmatrix},\quad (28)$$

equation (27) is expressed as

$$y = H x_k + \varepsilon$$

and the solution can be obtained similarly to equation (22) as

$$\hat{x}_k = (H^T R^{-1} H)^{-1} H^T R^{-1} y.$$

Using definition in equation (28) and the similar expansion procedure to equation (21),

$$\begin{aligned}\hat{x}_k &= \left\{ (I | \bar{H}_k^T) \begin{pmatrix} \bar{P}_k^{-1} & | & O \\ O & | & R_k^{-1} \end{pmatrix} \begin{pmatrix} I \\ \bar{H}_k \end{pmatrix} \right\}^{-1} \left\{ (I | \bar{H}_k^T) \begin{pmatrix} \bar{P}_k^{-1} & | & O \\ O & | & R_k^{-1} \end{pmatrix} \begin{pmatrix} \bar{x}_k \\ y_k \end{pmatrix} \right\} \\ &= (\bar{H}_k^T R_k^{-1} \bar{H}_k + \bar{P}_k^{-1})^{-1} (\bar{H}_k^T R_k^{-1} y_k + \bar{P}_k^{-1} \bar{x}_k),\end{aligned}\quad (29)$$

Namely the equation (29) also gives the best estimate of  $x$  in the case to add new observation to an a priori information as  $\bar{x}_j$  and  $\bar{P}_j$ .

The discussion above indicates that the covariance matrix  $P_k$  associated with estimate  $x_k$  is expressed as

$$P_k = (\bar{H}_k^T R_k^{-1} \bar{H}_k + \bar{P}_k^{-1})^{-1},\quad (30)$$

or

$$P_k^{-1} = \bar{H}_k^T R_k^{-1} \bar{H}_k + \bar{P}_k^{-1},\quad (31)$$

Pre-multiplying to equation (31) by  $P_k$  and then post-multiplying by  $\bar{P}_k$  lead to

$$\bar{P}_k = P_k \bar{H}_k^T R_k^{-1} \bar{H}_k \bar{P}_k + P_k\quad (32)$$

or

$$P_k = \bar{P}_k - P_k \bar{H}_k^T R_k^{-1} \bar{H}_k \bar{P}_k.\quad (33)$$

Post-multiplying to equation (32) by  $\bar{H}_k^T R_k^{-1}$ , the following expression is given as :

$$\begin{aligned}P_k \bar{H}_k^T R_k^{-1} &= P_k \bar{H}_k^T R_k^{-1} \cdot [\bar{H}_k^T \bar{P}_k \bar{H}_k^T R_k^{-1} + I] \\ &= P_k \bar{H}_k^T R_k^{-1} [\bar{H}_k \bar{P}_k \bar{H}_k^T + R_k] R_k^{-1},\end{aligned}\quad (34)$$

and  $P_k \bar{H}_k^T R_k^{-1}$  is solved as

$$P_k \tilde{H}_k^T R_k^{-1} = \bar{P}_k \tilde{H}_k^T [\tilde{H}_k \bar{P}_k \tilde{H}_k^T + R_k]^{-1}. \quad (35)$$

The equation (35) is inserted to the right hand side of equation (33), then  $P_k$  is expressed as

$$P_k = \bar{P}_k - \bar{P}_k \tilde{H}_k^T [\tilde{H}_k \bar{P}_k \tilde{H}_k^T + R_k]^{-1} \tilde{H}_k \bar{P}_k. \quad (36)$$

The equation (36) means that to obtain the covariance matrix  $P_k$ , the matrix to be inverted is of dimension  $m \times m$  ( $m$ : number of observation set at an instant of time,  $t_k$ ), e.g., the same as the observation error covariance matrix. If only a scalar observation as laser ranging data is involved, the inverse is obtained through only one scalar division. If the weighting matrix,  $K_k$ , is defined as

$$K_k = \bar{P}_k \tilde{H}_k^T [\tilde{H}_k \bar{P}_k \tilde{H}_k^T + R_k]^{-1} \quad (37)$$

then, equation (36) can be expressed as simple form as

$$P_k = [I - K_k \tilde{H}_k] \bar{P}_k. \quad (38)$$

If equation (38) is substituted into (29), then the sequential form for computing  $x_k$  can be obtained as

$$\hat{x}_k = [I - K_k \tilde{H}_k] \bar{P}_k [\tilde{H}_k^T R_k^{-1} y_k + \bar{P}_k^{-1} \bar{x}_k].$$

Rearranging leads to

$$\hat{x}_k = [I - K_k \tilde{H}_k] \bar{x}_k + [I - K_k \tilde{H}_k] \bar{P}_k \tilde{H}_k^T R_k^{-1} y_k. \quad (39)$$

The coefficient of  $y_k$  in equation (39) can be reduced to  $K_k$ , namely,

$$\begin{aligned} [I - K_k \tilde{H}_k] \bar{P}_k \tilde{H}_k^T R_k^{-1} &= \bar{P}_k \tilde{H}_k^T R_k^{-1} - \bar{P}_k \tilde{H}_k^T [\tilde{H}_k \bar{P}_k \tilde{H}_k^T + R_k]^{-1} \tilde{H}_k \bar{P}_k \tilde{H}_k^T R_k^{-1} \\ &= \bar{P}_k \tilde{H}_k^T (R_k^{-1} - [\tilde{H}_k \bar{P}_k \tilde{H}_k^T + R_k]^{-1} \{ \tilde{H}_k \bar{P}_k \tilde{H}_k^T R_k^{-1} + R_k R_k^{-1} - I \}) \\ &= \bar{P}_k \tilde{H}_k^T (R_k^{-1} - [\tilde{H}_k \bar{P}_k \tilde{H}_k^T + R_k]^{-1} [\tilde{H}_k \bar{P}_k \tilde{H}_k^T + R_k] R_k^{-1} + [\tilde{H}_k \bar{P}_k \tilde{H}_k^T + R_k]^{-1}) \\ &= \bar{P}_k \tilde{H}_k^T [\tilde{H}_k \bar{P}_k \tilde{H}_k^T + R_k]^{-1} \\ &= K_k \end{aligned}$$

and substituting this result into equation (39), the following result is lead,

$$\hat{x}_k = \bar{x}_k + K_k [y_k - \tilde{H}_k \bar{x}_k]. \quad (40)$$

Equation(40) can be used recursively with equations (23), (26), (37) and (38) to compute the estimate of  $x_k$ , incorporating the observation,  $y_k$ .

##### (5) Estimation of precision of a baseline length

By using the procedure described in the previous sections, station coordinates for unknown SLR sites can be obtained with the covariance matrix  $P$ . The error estimate for the unknown parameters is given by the diagonal elements of the covariance matrix of the well converged case when the range residuals for each station is applied to the observation noise covariance matrix,  $R$ , in equation (14). The variance/covariance information for three diagonal components of each determined station coordinates is involved in the associated elements of the covariance matrix.

According to the error estimation theory [e.g. Tajima and Komaki 1986], the propagation of error is treated as follows :

At first let us consider the case that there is a linear relation as

$$Y = a + BX \quad (41)$$

with a  $k$ -dimensional random variable  $Y$  and an  $n$ -dimensional random variable  $X$ , where  $a$  is a  $k$ -dimensional constant column vector and  $B$  is a  $(k \times n)$  dimensional constant matrix. If the mean value of  $X$  is defined by  $\mu$  and the covariance matrix of  $X$  is defined by  $P$ , the following relations are given :

$$\begin{aligned} E(X) &= \mu \text{ and } E[(X - \mu)(X - \mu)^T] = P, \\ E(Y) &= a + B E(X) = a + B\mu \end{aligned} \quad (42)$$

and

$$E[(Y - E(Y))(Y - E(Y))^T] = [B(X - \mu)] [B(X - \mu)]^T$$

$$\begin{aligned} &= B E \{ (X-\mu) (X-\mu)^T \} B^T \\ &= B P B^T. \end{aligned} \tag{43}$$

Therefore if there is a relation as equation (41) with  $Y$  and  $X$ , the mean value of  $Y$  becomes  $a + B\mu$  and the covariance matrix of  $Y$  becomes  $B P B^T$ .

The relation between two covariance matrix as given in equation (43) is called the propagation law of error. If the relation between two random variables is non-linear as  $Y=f(X)$ , the similar relation with equation (41) as

$$Y = f(\mu) + \left( \frac{\partial f}{\partial X} \right)_\mu (X-\mu)$$

can be formed approximately and the relation between the covariance matrices of  $X$ ,  $P_x$ , and of  $Y$ ,  $P_y$ , becomes

$$P_y = \left( \frac{\partial f}{\partial X} \right)_\mu P_x \left( \frac{\partial f}{\partial X} \right)_\mu^T.$$

The propagation law of error above gives a result for error estimate of baseline length. For the simplicity, the case of a baseline between a fixed station  $X_0(x_0, y_0, z_0)$  and an unknown station  $X_1(x_1, y_1, z_1)$  is considered.

As the mean baseline length is given as

$$\bar{r} = \{ (\bar{x}_1 - x_0)^2 + (\bar{y}_1 - y_0)^2 + (\bar{z}_1 - z_0)^2 \}^{1/2}$$

and

$$dr = \frac{(\bar{x}_1 - x_0)}{\bar{r}} dx_1 + \frac{(\bar{y}_1 - y_0)}{\bar{r}} dy_1 + \frac{(\bar{z}_1 - z_0)}{\bar{r}} dz_1,$$

the error budget can be obtained from the 3 x 3 covariance matrix,  $P_x$ , of the associated part of  $P$  by the following expression,

$$\begin{aligned} P_r &= \left( \frac{\partial f}{\partial X} \right) P_x \left( \frac{\partial f}{\partial X} \right)^T \\ &= \left( \frac{\bar{x}_1 - x_0}{\bar{r}}, \frac{\bar{y}_1 - y_0}{\bar{r}}, \frac{\bar{z}_1 - z_0}{\bar{r}} \right) P_x \left( \frac{\bar{x}_1 - x_0}{\bar{r}}, \frac{\bar{y}_1 - y_0}{\bar{r}}, \frac{\bar{z}_1 - z_0}{\bar{r}} \right)^T. \end{aligned}$$

The similar formulation can be made for other necessary relations.

## 2. Dynamical Models and Their Formulation

In the processor/analyzer to estimate the position and velocity of a satellite, station coordinates, earth rotation parameters and geophysical parameters, many time and coordinate systems and dynamical models are used. The principal dynamical models adopted in the processor/analyzer are given in Table III-1 and description on the systems and models are given in the following sections.

### (1) Time systems

There are some time systems to express dynamical models conveniently. As the basic time of the processor/analyzer it is expected to use a precise-, invariable-, continuous- and widely observable time system. In such purpose *TAI* (International Atomic Time) is adequate and used in this processor/analyzer. To express the independent variable of motion of the earth, moon, sun and planets, *TDT* (Terrestrial Dynamical Time) is used. *UTI* (Universal Time one) is used to denote the earth rotation phase and *UTC* (Coordinated Universal Time) is used for time of observation. The relation,

$$TDT - TAI = 32.184^s,$$

is used. For *UTIR - TAI* and *UTC (BIPM, BIH or USNO) - TAI* at each observation time the values are provided by IERS, BIPM, (BIH) or USNO.

Table III — 1. Adopted dynamical systems of HYDRANGEA

Astronomical constants	after : IAU1976 system (1976)
Precession	: Lieske, et al. (1977)
Nutation	: Wahr (1979)
Definition of UT	: Aoki et al. (1982)
Geopotential	: GEM L2 (1983)/GEM-T1(1987)
Earth model	: 1066A(Gilbert and Dziewonski 1975)
Solid earth tide and its site displacement	: Shen and Mansinha (1976), Sasao et al. (1977) and Wahr (1979)
Ocean tide and its loading site displacement	: Goad (1980), Sasao and Kikuchi(1982),
Tidal variation in UT1	: Yoder et al. (1981)
Air drag	: exponential atmosphere
Radiation pressure	: MERIT Standards (1983)
Satellite constants	: <i>ibid.</i>
Luni-, solar- and planetary position	: Japanese Ephemeris(1983)

## (2) Coordinate systems

The equation (1) with a true perturbation acceleration,  $\mathbf{R}$ , caused by true forces is a correct expression for the motion of a satellite in the non-accelerating (inertial) and non-rotating frame in the solar system. This frame is realized to take the origin of a coordinate system at the center of mass of the solar system having non-rotating coordinate axis. However an earth centered non-rotating coordinate system to the inertial space can be used to express the equation of motion of a satellite moving around the earth simply if the perturbation acceleration due to the moon, the sun and the planets is not given by direct  $n$ -body accelerations but given by the difference of the  $n$ -body accelerations to the satellite from the  $n$ -body accelerations to the center of mass of the earth. Namely, if we take the origin of a coordinate system at the center of mass of the earth, the equation (1) of the motion of a satellite holds good only by subtracting the (apparent)  $n$ -body acceleration at the center of the earth due to the sun, the moon and planets from the original  $n$ -body acceleration of the satellite.

Considering the subject above, as the basic coordinate system to denote a motion of an earth-centered artificial satellite, the geocentric rectangular coordinates on the basis of J2000.0 mean equator is adopted. The direction of the  $X$ -axis is taken to the equinox of J2000.0 from the center of mass of the earth and  $Z$ -axis is to the axis of the mean equator. The  $Y$ -axis is to be taken to make a right hand system by the  $X$ ,  $Y$  and  $Z$  axes. This coordinate system and other associated coordinate systems to express positions on the earth or in the space are as followings :

$X_{20}(X_{20}, Y_{20}, Z_{20})$  or simply  $X(X, Y, Z)$  : Geocentric rectangular coordinates of the J2000.0 Mean equator,

$X_{TM}(X_{TM}, Y_{TM}, Z_{TM})$  : Geocentric rectangular coordinates of the Mean equator of Date,

$X_{TT}(X_{TT}, Y_{TT}, Z_{TT})$  : Geocentric rectangular coordinates of the True equator of Date,



$U_P (U_P, V_P, W_P)$  : Pseudo earth-fixed geocentric rectangular coordinates which does not account for the pole motion,

$U_E (U_E, V_E, W_E)$  : Earth-fixed geocentric coordinates whose reference plane is perpendicular to a line passing from the center of mass of the earth to the Conventional International Origin (CIO) and with  $U$ -axis passing through the Greenwich meridian (rigorously saying, the direction of the axis is defined by the coordinate values of fixed stations of SLR sites as shown later),

$\Phi_G (\varphi, \lambda, h)$  : Conventional geodetic coordinates referred an ellipsoid, namely, latitude, longitude and height from the ellipsoid,

$\Phi_L (R, A_z, El)$  : Topocentric spherical coordinates where  $R$  is distance from a local origin,  $A_z$  is eastward azimuth from north and  $El$  is elevation from the horizontal plane.

An example for a transformation matrices from one coordinates to another for position and velocity are given as the case between geocentric rectangular coordinates of the J2000.0 Mean equator and geocentric rectangular coordinates of the Mean equatos of Date as :

$$\begin{cases} \dot{X}_{TM} = P\dot{X}_{20} \\ \dot{X}_{TM} = P\dot{X}_{20} \end{cases} \quad \begin{cases} X_{20} = P^T X_{TM} \\ \dot{X}_{20} = P^T \dot{X}_{TM} \end{cases}$$

where it is assumed that  $\dot{P}$  can be neglected practically and the expression of  $P$  is

$$P = \begin{bmatrix} P_{11} & P_{12} & P_{13} \\ P_{21} & P_{22} & P_{23} \\ P_{31} & P_{32} & P_{33} \end{bmatrix},$$

and precise expression is given by e.g. Sasaki[1984a].

The precise definition, expression and transformation matrices for other coordinates are given also by e.g. Sasaki [1984a]. It should be careful to treat velocity transformation between a rotating coordinate system and other coordinates because of rotating effect of the coordinates. It is expected to adopt recent results for the numerical corrections introduced by Herring *et al.* [1986] or Kubo [1989] to the nutation terms of Wahr [1979].

(3) **Acceleration due to the perturbation force**

The acceleration due to the perturbation force,  $R$ , in equation (1) is divided into a modeled term,  $R_m$ , and an unmodeled term,  $\eta$ , as

$$R(r, v, t) = R_m(r, v, t) + \eta(r, v, t).$$

If the unmodeled term is small enough to be ignored or it can be assumed to be random and unbiased, the algorithm described above can be applied. The modeled terms are given as followings :

$$R_m = \alpha_{NS} + \alpha_{NB} + \alpha_{RP} + \alpha_{AD} + \alpha_{TD}$$

where  $\alpha_{NS}$  : non-spherical acceleration due to the earth gravity field,  $\alpha_{NB}$  : difference of two-body accelerations due to the sun, the moon and planets (=  $n$ -body forces) to the satellite from the  $n$ -body accelerations to the center of mass of the earth,  $\alpha_{RP}$  : acceleration due to the radiation pressure,  $\alpha_{AD}$  : acceleration due to the atmospheric drag and  $\alpha_{TD}$  : acceleration due to the solid earth tide and the ocean tide.

If  $Q$ -matrix defined by  $U_E = QX_{20}$  and  $X_{20} = Q^T U_E$  is the direct expression of the relation between  $X_{20}$  and  $U_E$ , the non-spherical acceleration due to the earth gravity field expressed in the non-rotating coordinates,  $\alpha_{NS}$ , and in the earth-fixed coordinates,  $\alpha_{NS,E}$ , is given as follows

$$\begin{aligned} \alpha_{NS} &= Q^T \alpha_{NS,E} \\ \alpha_{NS,E} &= -gradU \end{aligned}$$

where  $U$  is the non-spherical gravity potential as defined as

$$U = -\frac{\mu}{r} \left( \sum_{n=2}^N \left( \frac{A_e}{r} \right)^n J_n P_n(\sin \phi) + \sum_{n=2}^N \sum_{m=1}^n \left( \frac{A_e}{r} \right)^n P_n^m(\sin \phi) (C_{n,m} \cos m\lambda + S_{n,m} \sin m\lambda) \right).$$

The precise expression and interrelations for the modeled terms are also given by e.g., Sasaki [1984a] which mostly based on the MERIT Standards [Melbourne *et al.* 1983] and Sasaki [1988b]. Several improvements and corrections for the former papers above are given in this paper.

The acceleration due to solar radiation pressure including effect of solar eclipse by the moon is given as

$$\alpha_{\text{RP}} = \nu P_s A_A^2 \frac{r A_s}{m} \frac{X - X_s}{|X - X_s|^3}$$

where  $X$ ,  $X_s$  : position vectors of the satellite and the sun from geocenter and

$P_s = 4.5605 \times 10^{-6}$  : solar radiation pressure at  $|X - X_s| = A_A$ ,

$A_A = 1.49597870 \times 10^{11}$  m : astronomical unit,

$\gamma$  : reflectivity coefficient,

$A_s$  : cross section area of the satellite to  $(X - X_s)$ ,

$m$  : mass of the satellite

$\nu = 1$  : the satellite is located at out of umbrae and penumbrae of the earth and the moon,

$0 < \nu < 1$  : the satellite is located in the penumbrae of the earth or the moon,

$\nu = 0$  : the satellite is located in the umbrae of the earth or the moon.

The estimation of  $\nu$  is given as follows :

If we give names  $E$ ,  $M$ ,  $S$  and  $O$  for the centers of masses of the earth, the moon, the sun and the satellite considering in the space and also  $\theta_e$ ,  $\theta_m$  and  $\theta_s$  for parallax angles of the earth, the moon and the sun seen from the satellite as given Figure III-1. If we define angles as

$$\alpha_{\text{ES}} = \angle SOE = \cos^{-1} \left\{ \frac{(-X) \cdot (X_s - X)}{|X| \cdot |X_s - X|} \right\}$$

and

$$\alpha_{\text{MS}} = \angle SOM = \cos^{-1} \left\{ \frac{(X_M - X) \cdot (X_s - X)}{|X_M - X| \cdot |X_s - X|} \right\},$$

the effect of shadow of the solar light by the earth gives values of  $\nu$  as

$$\nu = 0, \text{ if } \alpha_{\text{ES}} < \theta_e - \theta_s,$$

$$\nu = 1, \text{ if } \alpha_{\text{ES}} < \theta_e + \theta_s \text{ and}$$

$$0 < \nu < 1 \text{ if others see Figure III-2 and consider eclipse seen from the satellite as follows.}$$

If we define the area of the surface of the sun covered with the earth or the moon as  $f$  and put the angles expressed in radian as  $\angle AES = A$  and  $\angle ASE = B$ ,

$$f = (r_e^2 A / \pi + r_s^2 B / \pi) - (r_e^2 \cos A \sin A + r_s^2 \cos B \sin B),$$

where

$$A = \cos^{-1} \left( \frac{\alpha_{\text{ES}}^2 + r_e^2 - r_s^2}{2 r_e \alpha_{\text{ES}}} \right) \text{ and } B = \cos^{-1} \left( \frac{\alpha_{\text{ES}}^2 + r_s^2 - r_e^2}{2 r_s \alpha_{\text{ES}}} \right).$$

And  $\nu$  is given as

$$\nu = 1 - f / \pi r_s^2.$$

For the shadow by the moon, the same procedure as above but changing the earth to the moon should be applied.

#### (4) Expression of A-matrix

The unknowns in this estimation procedure are denoted by  $X$  as already described. For the unknowns, satellite position,  $X$ , satellite velocity,  $v$ , and any astrogeodetic parameters which are associated with satellite orbit can be taken, e.g., geocentric constant of gravitation ( $\mu = GM$ ), dynamical

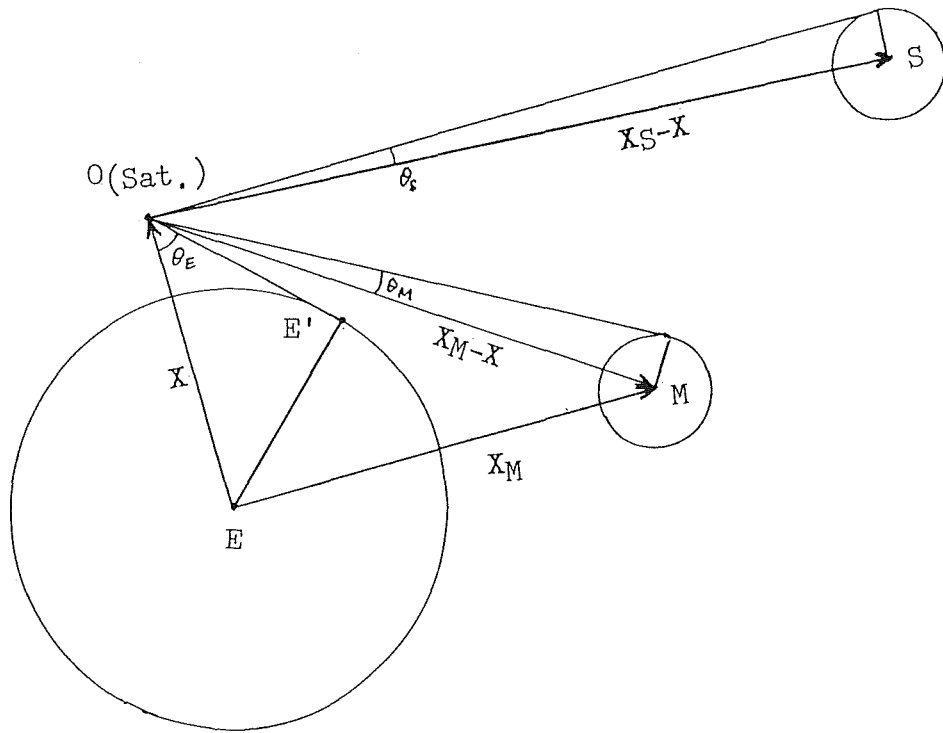


Figure III - 1. Positional relation of the earth, moon, sun and satellite.

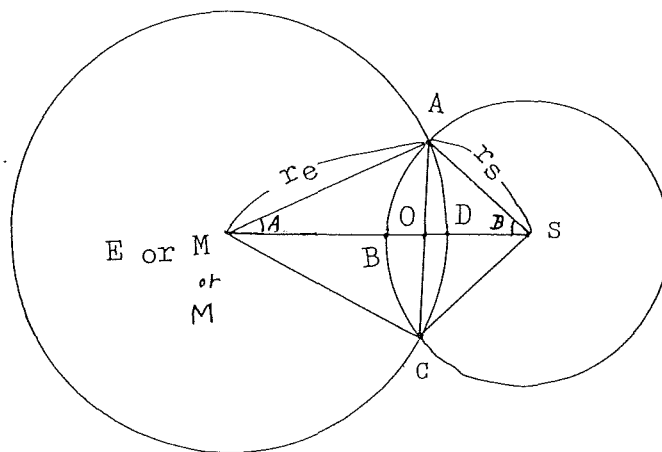


Figure III - 2. Ratio of covered surface at an eclipse.

form factor of the earth,  $J_2 (= -\sqrt{5} C_{2,0} > 0)$ , ballistic coefficient,  $\beta (= C_d A_s / 2m)$ , reflectivity coefficient of satellite surface,  $\gamma$ , pole position of the earth ( $x_p, y_p$ ), excess rotation per day (minus sign of the excess length of day) ( $\Delta\omega$ ), constant air drag acceleration ( $\Delta\alpha$ ), arbitrary degrees and orders of earth gravity potential coefficients,  $C_{n,m}, S_{n,m}$ , arbitrary number of three dimensional coordinates of observation stations, and latitude, longitude and height expression for other stations.

$$X = [X, v, \mu, J_2, \beta, \gamma, x_p, y_p, \Delta\omega, \Delta\alpha, C_{n,m}, S_{n,m}, U_1, U_2, \dots, U_M, \varphi_{M+1}, \lambda_{M+1}, h_{M+1}, \dots, \varphi_N, \lambda_N, h_N]^T \quad (44)$$

$$\dot{X} = F = [v, \alpha, 0, 0, 0, 0, 0, 0, 0, 0, \mathbf{0}, \mathbf{0}, \dots, \mathbf{0}, 0, 0, 0, \dots, 0]^T. \quad (45)$$

The expression of the  $A$ -matrix in equation (6) is :

$$A = \left[ \frac{\partial F}{\partial X} \right]^* = \begin{pmatrix} O_3 & I_3 & \mathbf{0} & \mathbf{0} & \mathbf{0} & \mathbf{0} & \mathbf{0} & \mathbf{0} & \mathbf{0} & \mathbf{0} & \mathbf{0} & \mathbf{0} & O_3 & O_3 & \dots & O_3 & \mathbf{0} & \mathbf{0} & \mathbf{0} & \dots & \mathbf{0} \\ \frac{\partial \alpha}{\partial X} & \frac{\partial \alpha}{\partial v} & \frac{\partial \alpha}{\partial \mu} & \frac{\partial \alpha}{\partial J_2} & \frac{\partial \alpha}{\partial \beta} & \frac{\partial \alpha}{\partial \gamma} & 0 & 0 & 0 & \frac{\partial \alpha}{\partial \Delta\alpha} & \frac{\partial \alpha}{\partial C_{n,m}} & \frac{\partial \alpha}{\partial S_{n,m}} & O_3 & O_3 & \dots & O_3 & \mathbf{0} & \mathbf{0} & \mathbf{0} & \dots & \mathbf{0} \\ \mathbf{0} & \mathbf{0} & 0 & 0 & 0 & 0 & 0 & 0 & 0 & 0 & 0 & 0 & \mathbf{0} & \mathbf{0} & \dots & \mathbf{0} & 0 & 0 & 0 & \dots & 0 \\ \vdots & \vdots \\ O_3 & O_3 & \mathbf{0} & \mathbf{0} & \mathbf{0} & \mathbf{0} & \mathbf{0} & \mathbf{0} & \mathbf{0} & \mathbf{0} & \mathbf{0} & \mathbf{0} & O_3 & O_3 & \dots & O_3 & \mathbf{0} & \mathbf{0} & \mathbf{0} & \dots & \mathbf{0} \\ \mathbf{0} & \mathbf{0} & 0 & 0 & 0 & 0 & 0 & 0 & 0 & 0 & 0 & 0 & \mathbf{0} & \mathbf{0} & \dots & \mathbf{0} & 0 & 0 & 0 & \dots & 0 \\ \mathbf{0} & \mathbf{0} & 0 & 0 & 0 & 0 & 0 & 0 & 0 & 0 & 0 & 0 & \mathbf{0} & \mathbf{0} & \dots & \mathbf{0} & 0 & 0 & 0 & \dots & 0 \\ \mathbf{0} & \mathbf{0} & 0 & 0 & 0 & 0 & 0 & 0 & 0 & 0 & 0 & 0 & \mathbf{0} & \mathbf{0} & \dots & \mathbf{0} & 0 & 0 & 0 & \dots & 0 \\ \vdots & \vdots \\ \mathbf{0} & \mathbf{0} & 0 & 0 & 0 & 0 & 0 & 0 & 0 & 0 & 0 & 0 & \mathbf{0} & \mathbf{0} & \dots & \mathbf{0} & 0 & 0 & 0 & \dots & 0 \end{pmatrix}$$

where

$$\alpha = \alpha_{2B} + (\alpha_{NS} + \alpha_{TD}) + \alpha_{NB} + \alpha_{RP} + \alpha_{AD},$$

$$\alpha_{2B} = -\mu \frac{X}{r^3},$$

$$O_3 = \begin{pmatrix} 0 & 0 & 0 \\ 0 & 0 & 0 \\ 0 & 0 & 0 \end{pmatrix} \quad \text{and} \quad I_3 = \begin{pmatrix} 1 & 0 & 0 \\ 0 & 1 & 0 \\ 0 & 0 & 1 \end{pmatrix}.$$

The expression of  $\frac{\partial \alpha}{\partial r}$ ,  $\frac{\partial \alpha}{\partial C_{n,m}}$ ,  $\frac{\partial \alpha}{\partial S_{n,m}}$  are given as

$$\frac{\partial \alpha}{\partial \gamma} = \frac{1}{\gamma} \alpha_{RP},$$

$$\frac{\partial \alpha}{\partial \Delta\alpha} = \frac{1}{\Delta\alpha} \alpha_{AD},$$

$$\frac{\partial \alpha}{\partial C_{n,m}} = \text{Real} [A_e^n \text{grad } U_{nm}],$$

$$\frac{\partial \alpha}{\partial S_{n,m}} = \text{Real} [-i A_e^n \text{grad } U_{nm}],$$

where the expression of  $\alpha_{RP}$ ,  $\text{grad } U_{nm}$  and other terms are also given by e.g. Sasaki [1984a] and Sasaki [1988b].

The other expression including corrections to the former paper of Sasaki [1984a] and additional descriptions of  $A$ -matrix are given here (where  $(i, j)$  expression is the  $i$ - $j$  component of  $(3 \times 3)$   $A$ -matrix):

$$\left. \frac{\partial \alpha_{2B}}{\partial X} \right|_{ij} = \frac{\partial \alpha_{2B}}{\partial X_j} = \frac{\mu}{r^3} \left\{ \frac{3X_i X_j}{r^2} - \delta_{ij} \right\},$$

$$\frac{\partial \alpha_{NS}}{\partial X} = Q^T \frac{\partial \alpha_{NS,E}}{\partial U} Q$$

and  $U : (U, V, W)$  earth fixed coordinates of the satellite

$$\frac{\partial \alpha_{NS,E}}{\partial U} = -\frac{\partial}{\partial U} \frac{\partial U}{\partial U} \text{ where } U \text{ is geopotential,}$$

$$\frac{\partial \alpha_{NS,E}}{\partial U} = -\frac{\partial^2 U}{\partial U_j \partial U_i} = \text{Real} \sum_{n=2}^N \sum_{m=0}^n A_n^m (C_{n,m} - i S_{n,m}) \frac{\partial^2 U_{n,m}}{\partial U_i \partial U_j}$$

where  $-\frac{\partial^2 U_{n,m}}{\partial U_i \partial U_j}$  is given in Sasaki [1984a],

$$\frac{\partial \alpha_{NB}}{\partial X} \Big|_{ij} = \mu \sum_{k=1}^6 \frac{M_k}{M} \frac{1}{R_k^3} \left\{ \frac{3(X_i - X_{ki})(X_j - X_{kj})}{R_k^2} - \delta_{ij} \right\},$$

where  $R_k = \{(X_1 - X_{k1})^2 + (X_2 - X_{k2})^2 + (X_3 - X_{k3})^2\}^{1/2}$ ,

$$\frac{\partial \alpha_{RP}}{\partial X} \Big|_{ij} = \nu P_s A_A^2 \frac{\gamma A_s}{m} \frac{1}{R_k^3} \{ \delta_{ij} - \frac{3(X_i - X_{2i})(X_j - X_{2j})}{R_k^2} \},$$

$$-\frac{\partial \alpha_{AD}}{\partial X} \Big|_{ij} = -\beta \rho \left\{ -\frac{K v_r}{r} (v_{ri} X_j) + \frac{1}{v_r} v_{ri} (\omega \times v_r)_j + v_r \Omega_{ij} \right\},$$

where  $r = (X_1^2 + X_2^2 + X_3^2)^{1/2}$  and

$$\Omega = \begin{bmatrix} 0 & \omega_z & -\omega_y \\ -\omega_z & 0 & \omega_x \\ \omega_y & -\omega_x & 0 \end{bmatrix}$$

$v_{ri} = (V - \omega \times X)_i$  and  $v_r = (v_{r1} + v_{r2} + v_{r3})^{1/2}$ ,

$$\frac{\partial \alpha}{\partial V} \Big|_{ij} = \frac{\partial \alpha_{AD}}{\partial V} \Big|_{ij} = -\beta \rho \frac{1}{v_r} (v_{ri} v_{rj} + \delta_{ij} v_r^2)$$

$$\frac{\partial \alpha}{\partial \mu} = -\frac{X}{r^3} + \frac{1}{\mu} \alpha_{NS},$$

$$\frac{\partial \alpha}{\partial J_2} = \frac{1}{J_2} \alpha_{J_2}$$

where  $\alpha_{J_2}$  is obtained by the  $J_2$  term of  $\alpha_{NS}$  and

$$\frac{\partial \alpha}{\partial \beta} = \frac{1}{\beta} \alpha_{AD}.$$

(5) Formulation of observational variables

If the unknown parameters are estimable from observed values, the observed values as range data should have relations with dynamical systems described above. We limit for simplicity that the observation to combine the earth dynamical system and satellite motion is only range measurement made from the ground stations to the satellite.

Roughly saying, the positions of the ground stations seem to be fixed. But if we see precisely, the real station positions on the ground are vibrated periodically by the solid earth tide and ocean tide loading site displacement. In order to make the treatment simple, not moving station coordinates are considered. As we know that the tidal motion includes permanent tide [Melbourne *et al.* 1983], we remove the tidal effect and consider constant station coordinates for observation stations. If we use the concept of such not-moving station positions in the frame of the earth fixed coordinates, we can express a  $j$ -th observation stations by using constant values as  $(U_j, V_j, W_j)$  in the earth fixed geocentric rectangular coordinates and distance from these not-moving stations to the center of mass of the satellite considering, whose rectangular coordinates are expressed as  $(U, V, W)$ , can be given as

$$R_j = \{(U - U_j)^2 + (V - V_j)^2 + (W - W_j)^2\}^{1/2}.$$

The distance is also expressed by using non-rotating (space fixed) coordinates of the  $j$ -th station,  $(X_j, Y_j, Z_j)$ , and of the satellite,  $(X, Y, Z)$  as

$$R_j = \{(X - X_j)^2 + (Y - Y_j)^2 + (Z - Z_j)^2\}^{1/2}.$$

On the other hand, the measured raw range data to the satellite obtained at a  $j$ -th station contain the effects of the atmospheric refraction, the positional difference between the center of mass of the satellite and reflector, the individual range offset of each ranging system and the effect of the solid earth tide and ocean tide loading site displacement. So, if the raw range obtained at  $j$ -th station is denoted by  $Y_j^*$  in the equation (4) and the algorithm given in the previous sections,  $Y_j^*$  is expressed with range error,  $\epsilon_j$ , as

$$Y_j^* = R_j + \Delta R_{DPj} + \Delta R_{RFj} + \Delta R_{CM} + \Delta R_{ROj} + \epsilon_j$$

where

- $\Delta R_{DPj}$  : component of tidal displacement along the direction from  $j$ -th site to the satellite,
- $\Delta R_{RFj}$  : change of range by the atmospheric refraction,
- $\Delta R_{CM}$  : center of mass correction of the satellite,
- $\Delta R_{ROj}$  : range offset of the laser ranging system at  $j$ -th site obtained by each system calibration.

The expression of  $R_{DPj}$  using upward-, northward- and eastward unit vectors,  $\mathbf{h}$ ,  $\mathbf{n}$ ,  $\mathbf{e}$ , is

$$\Delta R_{DPj} = [\Delta U_j + (\delta h_j^{(2)} + \delta h_j^{(1)} + \delta h_j^{(0)}) \mathbf{h}_j + (\delta n_j^{(2)} + \delta n_j^{(1)} + \delta n_j^{(0)}) \mathbf{n}_j + (\delta e_j^{(2)} + \delta e_j^{(1)} + \delta e_j^{(0)}) \mathbf{e}_j] \frac{(\mathbf{r}_j - \mathbf{r})}{|\mathbf{r}_j - \mathbf{r}|}$$

where

- $\Delta U_j$  : frequency independent vector displacement of the  $j$ -th site due to tidal deformation of the solid earth,
- $\delta h_j^{(2)}$  : frequency dependent upward displacement,
- $\delta n_j^{(2)}$  : frequency dependent northward displacement,
- $\delta e_j^{(2)}$  : frequency dependent eastward displacement,
- $\delta h_j^{(1)}$  : zero frequency permanent deformation to upward,
- $\delta n_j^{(1)}$  : zero frequency permanent deformation to northward in the horizontal plane,
- $\delta e_j^{(1)}$  : zero frequency permanent deformation to eastward in the horizontal plane,
- $\delta h_j^{(0)}$  : ocean tide loading site displacement to upward,
- $\delta n_j^{(0)}$  : ocean tide loading site displacement to northward in the horizontal plane,
- $\delta e_j^{(0)}$  : ocean tide loading site displacement to eastward in the horizontal plane.

For the concrete expression for tidal displacements and other effects, see Sasaki [1984a]. The center of mass corrections of LAGEOS and STARLETTE referred to the MERIT Standards are  $-0.24$  m and  $-0.075$  m, respectively. The center of mass correction of AJISAI is investigated by Sasaki and Hashimoto [1987] and  $-1.01$  m given is recommended to use.

The explicit expression of  $\partial G_i / \partial X$  or  $\tilde{H}_i(t)$  is also necessary in the estimation procedure of unknowns,  $X$ .

If we chose the component of  $X$  as equation (44), the  $\tilde{H}_i(t)$  for the  $i$ -th observation made at  $j$ -th station is given as

$$\tilde{H}_i(t) = \left[ \frac{\partial G_i}{\partial X} \right]^* = \left[ \frac{\partial (R_j + \Delta R_{DPj} + \Delta R_{RFj} + \Delta R_{CM} + \Delta R_{ROj})}{\partial X} \right]^*.$$

The effects of small corrections of  $\Delta R_{DPj}$ ,  $\Delta R_{RFj}$ ,  $\Delta R_{CM}$  and  $\Delta R_{ROj}$  to the selected set of unknowns,  $X$ , is nothing or very small and these terms can be ignored from the expression of  $\partial G_i / \partial X$  in this estimation procedure, namely,

$$\frac{\partial G_i}{\partial X} = \frac{\partial R_j}{\partial X}.$$

To make expression simple, the suffix " $i$ " for  $i$ -th observation is removed here and  $H(t)$  is given as

$$\hat{H}(t) = \left[ \frac{\partial G_i}{\partial X}, \frac{\partial G_i}{\partial V}, \frac{\partial G_i}{\partial \mu}, \frac{\partial G_i}{\partial J_2}, \frac{\partial G_i}{\partial \beta}, \frac{\partial G_i}{\partial \gamma}, \frac{\partial G_i}{\partial x_p}, \frac{\partial G_i}{\partial y_p}, \frac{\partial G_i}{\partial \Delta \omega}, \frac{\partial G_i}{\partial \Delta \alpha}, \frac{\partial G_i}{\partial C_{nm}}, \frac{\partial G_i}{\partial S_{nm}}, \frac{\partial G_i}{\partial U_1}, \frac{\partial G_i}{\partial U_2}, \dots, \frac{\partial G_i}{\partial U_M}, \frac{\partial G_i}{\partial \varphi_{M+1}}, \frac{\partial G_i}{\partial \lambda_{M+1}}, \frac{\partial G_i}{\partial h_{M+1}}, \dots, \frac{\partial G_i}{\partial \varphi_N}, \frac{\partial G_i}{\partial \lambda_N}, \frac{\partial G_i}{\partial h_N} \right]^T,$$

where

$$\frac{\partial G_i}{\partial X} = \frac{X^T - X_j^T}{R_j},$$

$$\frac{\partial G_i}{\partial V} = 0^T,$$

$$\frac{\partial G_i}{\partial \mu} = \frac{\partial G_i}{\partial J_2} = \frac{\partial G_i}{\partial \beta} = \frac{\partial G_i}{\partial \gamma} = \frac{\partial G_i}{\partial C_{nm}} = \frac{\partial G_i}{\partial S_{nm}} = 0,$$

$$\frac{\partial G_i}{\partial x_p} = \frac{1}{R_j} \left\{ (X_j - X) \frac{\partial X_j}{\partial x_p} + (Y_j - Y) \frac{\partial Y_j}{\partial x_p} + (Z_j - Z) \frac{\partial Z_j}{\partial x_p} \right\},$$

$$\frac{\partial G_i}{\partial y_p} = \frac{1}{R_j} \left\{ (X_j - X) \frac{\partial X_j}{\partial y_p} + (Y_j - Y) \frac{\partial Y_j}{\partial y_p} + (Z_j - Z) \frac{\partial Z_j}{\partial y_p} \right\},$$

$$\frac{\partial G_i}{\partial \Delta \omega} = \frac{1}{R_j} \left\{ (X_j - X) \frac{\partial X_j}{\partial \Delta \omega} + (Y_j - Y) \frac{\partial Y_j}{\partial \Delta \omega} + (Z_j - Z) \frac{\partial Z_j}{\partial \Delta \omega} \right\},$$

The coordinate transformation from the non-rotating rectangular coordinates of J2000.0 to the earth fixed rectangular coordinates is given by 3 x 3 matrices as  $U = B \cdot S \cdot N \cdot P \cdot X$  or  $U_j = B \cdot S \cdot N \cdot P \cdot X_j$  and  $X = P^T \cdot N^T \cdot S^T \cdot B^T \cdot U$  or  $X_j = P^T \cdot N^T \cdot S^T \cdot B^T \cdot U_j$  where the concrete expression of  $B, S, N$  and  $P$  is given in [Sasaki 1984a].

The partial derivatives in equations above are given by differentiating the transformation matrices as

$$\frac{\partial X_i}{\partial x_p} = P^T N^T S^T \frac{\partial B^T}{\partial x_p} U_j,$$

$$\frac{\partial X_i}{\partial y_p} = P^T N^T S^T \frac{\partial B^T}{\partial y_p} U_j,$$

$$\frac{\partial X}{\partial \Delta \omega} = P^T N^T \frac{\partial S^T}{\partial \Delta \omega} B^T U_j,$$

$$\frac{\partial B^T}{\partial x_p} = \begin{bmatrix} 0 & 0 & -1 \\ 0 & 0 & 0 \\ 1 & 0 & 0 \end{bmatrix}, \quad \frac{\partial B^T}{\partial y_p} = \begin{bmatrix} 0 & 0 & 0 \\ 0 & 0 & 1 \\ -1 & 0 & 0 \end{bmatrix},$$

$$\frac{\partial S^T}{\partial \Delta \omega} = \begin{bmatrix} -t^* \sin \theta^* & , & -t^* \cos \theta^* & , & 0 \\ t^* \cos \theta^* & , & -t^* \sin \theta^* & , & 0 \\ 0 & , & 0 & , & 0 \end{bmatrix},$$

where  $\omega = \omega_0 + \Delta \omega$ ,  $\theta = 12^h + UT 1 + \alpha_m + \Delta \psi \cos \epsilon t + \Delta \omega t^* = \theta^* + \Delta \omega t^*$ .

When  $\theta$  is given by a unit of radian/day,  $t^*$  is the elapsed time from the start of integration in fraction of day.

As for the geocentric coordinates of an arbitrary  $k$ -th site,  $(\varphi_k, \lambda_k, h_k)$ , if one of the current  $i$ -th observation is made at the  $j$ -th site,  $\frac{\partial G_i}{\partial \varphi_k}$ ,  $\frac{\partial G_i}{\partial \lambda_k}$  and  $\frac{\partial G_i}{\partial h_k}$  are given by using the chain rule of partial derivative and Kronecker's delta as followings :

$$\frac{\partial G_i}{\partial \varphi_k} = \left( \frac{\partial G_i}{\partial U_k} \frac{\partial U_k}{\partial \varphi_k} + \frac{\partial G_i}{\partial V_k} \frac{\partial V_k}{\partial \varphi_k} + \frac{\partial G_i}{\partial W_k} \frac{\partial W_k}{\partial \varphi_k} \right) \delta_{jk},$$

$$\frac{\partial G_i}{\partial \lambda_k} = \left( \frac{\partial G_i}{\partial U_k} \frac{\partial U_k}{\partial \lambda_k} + \frac{\partial G_i}{\partial V_k} \frac{\partial V_k}{\partial \lambda_k} + \frac{\partial G_i}{\partial W_k} \frac{\partial W_k}{\partial \lambda_k} \right) \delta_{jk},$$

$$\frac{\partial G_i}{\partial h_k} = \left( \frac{\partial G_i}{\partial U_k} \frac{\partial U_k}{\partial h_k} + \frac{\partial G_i}{\partial V_k} \frac{\partial V_k}{\partial h_k} + \frac{\partial G_i}{\partial W_k} \frac{\partial W_k}{\partial h_k} \right) \delta_{jk},$$

By using relations of  $(U_k, V_k, W_k)$  and  $(\varphi_k, \lambda_k, h_k)$  as

$$\begin{aligned} U_k &= (N_k + h_k) \cos \varphi_k \cos \lambda_k, \\ V_k &= (N_k + h_k) \cos \varphi_k \sin \lambda_k, \\ W_k &= \{N_k (1 - e^2) + h_k\} \sin \varphi_k, \end{aligned}$$

where

$$N_k = A / (1 - e^2 \sin^2 \varphi_k)^{1/2},$$

the expression of  $\frac{\partial U_k}{\partial \varphi_k}$  is given as

$$\frac{\partial U_k}{\partial \varphi_k} = -(N_k + h_k) \sin \varphi_k \cos \lambda_k + \frac{\partial N_k}{\partial \varphi_k} \cos \varphi_k \cos \lambda_k,$$

where

$$\frac{\partial N_k}{\partial \varphi_k} = \frac{e^2 N_k \sin \varphi_k \cos \varphi_k}{(1 - e^2 \sin^2 \varphi_k)}.$$

Other expression as  $\frac{\partial V_k}{\partial \varphi_k}$ ,  $\frac{\partial W_k}{\partial \varphi_k}$ ,  $\frac{\partial U_k}{\partial \lambda_k}$ , ... and  $\frac{\partial W_k}{\partial h_k}$  are given in Sasaki [1988b].

For  $\frac{\partial G_1}{\partial U_k}$ ,  $\frac{\partial G_1}{\partial V_k}$  and  $\frac{\partial G_1}{\partial W_k}$ , a vector expression is given as

$$\frac{\partial G_1}{\partial U_k} = -\frac{U^T - U_k^T}{R_k} \delta_{jk}.$$

### 3. Programing

The programing to make an early version of the developed orbital processor/analyzer, HYDRANGEA, for satellite laser ranging data was originated in early 1981 when the author stayed at the University of Texas at Austin. The principle of the formation is given in lectures of Tapley for graduate students and papers of Tapley [1973], Tapley and Schutz [1973], Murata [1978] and Matsushima *et al.* [1978]. Some questions of the author were solved by a co-researching staff at the University, He Miaofu. However the programing was originally started from a small testing program and developed larger and larger later and the contents of the program developed have been made independently by the author since then. Intermediate status and preliminary results were published several times [Sasaki 1981, Sasaki 1984a, Sasaki 1984b, Sasaki 1988b].

In January 1988, a computer network system with four HP9000-825Ss (one of them was replaced later by HP9000/835S), four HP9000/350Cs, two HP9000/318Ms, several terminals of NEC PC9801 and several peripherals of two MT drives, several hard disc drives, plotters and printers were introduced in the Satellite Geodesy Office of Geodesy and Geophysics Division, JHD and the author converted the developing program from one for the current ACOS-650 to one for the new system being given many technical supports by staffs of the Office and in mid-1988 the processor/analyzer were revised including many additional functions and improvements. The developed orbital processor/analyzer was named the **HYdrographic Department RANGE data Analyzer**, ...HYDRANGEA... Some description on the HYDRANGEA is given in this section.

#### (1) Formation

The major structure of the processor/analyzer is as follows : There is a short main program mainly to take dimension area, to open files as astronomical ephemeris file, a priori earth rotation parameter file for initial use, geopotential coefficients file, initial station coordinate file, parameter index file and SLR data file. An arbitrary combination of unknown parameters and station coordinates can be selected in simple procedure. In the first subroutine many common areas are taken and necessary



constants are defined. Many index parameters are read from index file. Initializations of all the processes are made next according to the selected set of parameters and the current time for integration is set.

At the initial time for integration a subroutine named "ephemeris" is called, and every environmental conditions including time dependent space-earth dynamical system which any observers can not affect, are set. Just after the current time is advanced for integration, the subroutine "ephemeris" is always called to set such environments. Once the current time and environmental conditions of the space-earth dynamical system are fixed, all the forces and their derivatives concerned with the satellite are calculated.

The integrator is a type of a single step with no stepsize control and no interpolation process. However the stepsize is changed shorter to adjust the current time to any observation times to make the environmental conditions at each observation time if observation is given within the current step. A subroutine was made for this processor/analyzer according to the algorithm of 7-th order Runge-Kutta formulas given by Fehlberg [1968].

Once the current time reaches to an observed time, procedures for the range data correction, estimation and accumulation are made. And when the current time reaches to the end of integration, unknown parameters are estimated and improved. If the current number of convergence does not reach a limit, all the procedures are restarted using the improved unknown parameters.

Next, the computation procedure is summarized simply here for the batch estimation algorithm. The equations from (1) to (21) in this Chapter are used in the programing of this batch estimation algorithm as follows :

- A. Initialize            geophysical parameters and set the number of current convergence, iconv=1.
- B. Initialize             $X(t_0) = X_0^*$ ,  $\hat{x} = 0$ ,  $\Phi(t_0) = I$ ,  $P_0 = \sigma I$   
                               ( $\sigma \sim 10^{25} \gg I$ ) and set  $t_{k-1} = t_0$ .
- C. Read                    observation  $Y_k$  obtained at  $t = t_k$ .
- D. Integrate             $\dot{X} = F(X^*, t)$  and  $\dot{\Phi}(t, t_0) = A(t) \Phi(t, t_0)$  calculating  $A(t) = [\frac{\partial F}{\partial X}]^*$  from  
                                $t_{k-1}$  to  $t_k$  and set  $t = t_k$ .
- E. Calculate             $y_k = Y_k - G(X_k^*, t_k)$ ,  $\tilde{H}_k = [\frac{\partial G}{\partial X}]_k^*$ ,  $H_k = \tilde{H}_k \Phi(t_k, t_0)$ .
- F. Test                    that if iconv not equals to 1, is  $y_k > y_{limit} = 3 * y_{rms}$  at iconv-1? If yes, reject the  
                               observation  $Y_k$  and go to C.
- G. Compute and accumulate  
                                $L_k = L_{k-1} + H_k^T R_k^{-1} H_k$ ,  
                                $N_k = N_{k-1} + H_k^T R_k^{-1} y_k$ ,
- H. Test                    that is  $Y_k$  the last observation or is  $t > T_{end}$ ? If yes, go to I. If no, set  $k \rightarrow k-1$  and  
                               go to C.
- I. Estimate                 $P = L_k^{-1}$ ,  $N = L_k$  and  $\hat{x}_0 = PN$ .  
                               Calculate  $X_0 = X_0^* + \hat{x}_0$  and print out the results.
- J. Test                    that does iconv equal to the convergence limit? If no, set  $X_0^* = X_0$  and go to B.
- K. End.

Major geodetic or geodynamic results which will be given in the following Chapters of this paper are obtained by using this procedure.

However on the stage of early versions of the programing and testing the author made another

program using the sequential estimation algorithm and checked the availability of both programs each other. The results of both algorithm for the same initial conditions are well coincided with. A sequentially estimable program for each observation is made based on the algorithm given in III-1-(4). The simplified programing procedure is :

- A. Initialize      geophysical parameters,  $X(t_0) = X_0^*$ ,  $x = 0$ ,  $\Phi(t_0) = I$ ,  $P_0 = \sigma I$  ( $\sigma \gg I$ ) and set  
 $t_{k-1} = t_0$ ,
- B. Read            observation  $Y_k$  obtained at  $t = t_k$ ,
- C. Integrate       $\dot{X} = F(X^*, t)$  under initial condition of  $X^*(t_{k-1}) = X_{k-1}$  and  $\dot{\Phi}(t, t_{k-1}) = A(t)\Phi(t, t_{k-1})$ , initially  $\Phi(t_{k-1}, t_{k-1}) = I$  calculating  $A(t) = \left[ \frac{\partial F}{\partial X} \right]^*$  from  $t_{k-1}$  to  $t_k$  and set  $t = t_k$ ,
- D. Propagate       $\bar{x}_k = \Phi(t_k, t_{k-1}) \bar{x}_{k-1}$ ,  
 $\bar{P}_k = \Phi(t_k, t_{k-1}) P_{k-1} \Phi^T(t_k, t_{k-1})$ ,
- E. Compute       $y_k = Y_k - G(X_k^*, t_k)$ ,  
 $H_k = \frac{\partial G(X_k^*, t_k)}{\partial X}$ ,  
 $H_k = \bar{P}_k H_k^T (H_k \bar{P}_k H_k^T + R_k)^{-1}$ ,
- F. Estimate       $\hat{x}_k = \bar{x}_k + K_k (y_k - H_k \bar{x}_k)$ ,  
 $P_k = (I - K_k H_k) \bar{P}_k$ ,  
 $X_k = X_k^* + \hat{x}_k$ ,
- G. Test            that is  $Y_k$  the last observation or  $t > t$  and ?  
 If yes, go to End, If no, go to B,
- H. End.

## (2) Capability and computation

The capability of estimation of this orbital processor/analyzer is as followings :

As for the estimable parameters, six elements of satellite position (3 elements) and initial velocity (3) expressed in geocentric rectangular coordinates of J2000.0 are fixed. Other estimable parameters as  $GM$  (1),  $J_2$  (1), the atmospheric drag coefficient,  $C_d$  (1), the reflectivity coefficient of satellite,  $\gamma$  (1), the earth rotation position ( $x_p, y_p$ ) (2), the excess rotation per day of the earth,  $\Delta\omega$  (1), the empirical drag acceleration,  $\Delta\alpha$  (1) and arbitrary number of three dimensional station coordinates are selectable. The selection procedure in the processor/analyzer is only to keep dimension size according to the number of unknown parameters and to set flags to define unknown parameters.

In this processor the effect of the ocean loading site displacement can be treated. However recently many new sites started SLR observation and the information on the amplitudes of the effect on these new sites could not obtained. So, in the results derived from recent version of the HYDRANGEA given in the following Chapters, the effect of the ocean tide site displacement is not included. The mean effect of this treatment can be almost cancelled and the resultant effect to the results of station coordinates will be a level of 1 cm at most.

The computation time depends on the computation duration of integration of an arc, step size, the number of data, adopted degrees of geopotential and partial derivative of the geopotential. In the case of a five-day-arc of LAGEOS which includes around 10,000 range data, 30 s step size, 20 degrees of geopotential and 7 degrees of partial derivatives, the rough estimate of the CPU time for one conversion driven by HP9000/935S is 8 hours. If the observation data are decreased to 1000, it becomes less than half of that. For the case of a three-day-arc of AJISAI with 10,000 range data, 30 sec step size, 36 degrees

of geopotential and 7 degrees of partial derivatives, the CPU time of HP9000/935s for one conversion is around 16 hours.

#### IV. RESULTS OF DATA PROCESSING AND ANALYSIS

##### 1. Short Arc Solutions

###### (1) Successive Passes Orbit Revising Technique (SPORT)

The range precision of SLR technique reaches one centimeter level today by some NASA high precision systems as given in a NASA GSFC report of the Summary of Laser Quick-Look Data [Decker 1989]. An observation table with estimated range precisions in the report is summarized in Table IV-1. However the accuracy of ordinary orbital determination of a semi-long arc or a five-day-arc remains around 7 to 9 centimeters level [Tapley 1987] as given in a CSR (Center for Space Research at the University of Texas at Austin) report [Schutz 1986]. The status of precision of orbital determination is summarized in Table IV-2. It is clear that such high precision ranging data supplied by good SLR hardware have not been effectively used in the current SLR data analysis. And if we use longer arc technique to estimate precise baseline lengths, worldwide SLR data should be used and it takes time to obtain almost all the worldwide SLR data until a distribution of later version of SLR data made by the data center of the Crustal Dynamics Project at Goddard Space Flight Center (GSFC). To save these problems in the case of precise baseline length estimation in a region of a diameter of a few kilometers like the U.S. West Coast, southern Europe and Japan area, it can be shown that a specific short arc technique is very effective.

Namely the author and his colleagues of JHD tried to use two successive passes obtained both at two or more nearby SLR stations for estimation of baseline lengths between two of them and named the technique as the **Successive Passes Orbit Revising Technique**, SPORT [Sengoku and Kubo 1986, Sengoku *et al.* 1988, Sasaki *et al.* 1989]. The concept is given in Figure IV-1. For the estimation of baseline between two nearby SLR stations, the developed orbital processor/analyzer, HYDRANGEA is used.

###### (2) Station coordinates and baseline determination

The precise determination of baseline length between Quincy and Monument Peak of around 883.6km which crosses San Andreas fault, can show the efficiency of the SPORT [Sasaki *et al.* 1989]. The LAGEOS SLR data of 65 sets of successive passes observed at the two stations of Quincy and Monument Peak from August 1984 to July 1987 are used. Around a thousand of range data are included in a set of the simultaneously observed data at the two stations in average. In order to solve the baseline length, the coordinates of one station is fixed and the initial position and velocity of LAGEOS and the three dimensional coordinates of the other station are solved.

The estimated baseline length between Quincy-Monument Peak in the duration of observation is shown in Figure IV-2. The values given in the left side of the figure are for the straight line length between the reference points of each hardware system. The most of the plotted points are nearly on a straight line and best fit of the straight line has a slope of  $-31\text{mm/year}$  and the mean residual of each point from this line is 11mm.

Next, the SPORT is applied to the baseline determination between Simosato and Titi Sima. The SLR data to determine this baseline were obtained by the fixed SLR station at the Simosato

Table IV—1. Observation pass table with range precision

—November 1988— [after Decker 1989]

SLR station	satellite					
	LAGEOS		AJISAI		STARLETTE	
	Passes	RMS (cm)	Passes	RMS (cm)	Passes	RMS (cm)
Potsdam, GDR	4	22.2	3	10.0	—	—
Riga, USSR	11	22.0	—	—	—	—
Sant. de Cuba, Cuba	16	22.4	1	10.8	1	15.9
Mt. Fowlkes, Texas	32	2.0	—	—	—	—
Yarragadee, Australia	25	1.0	1	1.3	4	0.8
Easter Isl., Chili	5	2.8	—	—	—	—
GSFC, Maryland	15	0.9	12	1.3	16	0.7
Quincy, Calif.	13	0.8	8	1.0	13	0.7
Mon. Peak, Calif.	26	1.0	14	1.3	12	0.9
Mazatlan, Mexico	16	0.8	12	1.2	2	0.8
Haleakala, Hawaii	6	2.7	4	3.5	—	—
Metsahovi, Finland	—	—	3	15.1	—	—
Zimmerwald, Switz	30	6.0	11	6.6	12	6.1
Borowiec, Poland	—	—	1	4.7	—	—
Wetzell, FRG	16	5.8	8	7.1	11	5.0
Grasse, France	59	2.0	49	1.9	41	1.7
Shanghai, PRC	11	5.4	5	4.6	—	—
Simosato, Japan	12	2.6	28	3.6	8	5.8
Graz, Austria	12	2.0	17	2.4	10	2.4
RGO, United Kingdom	65	3.8	48	5.5	43	3.5
Orroral, Australia	21	1.4	—	—	—	—
Owens Valley, Calif.	13	4.9	—	—	—	—
Arequipa, Peru	13	14.2	15	9.1	11	10.9
GSFC, Maryland	21	*	16	*	22	*
Total stations/passes	22/442		19/256		14/206	
Weighted average (cm)	4.5		4.0		3.2	

Table IV—2. Range residuals to determined orbits — case of CSR quick-look analysis —  
 [after Schutz 1986 and 1988]  
 CSR : Center for Space Research at Univ. of Texas at Austin

Five-Day-arcs (Quick-look data)						Monthly arcs (Full-rate data)			
1987 M D	data (shots)	RMS (cm)	1987 M D	data (shots)	RMS (cm)	1985 M	data (shots)	RMS (cm)	rejected (%)
5 4	606	9.7	6 28	545	7.7	Jan	458,296	10.2	4.2
5 9	684	8.5	7 3	613	8.9	Feb	387,215	8.8	6.5
5 14	555	10.5	7 8	715	8.6	Mar	634,238	10.2	6.5
5 19	424	10.7	7 13	586	8.8	Apr	871,175	9.2	5.6
5 24	458	11.1	7 18	472	11.4	May	1,860,305	9.3	5.2
5 29	325	7.9	7 23	842	8.0				
6 3	466	7.6	7 28	795	7.1				
6 8	492	7.4	8 2	739	9.3				
6 13	759	8.6	8 7	904	8.3				
6 18	756	7.8	8 12	717	8.5				
6 23	479	9.0	8 17	778	9.6				
total/average				(623)	8.86				

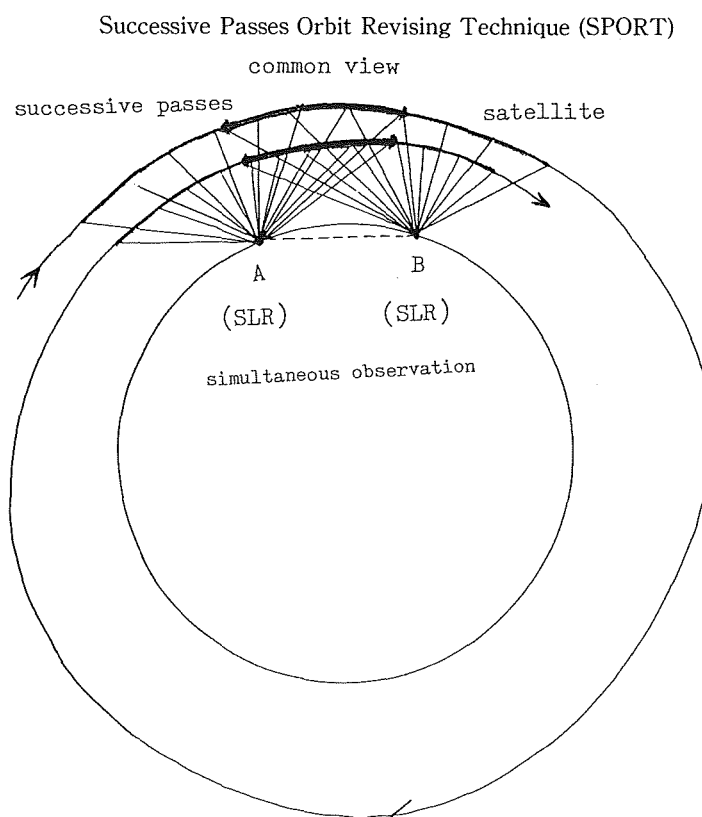


Figure IV — 1. Concept of the Successive Passes Orbit Revising Technique (SPORT).

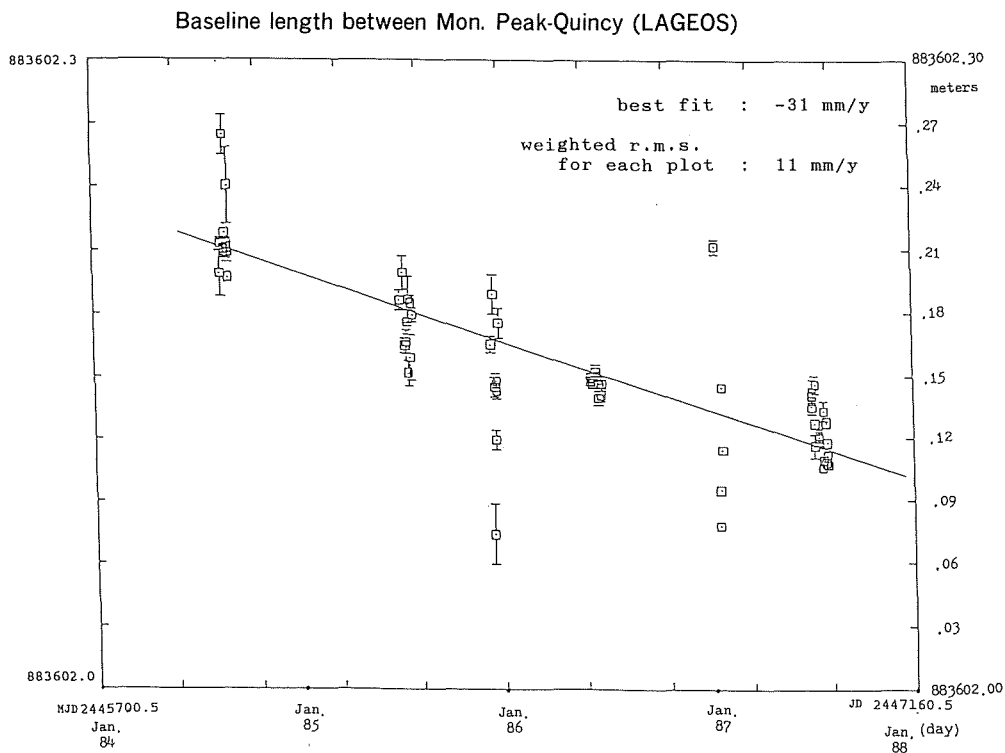


Figure IV — 2. Baseline length between Monument Peak and Quincy across San Andreas Fault (August 1984—July 1987). Results of the specific short arc technique, SPORT. <HYDRANGEA results>

Table IV — 3. Analyzed passes for SPORT to estimate the baseline between Simosato and Titi Sima. <HYDRANGEA results>

No.	date ( UT )		number of returns			r.m.s.		
			HTLRS	SHO	total	HTLRS	SHO	
		d h m	h m	cm				
1	1988 Jan.	24 18 48	- 19 01	493	326		4.7	9.0
		20 49	- 21 06	349	495	1663	5.2	9.7
2		25 11 42	- 11 55	776	184		5.2	9.7
		13 44	- 13 57	255	428	1648	5.2	10.1
3	Feb.	4 17 01	- 17 16	1125	641		3.5	10.3
		19 06	- 19 16	568	11	2345	3.7	2.2
4		5 16 07	- 16 21	58	622		3.4	9.4
		18 10	- 18 24	1092	537	2309	3.3	9.7
5		12 13 55	- 14 05	271	115		3.0	10.6
		15 54	- 16 09	543	343	1272	3.8	10.8
6		14 14 06	- 14 20	971	288		3.5	11.3
		16 09	- 16 22	15	141	1415	2.4	10.7
7		22 10 57	- 11 06	68	189		3.4	8.8
		13 00	- 13 13	179	161	597	3.7	8.9

Hydrographic Observatory and by the HTLRS in the duration from mid-January to mid-March in 1988 described in Chapter II.

Titi Sima is an isolated island which is around 940km southeast from Simosato and is supposed to be on the Philippine Sea plate while Simosato is believed to be located on the east edge of Eurasian plate. The SLR observations were made by the HTLRS at Titi Sima obtaining 25,818 shots in 38 passes of AJISAI, 11 passes of LAGEOS and 4 passes of STARLETTE as seen in Table II-9.

The SPORT is applied to the first baseline determination within Japan between Simosato and Titi Sima by using AJISAI SLR data taken only by both the fixed system at Simosato and the HTLRS at Titi Sima. The three dimensional solution of LSC8402 [Tapley *et al.* 1985] of Simosato

$$(-3,822,388.295\text{m}, 3,699,363.512\text{m}, 3,507,572.967\text{m})$$

is used for the fixed station coordinates. Seven sets of successive passes simultaneously observed at two stations within a month are used for the analysis of the SPORT. These data sets used are summarized in Table IV-3. The adopted center of mass correction of AJISAI is 1.01m [Sasaki and Hashimoto 1987]. The resulting values for the station coordinates of Titi Sima and the baseline length between Simosato and Titi Sima are given in Table IV-4. The range residuals for determined orbits are the level of each hardware precision as shown in the table. The results indicate a very good stability and repeatability of the determined baseline lengths for each set of the successive passes comparing with the values of station coordinates. Namely, the estimated precision of the rectangular coordinates of Titi Sima is around 4cm and, on the other hand, the baseline length is determined in the precision of 4mm as ten times better than the station position.

The next application of the SPORT is made to the baseline between Simosato and Minamitori Sima (Marcus island located at around 2000km southeast from Tokyo) [Sengoku *et al.* 1989]. The SLR observation was made from early January to mid-March in 1989 and observed data by the HTLRS in the duration were already given (Table II-10). The data used for the estimation of the baseline length are four sets of simultaneously observed passes as shown in Table IV-5. The estimation procedure and adopted values are the same as the case of the baseline determination of Simosato-Titi Sima. The estimated results are given in Table IV-6. The internal error estimate for the determined baseline length is 7mm.

The precision is extremely good in comparison with any other methods, especially in this kind of low orbit satellite, AJISAI, and also in such a short number of data used.

## 2. Global Solutions

### (1) Geophysical parameters

The developed orbital processor/analyzer, HYDRANGEA, can determine the unknown parameters of  $GM$ ,  $J_2$ , reflectivity coefficient,  $\gamma$ , atmospheric drag coefficient,  $Cd$ , along track acceleration,  $\Delta\alpha$ , earth rotation parameters,  $(x_p, y_p, \Delta\omega)$  and station coordinates,  $(U_i, V_i, W_i)$ ,  $i=1,2,\dots, n$ . If we call these parameters except the earth rotation parameters and station coordinates as "geophysical parameters" here, any combination of geophysical parameters can be obtained by using the HYDRANGEA. At first, to estimate  $GM$ ,  $J_2$ ,  $\gamma, \Delta\alpha$ , the HYDRANGEA is applied to a set of LAGEOS compressed SLR data named "normal point data" made by the Center for Space Research of the University of Texas at Austin (CSR) and supplied through Goddard Space Flight Center (GSFC). The number of the normal point data used are 5965 and the data span is in successive 8 five-day-arcs from late September to early November in 1984. The dynamical models and constants for LAGEOS adopted

Table IV-4. Estimated station coordinates of Titi Sima and baseline length between Simosato and Titi Sima. &lt;HYDRANGEA results&gt;

No.	$x_t$		$y_t$		$z_t$		r		residuals
	m	m	m	m	m	m	m	m	m
1	-4491072.416	±.006	3481527.856	±.013	2887391.639	±.012	937665.029	±.006	.048
2	.542	±.011	.842	±.010	.748	±.013	.050	±.010	.046
3	.464	±.015	.946	±.022	.656	±.014	.031	±.006	.045
4	.479	±.013	.824	±.015	.689	±.012	.048	±.006	.049
5	.527	±.014	.879	±.024	.723	±.014	.047	±.006	.046
6	.352	±.022	.865	±.017	.559	±.016	.034	±.007	.045
7	.213	±.036	.731	±.052	.433	±.065	.049	±.020	.058
mean	-4491072.427	±.043	3481527.849	±.025	2887391.635	±.041	937665.041	±.004	.048

Table IV-5. Analyzed Passes for SPORT—Simosato—Minamitori Sima—

	date (UT)			satellite	SHOLAS	HTLRS	total
1	1989	1	20 16 : 36—18 : 50	AJISAI	693	845	1539
2		2	14 10 : 18—12 : 33	AJISAI	2213	310	2524
3		2	15 9 : 25—11 : 39	AJISAI	703	334	1038
4		3	9 12 : 16—16 : 24	LAGEOS	300	791	1091

Table IV-6. Estimated station coordinates of Minamitori Sima and baseline length between Simosato and Minamitori Sima.

&lt;HYDRANGEA results&gt;

	x	y	z	baseline length	residual				
1 *	-5227189.507	±.085	2551881.121	±.250	2607610.396	±.159	2024874.049	±.017	.065
2	.992	±.018	2.236	±.037	09.716	±.040	.055	±.018	.076
3	.828	±.124	.211	±.170	.519	±.081	.040	±.035	.074
4	90.084	±.014	.381	±.089	.749	±.038	.022	±.039	.044
1.2.3.4	-5227189.853	±.110	2551881.987	±.291	2607609.845	±.191	2024874.042	±.007	.065
2.3.4	.968	±.075	2.276	±.053	.661	±.072	.039	±.010	.065

\* insufficient separation of parameters.



Table IV-7. Dynamical models and constants for LAGEOS orbit determination  
(assumed values or initially adopted values)

Light velocity	:	$c = 2.99792458 \times 10^8 \text{m/s}$
Atmospheric density at $h=5000 \text{ km}$	:	$\rho_o = 3.98 \times 10^{-9} \text{kg/km}^3$
Scale constant of the atmospheric density at $h=5000 \text{ km}$	:	$k = 1.61 \times 10^{-3} / \text{km}$
LAGEOS mass	:	$m = 407.0 \text{ kg}$
LAGEOS cross section area	:	$A_s = 0.283 \text{ m}^2$
LAGEOS reflectivity coefficient	:	$\gamma = 1.17$ (initially assumed)
LAGEOS atmospheric drag coefficient	:	$C_d = 3.8$ (initially assumed)
LAGEOS center of mass correction	:	$R_{CM} = -0.24 \text{ m}$
LAGEOS empirical along track acceleration	:	$\Delta\alpha = -2.9 \times 10^{-12} \text{m/s}^2$

for this estimation are tabulated in Table IV-7. The gravity field model used is the lower degrees and orders than  $(21 \times 21)$  of GEM-T1. The resulting geophysical parameters are :

<HYDRANGEA results>

$GM$ (geocentric constant of gravitation : GEM-T1)

$$= 398600.4453 \pm 0.0003 \text{km}^3/\text{s}^2$$

$J_2$ (dynamical form factor of the earth which does not include the permanent deformation)

$$= (1082.571 \pm 0.015) \times 10^{-6}$$

$\gamma$ (solar reflectivity coefficient of LAGEOS)

$$= 1.111 \pm 0.008$$

$\Delta\alpha$ (mean along track acceleration of LAGEOS)

$$= (-2.5 \pm 3.7) \times 10^{-12} \text{m/s}^2,$$

where error estimate of each parameter is given by standard deviation of the 8 estimates of arcs. The mean range residual (observed range minus range to the determined orbit : O-C) for normal point range data is 7.1cm. The earth rotation parameters and station coordinates for 16 sites are also solved with these geophysical parameters in this case. The values of SSC (CSR) 85L07 given by Tapley *et al.* [1985] are used for the station coordinates of several a priori fixed stations. The description of estimation of other parameters are given in the following sections.

The reflectivity coefficient of LAGEOS and mean along track acceleration are also estimated using 49,576 LAGEOS normal point data in 85 five-day-arcs from September 1983 to October 1984. The gravity field model used is the lower orders and degrees than  $(21 \times 21)$  of GEM-L2. The results obtained are :

<HYDRANGEA results>

$$\gamma = 1.121 \pm 0.01$$

$$\Delta\alpha = (-3.4 \pm 0.9) \times 10^{-12} \text{m/s}^2,$$

where error estimates are given by standard deviation of the 85 estimates of the arcs. The mean range residual for each normal point is 9.77cm. In this case only the earth rotation parameters with these parameters are estimated, but all the station coordinates are fixed as the station coordinates of the SSC (CSR) 85L07.

The estimation of geophysical parameters similarly to the case above is made by using LAGEOS raw data of 8 five-day-arcs with 87275 ranges from mid-September to late October in 1986 and of 9 five-day-arcs with 91634 ranges from early January to mid-April in 1988. The results are shown in

Table IV-8. The error estimates in the table are given by the standard deviation of each mean value derived from 8 and 9 estimates of respective arcs. The range residuals for the case of 1986 and 1988 are 5.3 and 4.7cm, respectively. The earth rotation parameters and station coordinates are also solved with these parameters as given later.

Some geophysical parameters of AJISAI can be also estimated. Since the altitude of AJISAI is 1500km, the effect of atmospheric drag is not so stable as that of LAGEOS. So, shorter arc than LAGEOS is better to estimate unknown parameters as reflectivity coefficient, along track acceleration and earth rotation parameters. On the other hand, sufficient number of data to determine the orbit and parameters are also necessary. Therefore the three-day-arcs are selected for the duration of computation of AJISAI in this case. Basic constants of AJISAI [Sasaki and Hashimoto 1987] are shown in Table IV-9.

Table IV-8. Geophysical parameters estimated by LAGEOS SLR  
— case of GEM-L2 gravity field used —  
<HYDRANGEA results>

	average of 8 arcs in 1986	average of 9 arcs in 1988	weighted mean
$GM$	$398600.44755 \pm 0.00059$	$398600.44811 \pm 0.00087$	$398600.44773 \text{ km}^3/\text{s}^2$
$J_2$	$(1082.532 \pm 0.031) \times 10^{-6}$	$(1082.657 \pm 0.021) \times 10^{-6}$	$1082.618 \times 10^{-6}$
$\gamma$	$1.144 \pm 0.015$	$1.129 \pm 0.026$	1.140
$\Delta\alpha$	$(-4.4 \pm 2.3) \times 10^{-12}$	$(-0.9 \pm 5.3) \times 10^{-12}$	$-3.8 \times 10^{-12} \text{ m/s}^2$

Table IV-9. Dynamical models and constants for AJISAI orbit determination  
(assumed values or initially adopted values)

Atmospheric density at $h=1500$ km	: $\rho_o = 3.55 \times 10^{-7} \text{ kg}/\text{km}^3$
Scale constant of the atmospheric density at $h=1500$ km	: $k = 1.73 \times 10^{-3}/\text{km}$
AJISAI mass	: $m = 685.2 \text{ kg}$
AJISAI cross section area	: $A_s = 3.631 \text{ m}^2$
AJISAI reflectivity coefficient	: $\gamma = 1.3$ (initially assumed)
AJISAI atmospheric drag coefficient	: $C_d = 3.8$ (initially assumed)
AJISAI empirical along track acceleration	: $\Delta\alpha = 0$
AJISAI center of mass correction	: $R_{CM} = -1.01 \text{ m}$

The AJISAI SLR data used are 136369 ranges in 35 three-day-arcs from August 16, 1986 at just after the launch of AJISAI to November 28, 1986. The gravity field model used is  $36 \times 36$  (full coefficients) of GEM-T1. The reflectivity coefficient ( $\gamma$ ) and atmospheric drag coefficient ( $C_d$ ) estimated are given in Table IV-10. The mean range residual is 18.2cm.

Table IV-10. Ballistic parameters of AJISAI estimated by SLR  
— case of GEM-T1 used —

	<HYDRANGEA results>
Reflectivity coeff. ( $\gamma$ )	: $1.01 \pm 0.07$
Atmospheric drag coeff. ( $C_d$ )	: $3.5 \pm 0.6$

## (2) Earth rotation parameters

The earth rotation parameters are estimated by using the LAGEOS SLR data. As a test, a

five-day-arc with 749 normal point data in the duration from 12h (UTC), October 8 to 12h (UTC) October 13, 1984 is used. The estimated parameters are the pole position  $(x_p, y_p)$ , the excess rotation per day (*ex. RPD* : minus sign of the excess length of day), reflectivity coefficient and along track acceleration. The input parameters for dynamical models and constants of LAGEOS are the same as given in the previous section. The resultant values for earth rotation parameters are :

<HYDRANGEA results>

$$(x_p, y_p) = (296.2 \pm 0.3 \text{milliarcsec} [= \text{mas}], 206.1 \pm 0.2 \text{mas}),$$

$$(\text{ex. RPD}) = (-1.80 \pm 0.02 \text{milliseconds of time/day} [= \text{ms/d}]).$$

Next, all the earth rotation parameters in the MERIT Campaign are estimated. The SLR data used are 49,576 LAGEOS normal point data of 85 five-day-arcs from September 1983 to October 1984. The gravity field used is GEM-L2 and the reference station coordinates adopted are SSC (CSR) 85 L 07 [Tapley *et al.* 1985]. The simultaneously estimated parameters are initial satellite position and velocity, pole position, excess rotation per day, reflectivity coefficient and along track acceleration. The mean residual for all the normal point data is 9.77cm and most of the internal errors for the derived pole positions and excess rotation per day are less than 0.5mas. The number of data used, range residual, resultant pole position, excess rotation per day, reflectivity coefficient and their standard deviations are given in Table IV-11. The resulting pole position and excess rotation per day are given in Figures IV-3 and IV-4. The result of the earth rotation parameters well coincides with ERP (CSR) 85 L 07. The mean systematic difference of this result from the result of ERP (CSR) 85 L 07 is  $(\delta x_p, \delta y_p, \delta \omega) = (-0.51 \text{milliarcseconds (mas)}, -0.13 \text{mas}, -0.87 \text{ms/d})$  and the standard deviation of each five-day-result is  $(\Delta x_p, \Delta y_p, \Delta \omega) = (\pm 1.1 \text{mas}, \pm 1.4 \text{mas}, \pm 0.42 \text{ms/d})$ .

The pole position of the earth is also solved by using worldwide AJISAI SLR data of three-day-arcs. The dynamical models, constants of AJISAI and SLR data used are the same as the case of the previous section. 136369 ranges in 35 three-day-arcs from mid-August to late-November in 1986 are used. The gravity field model used is full model of GEM-T1. The number of range data used and observed station, range residuals, resulting pole positions, reflectivity coefficients and their standard deviations for each arc are given in Table IV-12. The resultant pole position are shown in Figure IV-5 with VLBI results of IRIS [Campbell *et al.* 1987] for a reference in solid line.

### (3) Station coordinates

The geocentric station coordinates of the reference point of hardware of the SLR system in each observation station are also estimated. As the first case, the LAGEOS normal point data of 5965 ranges in the successive 8 five-day-arcs from late-September to early-November in 1984 are used. The solved for parameters are 61 unknowns of LAGEOS initial position and velocity,  $GM, J_2$ , reflectivity coefficient,  $\gamma$ , along track acceleration,  $\Delta \alpha$ , earth rotation parameters  $(x_p, y_p, \Delta \omega)$ , and three dimensional station coordinates for 16 sites,  $(U_i, V_i, W_i)$ ,  $i=1, 2, 3, \dots, 16$ . The gravity field model used is GEM-T1 of the lower degrees and orders than  $21 \times 21$ . The other parameters for dynamical models and constants of LAGEOS are the same as previous sections. The number of normal point data used and their observation station, mean range residuals are given in Table IV-13.

Since the pole position and excess rotation per day of the earth are also solved simultaneously with station coordinates, the longitude of one station and latitudes of two SLR stations, of which longitudes are expected to be different by around 90 degrees for good geometrical separation of station location and pole position, should be fixed numerically in principle in the procedure for each five-day-arc. However such numerically fixed and defining three stations which produce sufficient amount of

Table IV -11. Pole position and excess rotation per day (LAGEOS SLR)

-from September 1983 to October 1984-

&lt;HYDRANGEA results&gt; JHDERP-L1 [Sasaki]

UNITS : MILLI ARCSECOND(mas)FOR POLE POSITION AND MILLISECOND PER  
 DAY(ms/d)FOR EXCESS ROTATION PER DAY(ex-RPD=minus LOD)

DATE			M J D	RANGE			S I G M A				
y	m	d	d	DATA	RESIDUAL	Xp	Yp	ex-RPD	Xp	Yp	exRPD
				(npt)	cm	mas	mas	ms/d	mas	mas	ms/d
1983	SEP	7.56	45584.56	408	11.3	287.0	144.7	-1.69	0.5	0.7	0.03
1983	SEP	12.56	45589.56	333	9.1	273.1	125.7	-2.08	0.5	0.7	0.02
1983	SEP	16.74	45593.74	520	10.0	263.8	109.5	-1.86	0.4	0.6	0.02
1983	SEP	21.82	45598.82	495	11.1	249.2	94.0	-1.73	0.5	0.6	0.02
1983	SEP	27.50	45604.50	392	8.3	227.4	75.6	-2.20	0.4	0.5	0.02
1983	OCT	2.55	45609.55	263	10.7	208.2	60.9	-2.15	0.5	1.0	0.03
1983	OCT	6.60	45613.60	655	11.3	197.1	51.2	-2.24	0.4	0.5	0.02
1983	OCT	12.34	45619.34	555	9.2	176.7	37.7	-2.55	0.3	0.4	0.02
1983	OCT	16.94	45623.94	544	9.5	157.9	31.0	-2.03	0.4	0.5	0.01
1983	OCT	21.96	45628.96	529	9.9	137.2	24.1	-2.32	0.4	0.5	0.02
1983	OCT	27.21	45634.21	829	10.5	112.4	17.2	-2.67	0.3	0.4	0.02
1983	NOV	1.24	45639.24	559	10.5	89.4	12.1	-2.55	0.5	0.4	0.02
1983	NOV	6.19	45644.19	466	10.9	67.8	14.5	-2.89	0.6	0.5	0.02
1983	NOV	10.73	45648.73	559	11.3	45.5	11.8	-2.66	0.5	0.4	0.02
1983	NOV	16.40	45654.40	473	10.2	21.6	13.3	-2.39	0.4	0.5	0.03
1983	NOV	21.70	45659.70	460	16.0	-1.5	17.0	-2.66	0.7	0.6	0.03
1983	NOV	25.17	45663.17	299	9.2	-19.6	23.2	-2.38	0.5	0.5	0.03
1983	DEC	1.14	45669.14	424	12.0	-42.4	27.9	-2.08	0.5	0.6	0.02
1983	DEC	6.57	45674.57	473	10.1	-63.3	36.5	-2.33	0.4	0.4	0.03
1983	DEC	10.90	45678.90	426	11.9	-76.5	41.9	-2.02	0.5	0.5	0.02
1983	DEC	15.83	45683.83	392	13.1	-92.3	53.6	-2.06	0.6	0.5	0.03
1983	DEC	21.13	45689.13	345	10.0	-107.8	62.9	-2.24	0.5	0.5	0.03
1983	DEC	25.45	45693.45	221	9.0	-118.6	70.7	-2.17	0.5	0.7	0.03
1983	DEC	30.71	45698.71	366	7.6	-132.0	85.1	-2.22	0.4	0.4	0.02
1984	JAN	5.35	45704.35	380	9.5	-149.7	99.1	-2.32	0.6	0.5	0.03
1984	JAN	11.24	45710.24	385	6.3	-165.7	117.2	-1.69	0.4	0.3	0.03
1984	JAN	15.41	45714.41	440	10.0	-173.3	127.7	-1.66	0.4	0.4	0.02
1984	JAN	19.67	45718.67	530	11.1	-180.1	143.0	-1.90	0.4	0.4	0.03
1984	JAN	25.77	45724.77	620	7.6	-197.1	164.5	-1.34	0.3	0.4	0.02
1984	JAN	30.18	45729.18	381	7.5	-205.1	179.0	-1.62	0.4	0.5	0.02
1984	FEB	3.23	45733.23	267	7.3	-210.6	191.6	-1.60	0.7	0.8	0.03
1984	FEB	9.01	45739.01	628	7.9	-223.7	209.7	-1.73	0.4	0.4	0.02
1984	FEB	14.05	45744.05	313	9.5	-230.9	223.9	-2.08	0.5	0.6	0.04
1984	FEB	19.15	45749.15	456	11.9	-235.5	242.7	-1.63	0.5	0.5	0.03
1984	FEB	23.60	45753.60	397	11.7	-239.9	259.1	-1.69	0.7	0.5	0.03
1984	FEB	29.49	45759.49	476	12.4	-243.8	282.6	-2.02	0.5	0.5	0.03
1984	MAR	4.55	45763.55	281	10.6	-247.9	300.3	-1.84	0.6	0.5	0.04
1984	MAR	9.74	45768.74	289	10.0	-248.6	319.7	-2.07	0.5	0.6	0.04
1984	MAR	14.58	45773.58	329	13.3	-242.9	342.1	-2.05	0.6	0.9	0.04
1984	MAR	20.77	45779.77	442	11.7	-233.5	368.6	-1.86	0.5	0.5	0.05
1984	MAR	24.78	45783.78	425	11.6	-232.6	382.5	-2.17	0.5	0.5	0.04
1984	MAR	29.79	45788.79	512	8.5	-222.3	401.4	-2.30	0.3	0.4	0.03
1984	APR	4.39	45794.39	447	9.8	-210.8	420.1	-1.79	0.5	0.6	0.02
1984	APR	8.81	45798.81	524	8.8	-196.6	437.3	-2.11	0.4	0.4	0.02
1984	APR	14.31	45804.31	824	10.1	-182.6	459.0	-2.12	0.3	0.4	0.02

Table IV —11. Pole position and excess rotation per day(LAGEOS SLR)

—from September 1983 to October 1984—

JHDERP-L1 [Sasaki]

(continued)

UNITS : MILLI ARCSECOND(mas)FOR POLE POSITION AND MILLI SECOND PER  
DAY(ms/d)FOR EXCESS ROTATION PER DAY(exRPD)

D A T E			M J D	DATA	RANGE RESIDUAL	Xp	Yp	exRPD	S I G M A		
y	m	d	d	(npt)	cm	mas	mas	ms/d	mas	mas	ms/d
1984	APR	18.80	45808.80	578	10.5	-170.6	473.2	-1.87	0.5	0.5	0.03
1984	APR	24.82	45814.82	791	10.0	-154.8	490.7	-2.25	0.3	0.3	0.02
1984	APR	28.37	45818.37	658	10.8	-142.9	501.2	-1.83	0.4	0.4	0.02
1984	MAY	3.99	45823.99	607	10.1	-121.5	511.4	-2.08	0.4	0.3	0.02
1984	MAY	8.91	45828.91	577	8.5	-102.3	529.2	-1.83	0.3	0.3	0.02
1984	MAY	14.61	45834.61	582	10.5	-84.4	540.2	-1.43	0.4	0.3	0.02
1984	MAY	19.03	45839.03	896	9.0	-67.9	545.5	-1.62	0.3	0.3	0.01
1984	MAY	24.01	45844.01	1086	9.3	-48.8	552.2	-1.45	0.3	0.2	0.01
1984	MAY	30.02	45850.02	646	8.5	-22.7	556.7	-1.15	0.3	0.3	0.02
1984	JUN	2.84	45853.84	1014	8.5	-4.6	559.1	-1.55	0.2	0.2	0.01
1984	JUN	8.24	45859.24	689	9.9	19.4	556.5	-1.16	0.4	0.3	0.02
1984	JUN	13.18	45864.18	759	10.3	40.0	556.4	-1.13	0.4	0.3	0.02
1984	JUN	18.27	45869.27	818	8.0	60.2	554.1	-1.23	0.2	0.2	0.01
1984	JUN	22.79	45873.79	503	9.6	78.4	552.1	-0.94	0.4	0.4	0.03
1984	JUN	27.87	45878.87	868	9.8	98.9	546.6	-1.03	0.3	0.3	0.02
1984	JUL	3.24	45884.24	451	7.3	125.7	540.6	-0.69	0.3	0.4	0.02
1984	JUL	8.24	45889.19	594	7.8	145.3	531.2	-0.36	0.3	0.3	0.02
1984	JUL	12.48	45893.48	651	8.2	161.9	520.0	-0.77	0.3	0.3	0.03
1984	JUL	18.57	45899.57	581	7.5	183.7	504.2	-0.75	0.3	0.3	0.02
1984	JUL	23.25	45904.25	623	8.5	202.3	493.2	-0.14	0.4	0.3	0.02
1984	JUL	27.97	45908.97	563	10.5	218.3	479.4	-0.97	0.4	0.4	0.03
1984	AUG	2.07	45914.07	968	10.8	237.2	464.8	-1.53	0.3	0.3	0.02
1984	AUG	7.92	45919.92	706	8.1	255.9	446.4	-0.91	0.3	0.3	0.02
1984	AUG	12.03	45924.03	735	7.1	268.5	432.5	-1.29	0.2	0.2	0.01
1984	AUG	16.65	45928.65	710	7.4	280.5	417.7	-1.16	0.3	0.2	0.02
1984	AUG	22.35	45934.35	1016	8.3	291.6	396.5	-1.33	0.3	0.2	0.02
1984	AUG	27.45	45939.45	729	9.9	294.4	374.2	-1.49	0.4	0.3	0.02
1984	AUG	31.80	45943.80	855	10.1	297.2	360.1	-1.26	0.4	0.3	0.02
1984	SEP	6.05	45949.05	786	9.8	300.8	340.1	-1.53	0.3	0.3	0.02
1984	SEP	11.73	45954.73	772	7.6	304.4	317.5	-1.42	0.3	0.2	0.01
1984	SEP	15.94	45958.94	617	10.1	306.6	299.9	-1.36	0.4	0.3	0.02
1984	SEP	21.00	45964.00	899	9.5	310.1	280.5	-1.71	0.3	0.2	0.02
1984	SEP	26.00	45969.26	841	9.5	310.7	259.9	-1.58	0.3	0.3	0.02
1984	OCT	1.57	45974.57	569	8.5	308.9	241.3	-1.84	0.3	0.3	0.02
1984	OCT	5.51	45978.51	623	9.2	304.0	225.2	-1.97	0.4	0.3	0.02
1984	OCT	10.71	45983.71	750	9.2	296.4	204.9	-1.57	0.4	0.3	0.02
1984	OCT	16.37	45989.37	821	10.6	286.6	186.2	-1.56	0.3	0.3	0.02
1984	OCT	20.57	45993.57	639	10.7	281.0	173.2	-1.85	0.4	0.3	0.02
1984	OCT	25.71	45998.71	821	11.2	273.8	157.5	-1.48	0.3	0.3	0.02
1984	OCT	31.31	46004.31	901	9.0	259.3	138.8	-1.75	0.3	0.2	0.02

(mean 9.77cm)

Pole Position (HYDRANGEA) LAGEOS 5-day-arcs

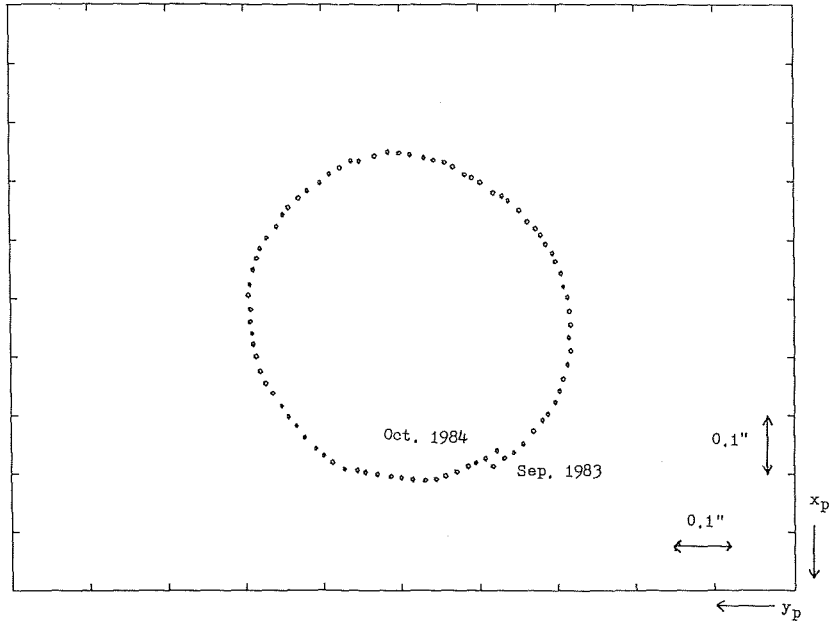


Figure IV - 3. Pole position derived from LAGEOS SLR data by using HYDRANGEA.

Excess Rotation per Day (HYDRANGEA) LAGEOS 5-day-arcs

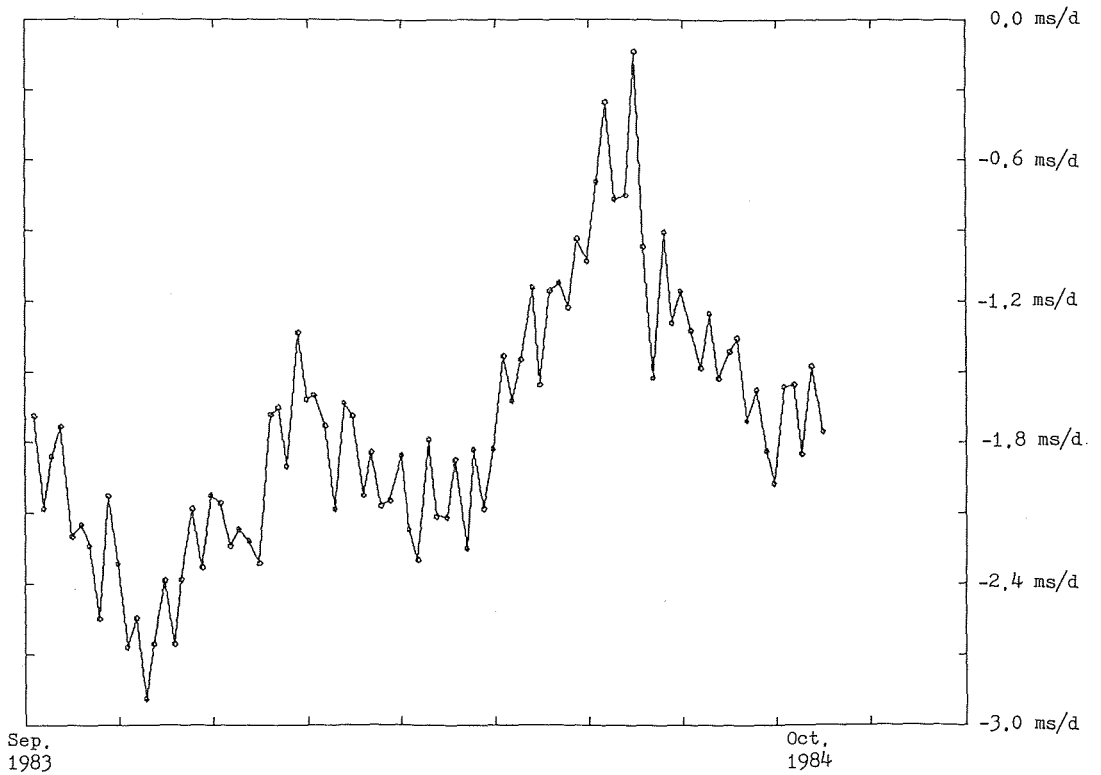


Figure IV - 4. Excess rotation per day derived from LAGEOS SLR data by using HYDRANGEA.

Table IV -12. Pole position and reflectivity coefficients derived from AJISAI three-day-arcs  
 —from August 1986 to November 1986—

<HYDRANGEA results> JHDERP-A1 [Sasaki]

UNITS : MILLIARCSECOND(mas)FOR POLE POSITION

DATE			MJD	DATA STN (RAW)	RANGE RESID.	Xp	Yp	$\gamma$	SIGMA		
y	m	d	d		cm	mas	mas		Xp	Yp	$\gamma$
1986	AUG	17.10	46659.10	2780 6	13.0	4.7	400.1	-0.476	0.4	0.5	0.018
1986	AUG	20.07	46662.07	9846 8	26.7	-8.3	379.6	0.726	0.3	0.3	0.005
1986	AUG	22.33	46664.33	3293 6	11.7	11.3	389.1	0.752	0.6	0.9	0.009
1986	AUG	26.77	46668.77	2499 10	17.4	11.4	387.8	1.078	0.4	0.4	0.005
1986	AUG	29.28	46671.26	4100 9	18.2	9.5	392.9	0.944	0.4	0.3	0.003
1986	SEP	1.72	46674.72	1744 6	17.3	18.3	393.6	0.930	0.6	0.5	0.005
1986	SEP	4.23	46677.23	8946 10	26.0	19.7	394.2	1.016	0.3	0.2	0.002
1986	SEP	7.81	46680.81	3877 11	28.5	17.3	397.8	0.904	0.6	0.6	0.004
1986	SEP	10.97	46683.97	6666 8	23.9	35.6	397.0	0.958	0.4	0.3	0.003
1986	SEP	12.76	46685.76	854 6	8.9	43.3	393.9	0.902	0.7	0.7	0.005
1986	SEP	15.81	46688.81	965 6	9.7	61.8	411.9	1.566	1.3	1.4	0.048
1986	SEP	19.32	46692.32	2457 5	18.4	47.0	394.5	1.090	0.5	0.5	0.003
1986	SEP	22.85	46695.85	4435 8	20.6	34.9	399.5	1.001	0.4	0.3	0.004
1986	SEP	25.72	46698.72	7742 12	23.9	43.6	393.8	1.029	0.3	0.3	0.002
1986	SEP	28.35	46701.35	2929 6	17.1	65.0	383.0	1.222	0.4	0.3	0.006
1986	OCT	1.50	46704.50	2889 8	19.8	56.0	378.5	1.105	0.5	0.4	0.004
1986	OCT	3.55	46706.55	2579 6	16.8	51.1	393.5	0.773	0.6	0.5	0.027
1986	OCT	7.84	46710.84	7253 10	15.7	56.1	393.2	0.970	0.3	0.2	0.002
1986	OCT	10.43	46713.43	4009 9	15.8	54.9	390.8	1.032	0.4	0.3	0.002
1986	OCT	13.89	46716.89	4367 9	23.0	72.0	392.0	0.940	0.4	0.3	0.004
1986	OCT	16.74	46719.74	5059 11	29.7	75.3	391.9	0.924	0.5	0.3	0.004
1986	OCT	20.06	46723.06	2167 7	14.7	80.6	383.0	0.970	0.5	0.3	0.003
1986	OCT	22.69	46725.69	4380 9	17.3	82.7	387.0	1.139	0.3	0.2	0.002
1986	OCT	25.05	46728.05	3933 7	11.5	85.0	377.1	1.107	0.3	0.5	0.003
1986	OCT	28.18	46731.18	3643 8	19.1	86.0	378.0	1.112	0.4	0.4	0.003
1986	OCT	30.07	46733.07	1558 5	13.6	104.0	386.4	1.076	0.6	0.4	0.008
1986	NOV	3.16	46737.16	4873 11	30.2	101.8	368.3	0.982	0.5	0.4	0.003
1986	NOV	6.16	46740.16	3806 10	21.1	106.2	361.1	0.913	0.5	0.4	0.003
1986	NOV	9.59	46743.59	2740 10	15.9	101.8	371.3	1.063	0.3	0.3	0.003
1986	NOV	11.78	46745.78	4275 11	22.7	107.9	381.4	0.977	0.4	0.4	0.005
1986	NOV	15.04	46749.04	3509 7	11.1	111.0	367.5	0.894	0.3	0.2	0.008
1986	NOV	17.54	46751.54	2622 10	19.8	104.3	357.8	1.057	0.6	0.4	0.004
1986	NOV	21.43	46755.43	2401 8	16.1	116.0	355.6	0.998	0.4	0.3	0.005
1986	NOV	24.62	46758.62	2734 9	13.9	119.2	353.9	1.055	0.4	0.3	0.003
1986	NOV	26.94	46760.94	4886 11	19.0	120.9	348.2	1.020	0.3	0.3	0.002

( mean 18.2 cm )

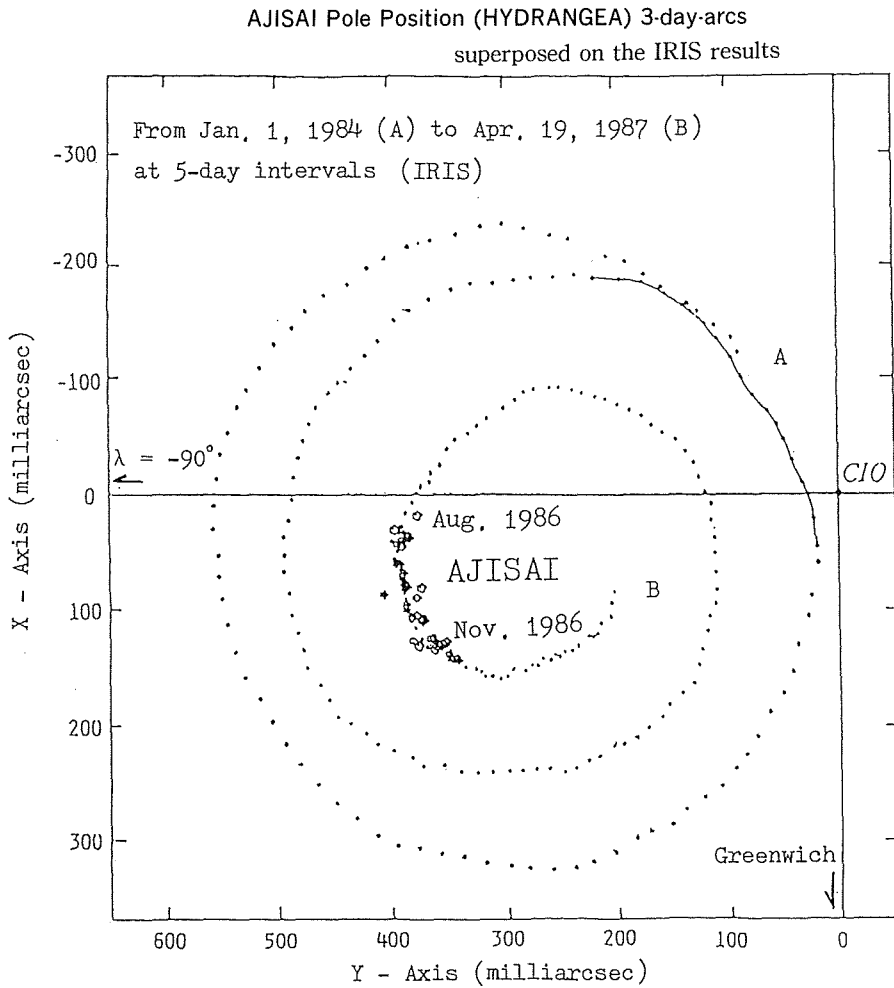


Figure IV — 5. Pole position derived from AJISAI SLR data by using HYDRANGEA.

Table IV—13. Data table for JHDSC-2 and range residuals  
<HYDRANGEA results>

mean	date	MJD	station number	ranges (normal point)	rms
1984		244			cm
SEP	26.26	5969.26	10	841	7.3
OCT	1.53	5974.53	12	569	5.6
OCT	5.51	5978.51	13	623	5.9
OCT	10.71	5983.71	16	750	6.8
OCT	16.37	5989.37	12	821	7.8
OCT	20.57	5993.57	13	639	7.2
OCT	25.71	5998.71	13	821	8.9
OCT	31.31	6004.31	12	901	6.9
(total/mean)				5965	7.1



SLR data for determination of unknown parameters in every five-day-arcs can not be selected from the station file because no station can obtain ideally sufficient SLR data for every five-day-arcs owing to weather- and operational conditions. Therefore the four major station coordinates of Yaragadee, in Australia (station ID 7090), Quincy, California (7109), Wettzell, West Germany (7834) and Matera, Italy (7939) are fixed to construct the frame of the geocentric coordinate system to make coincide with LSC (CSR) 85 L 07, (which was defined for the mean time of a half year before the epoch date of this estimation), as an original reference. Several station coordinates, of which numbers of ranges observed in the 40 days are small, are also fixed and the coordinates of 15 stations (16th station (Platteville, Colorado) has no sufficient data) are solved freely. The fixed station coordinates with a mark of "0" and the solved for stations with "1" for the first column are tabulated in Table IV-14. The resulting station coordinates named as JHDSC-2 (L84) are given in Table IV-15.

Table IV -15. JHD SLR station coordinate set 2 (JHDSC-2) for 1984. 80

&lt;HYDRANGEA results&gt;

STATION ID	U	V	W	SU	SV	SW	DU	DV	DW
	(diff. from LSC(CSR)8507)								
	m	m	m	mm	mm	mm	mm	mm	mm
FRF105 7105	1130720.328	-4831352.954	3994108.568	28	32	55	+45	+59	-73
MNPEAK 7110	-2386279.158	-4802356.889	3444883.211	14	6	13	-15	+9	0
HUAHIN 7121	-5345868.277	-2958248.487	-1824625.026	14	14	25	-30	+97	-63
MAZTLN 7122	-1660090.188	-5619103.211	2511639.243	16	21	19	+37	-6	+22
HOLLAS 7210	-5466007.043	-2404428.299	2242188.416	24	9	29	-13	-2	+5
METFIN 7805	2892595.259	1311808.051	5512609.850	468	347	307	+80	-125	-87
ZIMERW 7810	4331283.534	567549.240	4633140.238	18	41	18	+14	-1	+1
GRASSE 7835	4581691.869	556159.276	4389359.474	32	13	11	+59	-23	+29
SHANHI 7837	-2831087.666	4676203.584	3275172.901	43	24	43	+96	-69	+160
SIMOST 7838	-3822388.330	3699363.577	3507573.186	27	40	29	-31	+46	+39
GRAZ 7839	4194426.797	1162693.822	4647246.852	41	60	61	+5	-7	+196
RGO 7840	4033463.840	23662.263	4924305.153	18	11	14	-28	+23	+12
ORRLR 7843	-4446476.890	2678127.310	-3696252.010	35	26	43	-56	-74	+101
QUINC3 78863	-2517244.864	-4198552.155	4076572.977	17	7	12	+22	+5	+16
AREQPA 7907	1942791.901	-5804077.812	-1796919.276	30	35	38	-33	+9	-5

\* averaged values of eight 5 day arcs

\* the values above are for the reference point of each SLR hardware

\* other derived parameters:  $(X, Y, Z, V_x, V_y, V_z)$ ,  $(x_p, y_p, ex-RPD)$ ,  $GM: 398600.4453 \pm 0.0003 \text{ km}^3/\text{s}^2$ , reflectivity coeff. :  $1.111 \pm 0.008$ , mean empirical acceleration:  $-2.5 \times 10^{-12} \text{ m/s}^2$

Table IV —14. An input file for estimation of station coordinates  
 [after Tapley *et al.* 1986, SSC (CSR)85L07]  
 (averaged epoch:1984. 25)

"0" in the first column means fixed station,

"1" in the first column means free adjustment station

0	1	1181	3800.62133980	882.00530920	5028.85973880
0	2	7062	-2428.82645109	-4799.75197452	3417.27267390
0	3	7082	-1735.99714938	-4425.05163362	4241.43222929
0	4	7086	-1330.12100349	-5328.53225482	3236.14692650
0	5	7090	-2389.00748085	5043.33186767	-3078.52712417
1	6	7105	1130.72028300	-4831.35301273	3994.10864126
0	7	7109	-2517.23599413	-4198.55833712	4076.57182528
1	8	7110	-2386.27914274	-4802.35687951	3444.88321147
1	9	7112	-1240.67891517	-4720.46591694	4094.48299310
1	10	7121	-5345.86824739	-2958.24858418	-1824.62496221
1	11	7122	-1660.09022497	-5619.10321667	2511.63922112
1	12	7210	-5466.00703029	-2404.42829680	2242.18841078
0	13	7220	-2386.29249008	-4802.34964553	3444.88389930
0	14	7265	-2356.47824914	-4646.61993915	3668.42728893
0	15	7400	1769.70037043	-5044.61486135	-3468.26315879
0	16	7401	1815.51795893	-5213.46688609	-3188.00239597
0	17	7599	4075.51748510	931.75404810	4801.63040520
1	18	7805	2892.59517860	1311.80817580	5512.60993670
1	19	7810	4331.28351980	567.54924120	4633.14023710
0	20	7831	4728.28301690	2879.66963200	3156.89419850
0	21	7833	3899.22428920	396.74280480	5015.07400130
0	22	7834	4075.53018840	931.78123020	4801.61839170
1	23	7835	4581.69191040	556.15929930	4389.35944520
1	24	7837	-2831.08756980	4676.20365280	3275.17274110
1	25	7838	-3822.38829880	3699.36353070	3507.57314720
1	26	7839	4194.42679160	1162.69382910	4647.24665570
1	27	7840	4033.46386750	23.66224000	4924.30514080
1	28	7843	-4446.47694560	2678.12738440	-3696.25211100
0	29	7882	-1997.24221570	-5528.04259884	2468.35586606
0	30	78861	-2517.24252593	-4198.55420953	4076.57228296
0	31	78862	-2517.24253049	-4198.55420352	4076.57227541
1	32	78863	-2517.24484244	-4198.55214964	4076.57296010
1	33	7907	1942.79193440	-5804.07782100	-1796.91927060
0	34	7935	-3910.42362630	3376.35799700	3729.23900670
0	35	7939	4641.96518490	1393.06984770	4133.26234580
0	36	7940	4595.21695840	2039.46449720	3912.61323340
0	37	8833	3899.23788300	396.76913070	5015.05538700

The mean internal error of the station coordinates for 14 stations determined except a Finland station (Metsahovi) with much larger range residuals than other stations is (2.6cm, 2.4cm, 2.9cm). A comparison with the original SSC (CSR) 85L07 for the same 14 stations gives good coincidence as (+0.5cm, +0.5cm, +3.1cm) for the systematic difference of the coordinates and as (3.4cm, 3.1cm, 5.1cm) for the mean individual difference. The internal error is very small despite of the derived results from averaging of 8 five-day-arcs. A part of the reason of the external difference from original SSC (CSR) 85L07 might be explained by the half year difference of epoch of time of determination. These facts show a semi-long arc method as such five-day-arcs is powerful to determine dynamical parameters well because there is usually no large dynamical error owing to short duration of integration as five days, and mean range residual is kept small in a five-day-arcs.

As for the station coordinates of the Simosato Hydrographic Observatory, the resulting value of the reference point of the fixed SLR system is ;

<HYDRANGEA results>

SIMOSATO ( $-3822388.330 \pm 0.027\text{m}$ ,  $3677363.822 \pm 0.040\text{m}$ ,  $3507573.186 \pm 0.029\text{m}$ ) [JHDSC-2 (L84)]  
 or  $+33^{\circ} 34^{\text{M}} 39.6994^{\text{S}}$  (Lat.),  $135^{\circ} 56^{\text{M}} 13.3384^{\text{S}}$  (Lon.),  $101.652\text{m(H)}$  (semi-major axis =  $6378137.0\text{m}$ , flattening =  $1/298.257$ ).

On the other hand, the surveyed coordinates for the same point referring to the Tokyo Datum is

$+33^{\circ} 34^{\text{M}} 27.496^{\text{S}}$  (Lat.),  $135^{\circ} 56^{\text{M}} 23.537^{\text{S}}$  (Lon.),  $62.44\text{m (H)}$ .

The geoid height of the Tokyo Datum at Simosato area is estimated as 0 meter by using a geoid map of Ganeko [1977]. The three dimensional coordinates of the reference point are calculated and therefore the interrelation of the global geocentric coordinates, JHDSC-2 and the Tokyo Datum is given as

<HYDRANGEA results>

$$U_{\text{JHDSC2}} - U_{\text{TOKYO}} = -146.28\text{m},$$

$$V_{\text{JHDSC2}} - V_{\text{TOKYO}} = +507.56\text{m},$$

$$W_{\text{JHDSC2}} - W_{\text{TOKYO}} = +681.87\text{m}.$$

The similar procedures are made for 8 five-day-arcs of LAGEOS in mid-1986 and 9 five-day-arcs of LAGEOS in early-1988 by using not the normal point data but raw range data. The 61 solved-for parameters are the same as previous case. However the earth gravity field model is GEM-L2 in these case. Other dynamical models and constants of LAGEOS are the same. The date of the central point of each duration of arc, raw range data used, number of stations involved in the data used, range residuals for determined orbit are given in Table IV-16 for the year 1986 and Table IV-17 for the year 1988. Total numbers of range data and mean range residuals are 87275, 5.3cm for 1986 and 91634, 4.7cm for 1988, respectively. The fixed stations are the same as previous case but the station positions are slightly shifted by using the plate motion model of AM0-2 given by Minster and Jordan [1978]. The calculation procedure is given by a subroutine supplied by Minster [1988] in IERS Standards [McCarthy *et al.* 1988]. The resulting station coordinates are named JHDSC-3 and JHDSC-4 and are given in Table IV-18 and Table IV-19, respectively.

The determination of the baseline length for Simosato-Titi Sima by using not short arcs but semi-long arc of a five-day-arc of worldwide LAGEOS SLR data is made. The number of solved-for unknowns are 61 and three dimensional station coordinates of Simosato and Titi Sima are simultaneously solved as unknown parameters. Only one set of five-day-arc can be used to determine the both station coordinates because of insufficient number of data. The duration of the one arc is from 12th to 16th of

Table IV—16. Data table for JHDSC-3 and range residuals  
 <HYDRANGEA results>

	mean	date	MJD	station number	ranges (raw data)	rms
1986			244			cm
	SEP	17.37	6690.37	10	9033	4.0
	SEP	23.98	6696.98	11	8462	5.0
	SEP	29.32	6702.32	13	7665	7.8
	OCT	2.72	6705.72	13	11046	5.1
	OCT	8.51	6711.51	12	6062	5.1
	OCT	14.25	6717.25	13	16561	4.3
	OCT	18.16	6721.16	12	14436	6.2
	OCT	22.88	6725.88	10	14010	4.5
	(total/mean)				87275	5.3

Table IV—17. Data table for JHDSC-4 and range residuals  
 <HYDRANGEA results>

	mean	date	MJD	station number	ranges (raw data)	rms
1988			244			cm
	JAN	12.58	7172.58	14	11638	3.9
	JAN	19.33	7179.33	10	3887	4.0
	JAN	25.73	7185.73	14	9865	5.1
	JAN	30.75	7190.75	11	9391	4.1
	FEB	4.21	7195.21	11	17370	5.2
	FEB	9.77	7200.77	11	12228	5.3
	FEB	14.11	7205.11	12	12817	7.0
	FEB	18.96	7209.96	12	9885	3.1
	APR	13.01	7264.01	9	4553	4.3
	(total/mean)				91634	4.7

Table IV—18. JHD SLR station coordinate set 3 (JHDSC-3) for 1986.76

〈HYDRANGEA results〉

STATION	ID	U	V	W	SU	SV	SW
		m	m	m	mm	mm	mm
GRF105	7105	1130720.392	-4831353.012	3994108.478	46	30	60
MNPEAK	7110	-2386279.216	-4802356.794	3444883.240	27	18	21
MAZTLN	7122	-1660090.204	-5619103.192	2511639.131	53	24	40
HOLLAS	7210	-5466007.001	-2404428.137	2242188.454	47	69	46
SIMOST	7838	-3822388.362	3699363.594	3507573.190	31	48	44
GRAZ	7839	4194426.800	1162693.823	4647246.696	28	66	39
RGO	7840	4033463.875	23662.353	4924305.137	42	71	47
AREQPA	7907	1942791.795	-5804077.799	-1796919.213	35	38	48

\* averaged values of eight 5 day arcs

\* the values above are for the reference point of each SLR hardware

\* other derived parameters : (X, Y, Z, V<sub>x</sub>, V<sub>y</sub>, V<sub>z</sub>), (x<sub>p</sub>, y<sub>p</sub>, ex-RPD), GM : 398600.4475 ± 0.0005 km<sup>3</sup>/s<sup>2</sup>, J<sub>2</sub> : (1082.532 ± 0.03) × 10<sup>-6</sup>, reflectivity coeff. : 1.144 ± 0.015, mean empirical acceleration : (-4.4 ± 2.3) × 10<sup>-12</sup> m/s<sup>2</sup>

Table IV—19. JHD SLR station coordinate set 4 (JHDSC-4) for 1988.11

〈HYDRANGEA results〉

STATION	ID	U	V	W	SU	SV	SW
		m	m	m	mm	mm	mm
GRF105	7105	1130720.259	-4831353.100	3994108.475	70	49	70
MNPEAK	7110	-2386279.222	-4802356.792	3444883.277	22	32	25
MAZTLN	7122	-1660090.255	-5619103.286	2511639.256	20	25	27
HOLLAS	7210	-5466007.127	-2404427.947	2242188.711	17	37	50
GRASSE	7835	4581691.850	556159.423	4389359.610	47	34	59
SIMOST	7838	-3822388.307	3699363.540	3507573.232	21	60	50
GRAZ	7839	4194426.760	1162693.831	4647246.703	20	15	21
RGO	7840	4033463.833	23662.357	4924305.282	28	36	34

\* averaged values of nine 5 day arcs

\* the values above are for the reference point of each SLR hardware

\* other derived parameters : (X, Y, Z, V<sub>x</sub>, V<sub>y</sub>, V<sub>z</sub>), (x<sub>p</sub>, y<sub>p</sub>, ex-RPD), GM : 398600.4481 ± 0.0009 km<sup>3</sup>/s<sup>2</sup>, J<sub>2</sub> : (1082.657 ± 0.02) × 10<sup>-6</sup>, reflectivity coeff. : 1.129 ± 0.026, mean empirical acceleration : (-0.9 ± 5.3) × 10<sup>-12</sup> m/s<sup>2</sup>

Table IV—20. Station coordinates of Simosato and Titi Sima and

baseline length between them      〈HYDRANGEA results〉

— case of a five-day-arc —

arc date    1988 FEB 12-16

Simosato			Titi Sima		
U	V	W	U	V	W
m	m	m	m	m	m
-3822388.250	3699363.676	3507573.084	-4491072.572	3481528.024	2887391.731
±0.011	±0.011	±0.016	±0.009	±0.009	±0.009
Simosato-Titi Sima baseline length : 937665.185 m					

February 1988. The parameters simultaneously determined are  $GM$ ,  $J_2$ , reflectivity coefficient, earth rotation parameters, along track acceleration and 16 unknown stations as same as described for estimation of JHDSC-4. The SLR data used are 154 of Simosato, 847 of Titi Sima and 13762 in total of 13 stations for the arc from Feb. 12 to 16th. The mean range residuals for SLR data of Simosato, Titi Sima and all stations are 10.9cm, 5.2cm and 6.8cm, respectively. The determined coordinates of both sites and baseline length are given in Table IV-20.

#### (4) Changes of baseline lengths and plate motions

As described in the previous section, the station coordinate estimation by using continuous 8 five-day-arcs from late-September to early-November of 1984 determined good U-, V- and W-components in several centimeters level for 14 stations.

The baseline lengths between any two stations of these stations and four major fixed stations of Yaragadee, Quincy, Wettzell and Matera are to be determined in the precision of several centimeters level. Even if some of these stations have errors for vertical (height) direction, the horizontal component, especially baseline lengths, can be determined well. Similar to the station coordinate determination for mid-1984, baseline determination can be done for the results derived by 8 five-day-arcs in mid-1986 and also for the results derived by 9 five-day-arcs in early 1988. There are many common baselines. However several station coordinates can not be determined well because of insufficient amount of SLR data. There are also some unstable stations for their station coordinates. At these stations there might be changes of their hardware systems, displacements of hardware or local crustal movements. The number of data is also not sufficient to estimate every baselines. Therefore stable stations as Monument Peak (International station ID : 7110) in California which is estimated to be on the Pacific plate, Hollas (7210) at Hawaii on the Pacific plate, Simosato (7838) at south edge of Kii Peninsula which is estimated to be on the Eurasian plate are selected as stations of completely free adjustment. The changes of baseline lengths between one of these free adjustment stations and one of fixed stations are also considered.

Before to consider a baseline length between two SLR stations, the angle which is made by two lines from the geocenter to a station and from the geocenter to another station is considered. If the angle is multiplied by a mean earth radius, the value expresses length of arc on the mean radius of the earth. As the amount of change of baseline length is a little more than 10cm level per year at most, the difference of the length of the arc above coincides with the change of the baseline length on a reference ellipsoid in sufficient precision. So, we only consider the change of the angles or length of arc on mean radius of the earth made by two lines from geocenter to a station and geocenter to another station for each pair of two observation stations.

The three epochs of station coordinate determinations in 1984, 1986 and 1988 are 1984.80, 1986.76 and 1988.11 and each time intervals from 1984 are 1.96 years and 3.31 years. The arc lengths between any of two stations freely determined and also arc lengths between a station freely determined and a fixed station are calculated for each year of 1984.80, 1986.76 and 1988.11.

To estimate yearly change of each arc length, the addition of the value of subtraction as the arc length for the year of 1986.76 minus the arc length for the year of 1984.80 and the other value of subtraction as the arc length for the year of 1988.11 minus the arc length for the year of 1984.80 is divided by the total years, 5.27. This is equivalent to give a constant error to measurements of any length of baseline, or in the other words, the weight for the measurement of yearly change rate of baseline length is proportional to the measurement interval.

The derived results are shown in Figures IV-6, IV-7 and IV-8 as followings : the amounts of arc

LAGEOS SLR PLATE MOTIONS (HYDRANGEA RESULTS) ... 1 ...

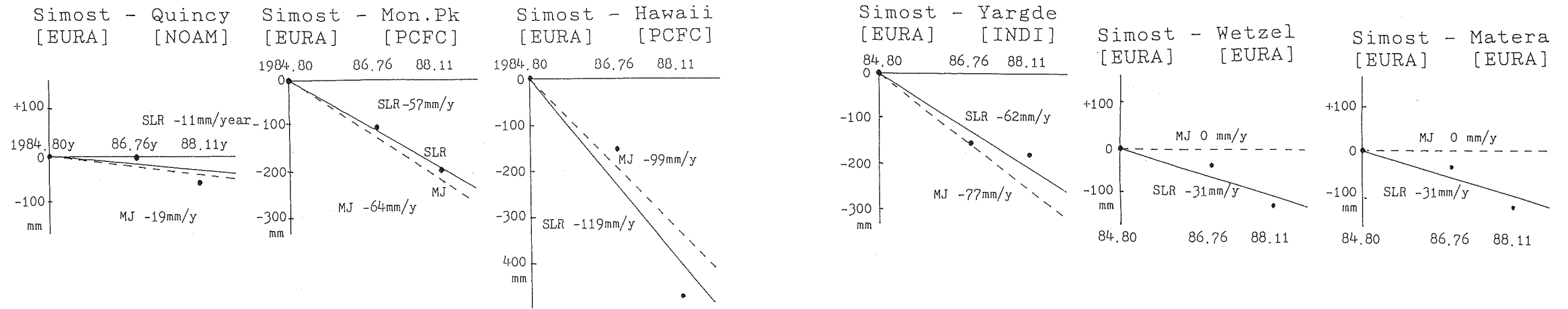


Figure IV - 6. Plate motions derived from LAGEOS SLR data by using HYDRANGEA(1).

LAGEOS SLR PLATE MOTIONS (HYDRANGEA RESULTS) ... 2 ...

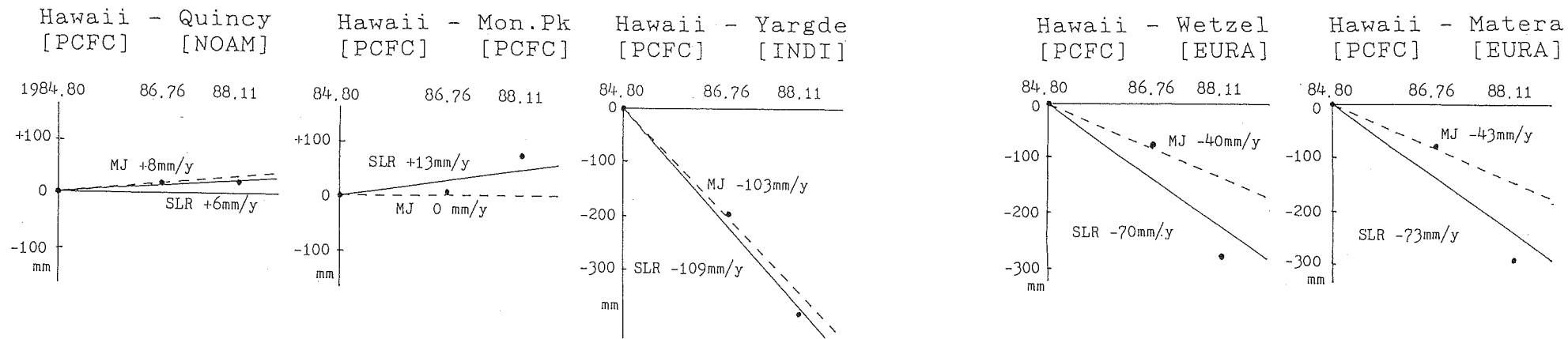


Figure IV - 7. Plate motions derived from LAGEOS SLR data by using HYDRANGEA(2).

LAGEOS SLR PLATE MOTIONS (HYDRANGEA RESULTS) ... 3 ...

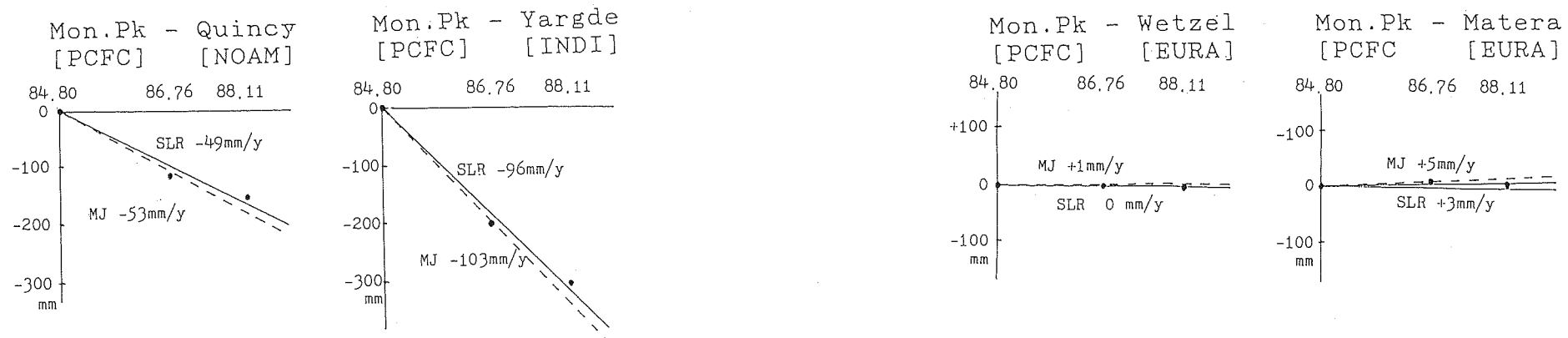


Figure IV - 8. Plate motions derived from LAGEOS SLR data by using HYDRANGEA(3).

length changes from 1984.80 to 1986.76 and from 1984.80 to 1988.11 are shown in two dots for each arc line ; the weighted yearly change rate is shown for each arc by a solid line and a value with "SLR" ; the calculated value of the AM0-2 model for each arc is given by a broken line and a value with "MJ" for comparison. These changes of arc lengths in the Figures indicate plate motions.

The results of yearly change of each arc length, namely the derived plate motions, are tabulated with the AM0-2 plate motions of Minster and Jordan [1978] in Table IV-21 as JHDPMTN-1 and also the results are shown on the worldwide map in Figure IV-9.

Table IV-21. JHD SLR derived plate motions 1 (JHDPMTN-1) from 1984, 80 to 1988, 11  
<HYDRANGEA results>

				JHD <HYDRANGEA>	M/J
				mm/y	mm/y
Simost	[EURA]	— Quincy	[NOAM]	-11	-19
Simost	[EURA]	— Mon. Pk	[PCFC]	-57	-64
Simost	[EURA]	— Hawaii	[PCFC]	-119	-99
Simost	[EURA]	— Yargde	[INDI]	-62	-77
Simost	[EURA]	— Wetzel	[EURA]	-31	0
Simost	[EURA]	— Matera	[EURA]	-31	0
Hawaii	[PCFC]	— Quincy	[NOAM]	+6	+8
Hawaii	[PCFC]	— Mon. Pk	[PCFC]	+13	0
Hawaii	[PCFC]	— Yargde	[INDI]	-109	-103
Hawaii	[PCFC]	— Wetzel	[EURA]	-70	-40
Hawaii	[PCFC]	— Matera	[EURA]	-73	-43
Mon. Pk	[PCFC]	— Quincy	[NOAM]	-49	-53
Mon. Pk	[PCFC]	— Yargde	[INDI]	-96	-103
Mon. Pk	[PCFC]	— Wetzel	[EURA]	0	+1
Mon. Pk	[PCFC]	— Matera	[EURA]	+3	+5

### 3. Discussions on Solutions

#### (1) On the short arc solutions

To avoid the effect of error of dynamical models for low altitude satellites as BEACON-C, once a method as named the "baseline estimate from simultaneous tracking-BEST [Christodoulidis and Smith, 1981] was used. This method is to use many simultaneously observed data in narrow region for an arc of around five days. An estimation between Quincy and Monument Peak was made but the very stable results were not obtained.

However as shown in the previous section, the specific very short arc method, the SPORT, looks much powerful to determine baseline lengths within a few thousands of kilometers despite of simple concept. The concept was once shown by a simulation using very simple model (Kepler motion) for the case of baseline between Simosato - Titi Sima first by Sengoku and Kubo [1986] according to discussions in JHD. The efficiency of the SPORT was proved by obtaining result of -31mm/year for the real estimation of baseline change for Quincy-Monument Peak using LAGEOS raw data. For the estimation of the contraction rate of this baseline, a recent NASA estimate of SL7.1 [Smith 1988] gives -24mm/year and the result of Murata [1988] is -32mm/year. The plate motion between the two



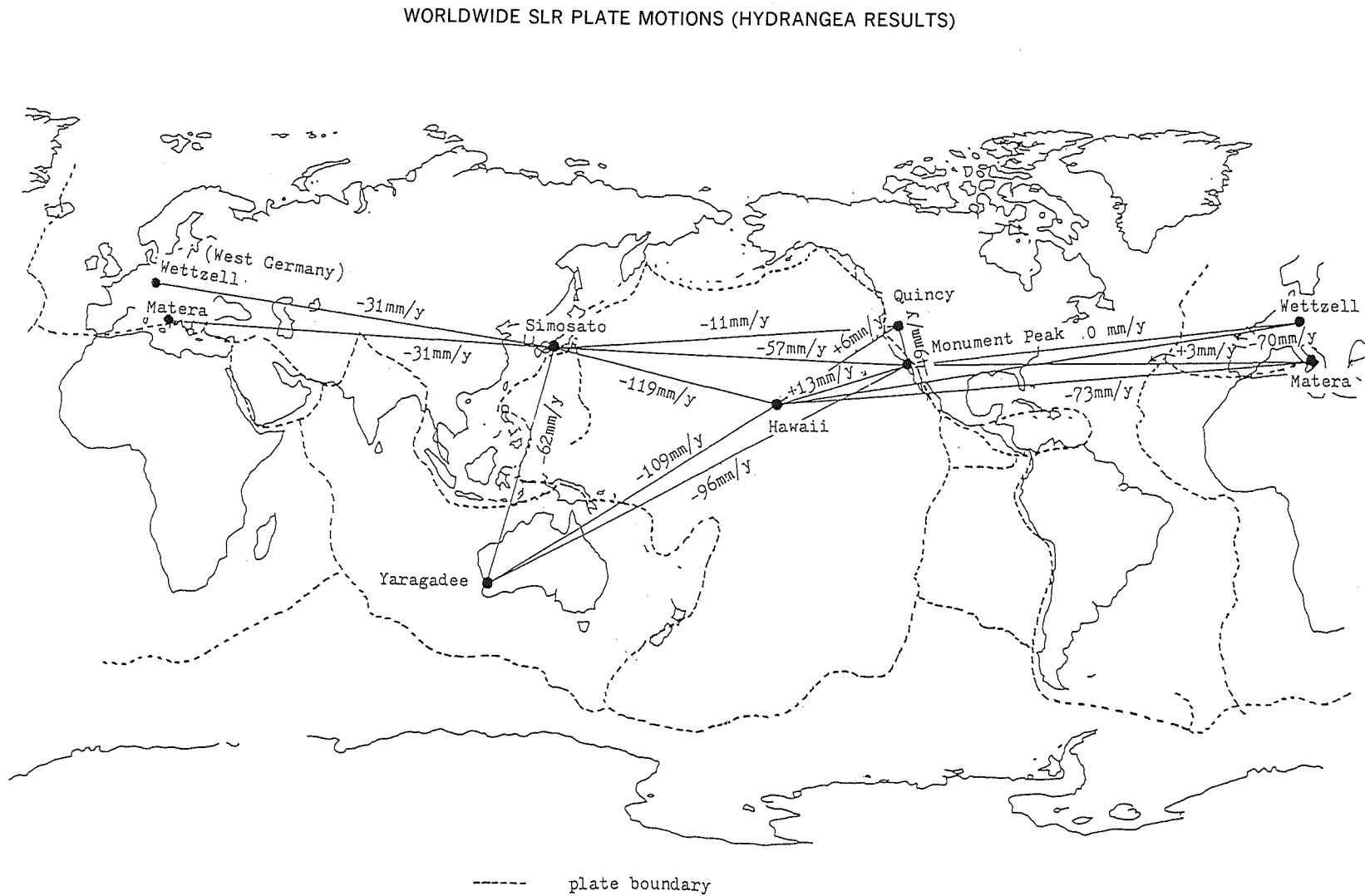


Figure IV — 9. Worldwide plate motions derived from LAGEOS SLR data.

stations estimated by Minster and Jordan [1978] is  $-53\text{mm/year}$ .

The results on the figure and comparison with other results show that the stability and repeatability of the SPORT for this baseline is good enough to detect a plate motion. Similarly each error estimate of actual baseline length determination for Simosato-Titi Sima gives 4mm and also for Simosato-Minamitori Sima gives 7mm. As was shown in Tables IV-4 and IV-6, the precision of the baseline length is determined better than three dimensional coordinates because of the geometrical effect among the orbit, geocenter, earth rotation axis and site location. The following considerations give an interpretation for this effect. Namely if an orbit of a satellite is polar orbit and the station configuration concerned is near north pole, absolute direction of the baseline can not determine well, but because of shape of orbit baseline length will be determined much better than direction.

The SPORT can not determine the direction of the baseline very well when the satellite orbit passes almost parallel to the direction of the baseline, however the baseline length can be determined very well. When the orbit passes almost perpendicular to the direction of the baseline, the baseline length can not be determined by the SPORT. The azimuth of the baseline is determined by the effect of the earth rotation within the subsequent passes and the gravitational force to geocenter. However the baseline length is determined by the effect of curvature of the orbit from both stations, caused by the gravitational acceleration. This can be also understood to consider a specific baseline almost on the equator and ranging to satellite of which orbit has zero inclination. In this case the direction of the baseline cannot determine well but the baseline length will be determined well.

For the Simosato- Titi Sima baseline, a semi-long arc estimate is treated as described in 2-(3) of this Chapter. The data used are five-day-arcs of LAGEOS. The difference of baseline length with the SPORT result given in Tables IV-4 is 14.4cm. The large difference is supposed to come from the insufficient number of LAGEOS passes and data obtained at Simosato and Titi Sima for the case of the five-day-arc. The discussion on the comparison with results of baseline lengths derived from both SPORT and semi-long arc technique should be continued.

## (2) On the treatment of the permanent tide

The solid earth tide model used in the orbital processor/analyzer, HYDRANGEA, is based on an abbreviated form of the Wahr model [Wahr 1979]. The free space potential induced by the earth tide is modeled as variations in the geopotential coefficients  $C_{nm}$  and  $S_{nm}$  by using the Love number,  $k$ , for the induced free space geopotential. The Wahr model is computed in two steps.

The first step uses a frequency independent Love number  $k_2$  and an evaluation of the tidal potential in the time domain from a lunar and solar ephemeris. The second step corrects those arguments of a harmonic expansion of the tide generating potential [Melbourne *et al.* 1983].

In order to estimate  $J_2$ , a careful treatment for the solid earth tide including permanent tide is necessary. The change in a normalized second degree geopotential coefficients  $J_2$  for step 1 is

$$\Delta \bar{J}_2 = -k_2 \frac{A_e^3}{GM} \sum_{j=2}^3 \frac{GM_j}{r_j^3} P_2(\sin \phi_j)$$

where

$k_2$  : nominal second degree Love number

$A_e$  : equatorial radius of the earth

$GM_j$  : gravitational parameter for the moon ( $j=2$ ) or sun ( $j=3$ )

$r_j$  : distance from geocenter to the moon or sun

$\phi_i$  : body fixed geocentric latitude of the moon or sun.

The mean value of  $J_2$  in the equation above is not zero and this non-zero-term is called the permanent tide and the deformation of the earth concerned this non-zero mean value is named the permanent deformation. The early ages in the field of the satellite dynamics, the practical situation was not so clear to derive  $J_2$  term in the meaning above. To make geopotential coefficient sets, there has been a mixture of method to apply or not to apply the permanent tide. However it may be assumed that the more recent data has most of the weight in the determination of  $J_2$  and the permanent deformation is not included in the  $J_2$  term of recent derived geopotential coefficient sets as GEM-L2 [Melbourne *et al.* 1983] and GEM-T1. If it is true the total tidal effect denoted by  $J_{2T}$  concerned  $J_2$  at an instant of time is given by addition of the term  $J_2$  given in a geopotential coefficient set denoted by  $\bar{J}_2$  which does not include permanent tide and  $\Delta\bar{J}_2$  as  $J_{2T} = \bar{J}_2 + \Delta\bar{J}_2$ .

The zero frequency change in  $J_2$  can be removed by computing  $\Delta\bar{J}_2$  [See Melbourne *et al.* 1983 or Sasaki 1984a] as

$$\Delta\bar{J}_2^* = \Delta\bar{J}_2 \text{ (in the equation above)} - \langle \Delta\bar{J}_2 \rangle$$

where

$\langle \Delta\bar{J}_2 \rangle$  : time-independent, permanent tidal deformation caused by the moon and sun

$$= -\sqrt{5} A_0 H_0 k_2$$

$$= -\sqrt{5} \frac{I}{A_e \sqrt{4\pi}} \cdot (\text{amplitude in meter}) \cdot k_2$$

$$= -\sqrt{5} (4.4228 \times 10^{-8}) \cdot (-0.31455) \cdot k_2$$

$\Delta\bar{J}_2^*$  : zero-mean time dependent tide caused by the moon and sun

Namely, the total tidal effect concerned  $J_2$  is given by

$$\begin{aligned} J_{2T} &= [\bar{J}_2 + \langle \Delta\bar{J}_2 \rangle] && \text{: constant term} \\ &+ \Delta\bar{J}_2^* && \text{: zero-mean time dependent term.} \end{aligned}$$

For the case of GEM-L2, value of  $\bar{J}_2$  is  $1082.6258 \times 10^{-6}$  and does not include the permanent deformation. The tidal corrections employed in the computations leading to GEM-L2 were equivalent to equation above with  $k_2 = 0.29$  [Lerch *et al.* 1985]. However this paper and the MERIT Standards adopt the value of 0.30 for  $k_2$ . If GEM-L2 is used in this stage, non tidal term  $\bar{J}_2$  does not seem to concern with  $k_2$  and only tidal term,  $\Delta\bar{J}_2$ , depends on  $k_2$ . However the permanent tide,  $\langle \Delta\bar{J}_2 \rangle$ , is not direct observable in the process for determination of  $k_2$  and actual observable is only zero-mean time dependent term,  $\Delta\bar{J}_2^*$ . The constant term of  $[\bar{J}_2 + \langle \Delta\bar{J}_2 \rangle]$  should be considered as one term to use with different  $k_2$  value. Namely if  $k_2 = 0.30$  is used with GEM-L2 geopotential coefficient set, only  $\Delta\bar{J}_2^*$  term should be changed to the case from  $k_2 = 0.29$  to  $k_2 = 0.30$  as followings;

$$\begin{aligned} J_{2T}(\text{GEM-L2}; k_2 = 0.29) &= [\bar{J}_2(\text{GEM-L2}) + \langle \Delta\bar{J}_2(k_2 = 0.29) \rangle] + \Delta\bar{J}_2^*(k_2 = 0.29) \\ &= 1082.6258 \times 10^{-6} + \Delta\bar{J}_2(k_2 = 0.29), \\ J_{2T}(\text{GEM-L2}; k_2 = 0.30) &= [\bar{J}_2(\text{GEM-L2}) + \langle \Delta\bar{J}_2(k_2 = 0.29) \rangle] + \Delta\bar{J}_2^*(k_2 = 0.30) \\ &= \bar{J}_2(\text{GEM-L2}) + \langle \Delta\bar{J}_2(k_2 = 0.29) \rangle - \langle \Delta\bar{J}_2(k_2 = 0.30) \rangle \\ &\quad + \Delta\bar{J}_2^*(k_2 = 0.30) + \langle \Delta\bar{J}_2(k_2 = 0.30) \rangle \\ &= \bar{J}_2(\text{GEM-L2}) + \langle \Delta\bar{J}_2(k_2 = 0.29) \rangle - \langle \Delta\bar{J}_2(k_2 = 0.30) \rangle + \langle \Delta\bar{J}_2(k_2 = 0.30) \rangle \\ &= 1082.6258 \times 10^{-6} + 9.0213 \times 10^{-9} - 9.3324 \times 10^{-9} + \langle \Delta\bar{J}_2(k_2 = 0.30) \rangle \\ &= 1082.6254 \times 10^{-6} + \Delta\bar{J}_2(k_2 = 0.30) \end{aligned}$$

$$\begin{aligned}
J_{2T}(\text{GEM-T1}; k_2=0.30) &= [\bar{J}_2(\text{GEM-T1}) + \langle \Delta \bar{J}_2(k_2=0.30) \rangle] + \Delta \bar{J}_2^*(k_2=0.30) \\
&= \bar{J}_2(\text{GEM-T1}) + \Delta \bar{J}_2(k_2=0.30) \\
&= 1082.6258 \times 10^{-6} + \Delta \bar{J}_2(k_2=0.30).
\end{aligned}$$

In order to use GEM-L2 for the case of  $k_2 = 0.30$ , the second equation is better to be used. To estimate  $k_2$  or better value for  $J_2$  (GEM-L2) and  $J_2$  (GEM-T1), the attention above is necessary for treatment of the permanent tide.

### (3) On the geophysical parameters

As for the geocentric constant of gravitation derived from LAGEOS, the derived  $GM$ , 398600.4453(km<sup>3</sup>/s<sup>2</sup>) in use of GEM-T1 earth gravity model is a little larger than the formal value of 398600.436, but in the case of use of GEM-L2, the derived value of 398600.4477 is reasonable comparing with the formal value of 398600.448.

The derived values of  $J_2$ ,  $1082.571 \times 10^{-6}$  for the case of GEM-T1 used and  $1082.618 \times 10^{-6}$  for the case of GEM-L2, seem a little smaller than the formal values for both models as  $1082.626 \times 10^{-6}$ , and  $1082.625 \times 10^{-6}$  which is revised in the previous section.

The weighted mean value of the solar radiation reflectivity coefficient of LAGEOS,  $\gamma$ , derived in this paper as  $1.111 \pm 0.008$ ,  $1.121 \pm 0.010$ ,  $1.144 \pm 0.015$  and  $1.129 \pm 0.026$  becomes 1.123. Once Murata [1988a] gave 1.121 for this value of LAGEOS. The first draft [1980] and last one [1983] of the MERIT Standards [Melbourne *et al.*] gave 1.17 and 1.14. The derived value in this paper, 1.123, well coincides with the result of Murata.

For the along track acceleration,  $\Delta\alpha$ , the weighted mean value of residuals in this paper,  $-2.5 \pm 3.7$ ,  $-3.4 \pm 0.9$ ,  $-4.4 \pm 2.3$  and  $-0.9 \pm 5.3$  (unit:  $1 \times 10^{-12}$  m/s<sup>2</sup>), is  $-3.26 \times 10^{-12}$  m/s<sup>2</sup>. The first draft and the last publication of the MERIT Standards gave  $-2.9 \times 10^{-12}$  m/s<sup>2</sup>,  $-3.1 \times 10^{-12}$  m/s<sup>2</sup> and Murata [1988a] gave  $-3.524 \times 10^{-12}$  m/s<sup>2</sup>. The resulting value in this paper,  $-3.26 \times 10^{-12}$  looks reasonable.

A recent draft of IERS Standards [McCarthy *et al.* 1989] adopted  $398600.440$  km<sup>3</sup>/s<sup>2</sup> for  $GM$  and  $1082.626 \times 10^{-6}$  for  $J_2$ . The fluctuation of the last digit seems unavoidable at present. It is difficult to determine absolute values of  $GM$  and  $J_2$  independently much better than other error source level by satellite dynamics because errors of many other force models and values cause errors of estimation of  $GM$  and  $J_2$ .

Murata [1988b] made a preliminary analysis for the AJISAI SLR data obtained in 1986, and the mean range residual in the case of adoption of five-day-arcs, GEM-T1 gravity model, Jacchia-Robert 71 model [Jacchia 1971] daily estimation of atmospheric drag coefficient was 27cm. However there is no determined value for along track acceleration in his paper. The resultant values given by the author of lic01 for the reflectivity coefficient ( $\gamma$ ) and 3.5 for the atmospheric drag coefficient ( $C_d$ ) of AJISAI with smaller mean range residuals of 18.2cm look good in comparison with the results of LAGEOS case in the first draft of MERIT Standard as 1.17 and 3.8, respectively.

More precise measurements of  $GM$  in the future may realize the change effect of gravitation constant, which might be caused by the relativity effect. The direct measurement of time variation of  $J_2$  also will support the change of earth's shape as given by Rubincam [1984].

### (4) On the earth rotation parameters

Comparisons of the results of earth rotation parameters estimated by using 49576 LAGEOS normal point data in 85 five-day-arcs, in the MERIT Campaign with the results of BIH (Bureau International de l'Heure) [smoothed one: Circular-D, 1983 and 1984; Figure IV-10] and ERP (CRS) 85L07 [raw values: Tapley *et al.* 1986: Figure IV-11] are made. If there is a mean difference between the

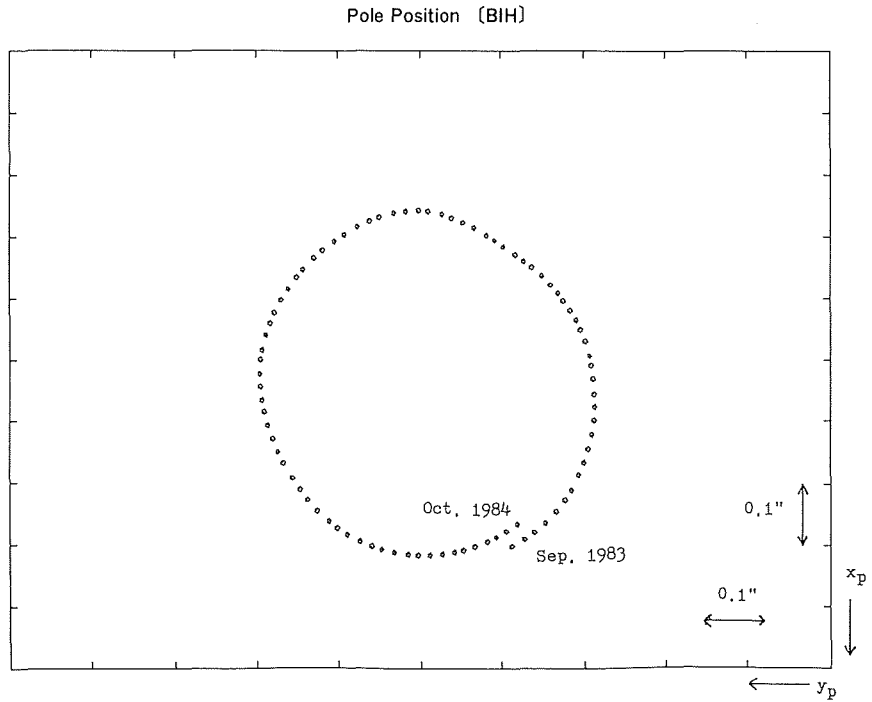


Figure IV -10. Pole position derived from LAGEOS SLR data(BIH results).

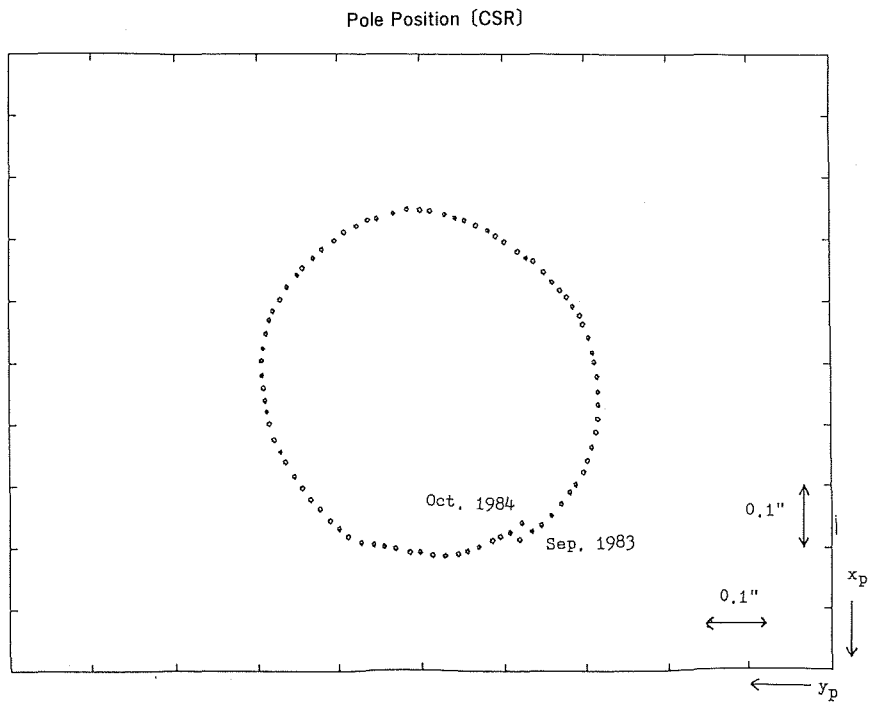


Figure IV -11. Pole position derived from LAGEOS SLR data(CSR results).

HYDRANGEA results in this paper and the interpolated BIH results for all the 85 five-day-arcs, it suggests an existence of a systematic difference of the pole position coordinates. The systematic differences expressed by  $dx_p$  and  $dy_p$  for  $x_p$ , and  $y_p$  components are given as followings. The standard deviations [s.d.] for each five day pole position are also shown in the following parentheses :

<HYDRANGEA results>

pole position ( $x_p$ ,  $y_p$ )

(Sasaki-BIH)

$$dx_p = -8.6 \pm 0.2 \text{milliarcseconds}[\text{mas}](4.1\text{mas of standard deviation [s.d.]})$$

$$dy_p = -1.8 \pm 0.1\text{mas} (2.3\text{mas s. d.})$$

(Sasaki-CRS)

$$dx_p = -0.56 \pm 0.01\text{mas} (1.1\text{mas s. d.})$$

$$dy_p = -0.13 \pm 0.02\text{mas} (1.4\text{mas s. d.})$$

The results above mean that there is almost no systematic difference between Sasaki and CSR pole positions, however the systematic differences of pole position coordinates with Sasaki/CSR system and BIH system are 8-9mas for  $x_p$  and 2mas for  $y_p$ . The author's Sasaki pole position coincides with CSR pole position in the level of almost 1mas for each five-day result.

As for the excess rotation per day the similar comparison is made. The results are :

<HYDRANGEA results>

excess rotation per day (ex.RPD) :  $\Delta\omega$

(Sasaki-BIH)

$$\text{ex. RPD} = -0.08 \pm 0.02 \text{ millisecond per day}[\text{ms/d}] (0.20\text{ms/d s.d.})$$

(Sasaki-CSR)

$$\text{ex. RPD} = -0.10 \pm 0.05\text{ms/d} (0.42\text{ms/d s.d.}).$$

The results for ex. RPD show the existence of a systematic difference between Sasaki results and BIH (smoothed one, Figure IV-12) / CSR (raw value, Figure IV-13) results in a level of 0.1ms/d. However the visual comparison of Sasaki in Figure IV-4 with Figure IV-13 gives an impression that the derived results show smaller deviation than CSR. This might be caused by the reason that the earth rotation parameters are not estimated directly like CSR but only the smaller differences with a reference earth rotation parameters (e. g. BIH results are used originally) are estimated in a arc in the HYDRANGEA.

The resultant excess rotation per day are plotted in Figure IV-14 roughly superposing with the atmospheric "excess rotation per day" estimated by Naito and Yokoyama [1985] from wind data supplied by the Japan Meteorological Agency (JMA) and the U. S. National Meteorological Center (NMC). The comparison shows a good correlation with the excess rotation per day and angular momentum of wind on the earth. According to Naito and Yokoyama [1985], the mass contribution is at most ten percent of the total effect of the angular momentum and most part of the change of the angular velocity of the earth is explained by the wind effect of the earth.

The more precise measurements of pole position and angular velocity of the earth by advanced SLR or VLBI technique in the near future will produce the detections of phenomena of a big earthquake, short time excitation of earth rotation by the atmosphere change, ocean currents or the core-mantle interaction in the inner side of the earth.

##### (5) On the station coordinates

The position of the earth rotation axis on the earth's surface and the SLR stations were determined by using the SLR technique in the precision of a few centimeters level today as already

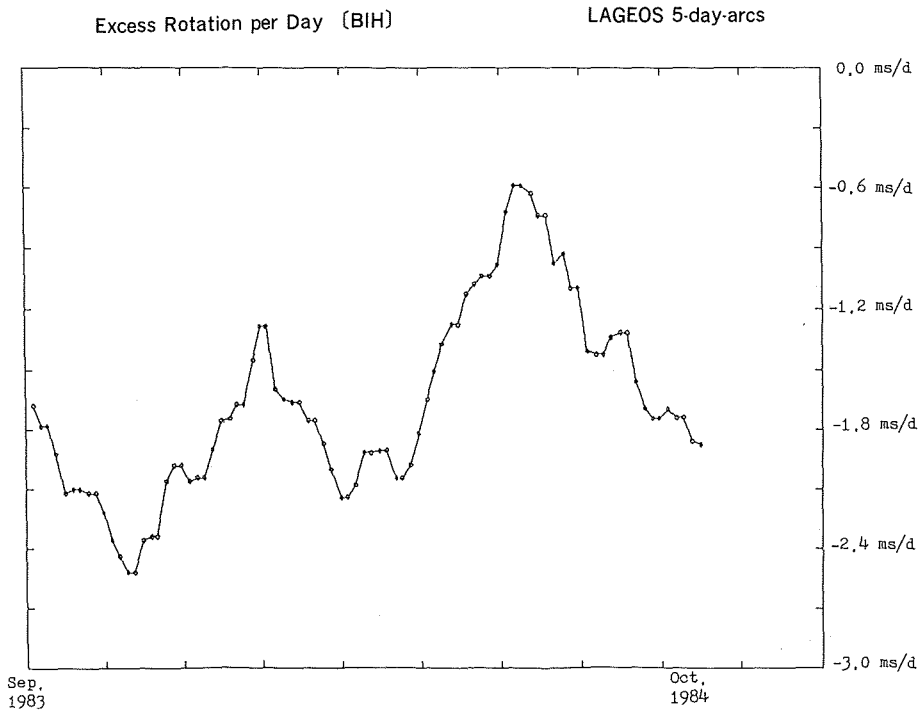


Figure IV -12. Excess rotation per day derived from LAGEOS SLR data(BIH results).—smoothed—

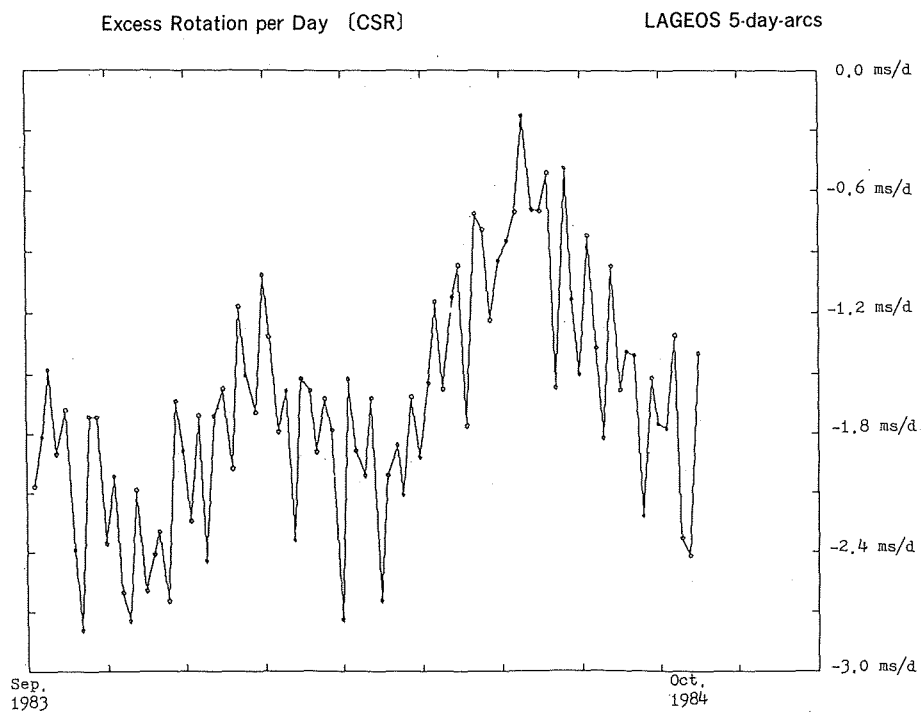


Figure IV -13. Excess rotation per day derived from LAGEOS SLR data (CSR results).—raw—

Excess Rotation per Day (HYDRANGEA) LAGEOS 5-day-arc and wind effects on earth rotation

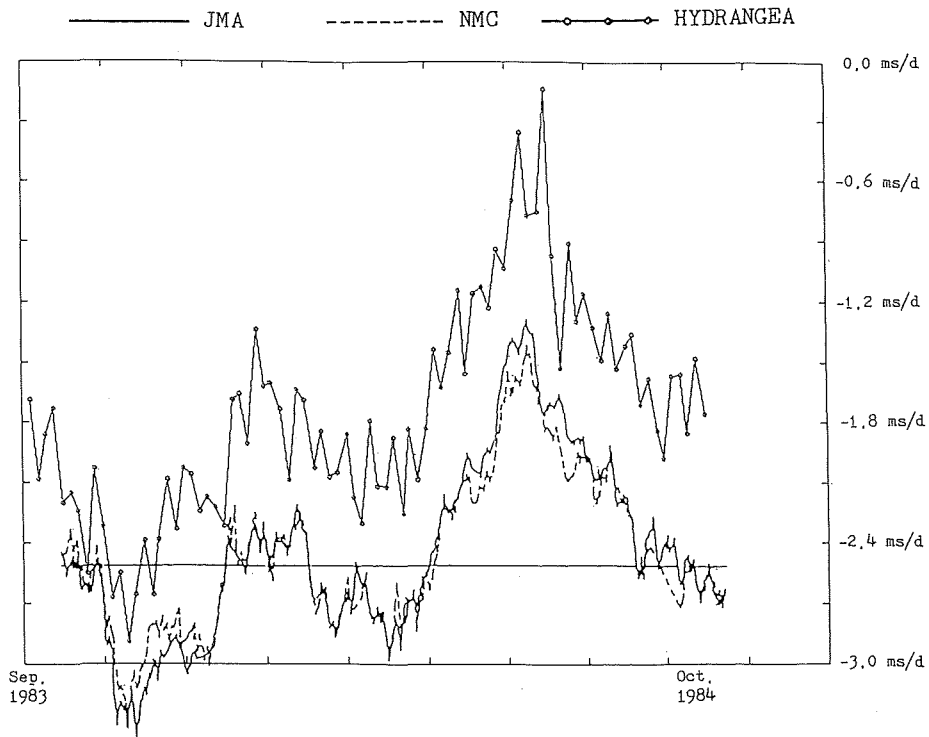


Figure IV —14. Comparison with excess rotation per day and wind effects on earth rotation [Naito and Yokoyama 1985] .

mentioned. At this kind of high precision determination of global positions, some attention should be paid, especially for the case of comparison with similar results obtained by other techniques or the same technique but different analysis systems.

One major merit of satellite-derived station coordinates is that the origin of the derived coordinate system can be based on the center of the mass of the earth, whereas the VLBI technique for fixed star, for instance, can only determine an interrelation of station positions relatively to a specific station. The VLBI technique can not make any relation between observation stations and the earth center but the SLR technique can show the actual position of the geocenter based on the positions of SLR stations.

Next, for the nominal values of expression of station coordinates, the largest discrepancy in some different results for the same point of a ground marker near observation facilities may occur because of a different definition of the longitude. As everyone knows the definition of the zero meridian is completely artificial in principle. Actually almost every zero meridian of the earth centered terrestrial coordinate systems might go through the "yard" of Greenwich Observatory, but these do not penetrate the same point. For instance the difference of longitude between WGS-72 and WGS-84 is 0.54 arcseconds (around 16 meters on the equator)[Leroy 1982]. There is no authorized definition of longitude in the



precision of several meters level and analysts can chose the definition freely at present (e. g. CSR longitude is combined with a lunar laser ranging (LLR) result.

The plate motions also should be considered for global precise positioning. Even if a precise coordinate system defined at an instant of time, interrelation of location of the observation stations may change by the plate motions at a rate of ten centimeters per year at most. This is the major problem for the definition of a static terrestrial reference frame. On the case of SLR technique it is sufficient to fix only one longitude of one defining SLR station in principle if the rotation axis of the earth is fixed on the surface of the earth. However in actual the earth rotation axis moves, and the latitude of two SLR stations, of which longitudes are expected to be different by around 90 degrees, should be fixed to solve and denote the pole position. In order to fix these values originally, the interrelation between the two defining stations for latitude should be known at first precisely. Even if one knows the interrelation of them at an instant of time, for the estimation of the future or past station coordinates the relative plate motions should be known precisely in a few centimeters level. Actually this is difficult except an assumption of plate motions.

Here is also a problem to determine the pole position by using SLR technique. As for the nominal values for expression of the pole position the largest discrepancy in some different results for the same time also occurs because of a different station coordinate system used for SLR stations. The expression of the pole position directly depends on the reference coordinate system, as CIO, BIH, CSR or other reference coordinate systems. There exist differences among them as described in the previous section.

Another problem is the effect of the earth gravity field. To develop a gravity field model for precise satellite orbital determination as GEM-T1 [Marsh *et al.* 1987] only the satellite tracking data were used. In such a process, a priori selection of station coordinates, pole position and earth rotation phase (UT1) is made, and the resultant earth gravity model contains the effect of such a priori selection a little. Namely there is a possibility that the earth rotation parameters estimated by using a specific gravity model contain some proper bias. Actually GEM-T1 caused some bias between a priori earth rotation parameters and resulting earth rotation parameters derived by using the same SLR data set. The systematic error of the SLR station coordinates also comes from the dynamical model used.

As the example of expression of station coordinates, Simosato station is adopted here. The three dimensional values are given with name of authors or coordinate systems in Table IV-22. The table Table IV-22. Three dimensional geocentric coordinates for the reference point of Simosato SLR system derived by several authors

U	V	W	authors
m	m	m	
-3822388.295	3699363.512	3507572.967	LSC 8402 [Tapley <i>et al.</i> 1985]
388.2988	363.5307	573.1472	SSC (CSR) 85L07 [Tapley <i>et al.</i> 1986]
388.419	367.939	567.617	SL6 [Smith <i>et al.</i> 1986]
388.551	363.359	573.188	Murata [1988a]
384.82	366.73	572.34	STALAS longitude definition [Sasaki 1984b]
388.5	363.1	572.3	McDonald LLR longitude definition [Sasaki 1984b]
388.330	363.577	573.186	JHDSC-2 [Sasaki 1989]

shows that the direct comparison of station coordinates with some other results is not meaningful. However, the baseline lengths among stations which are independent from the expression of adopted station coordinate systems are rather significant for comparison and detection of the motions of stations.

The discussion above indicates that in order to establish a terrestrial reference frame, it is expected to complete a precise and accurate plate motion model and other dynamical models by using several techniques recurring convergence of determination of the station coordinates and the earth rotation.

#### (6) On the changes of baseline lengths and plate motions

The local baseline change between Quincy-Monument Peak is considered here at first. The value of semi-long arc result of HYDRANGEA as 49mm/y which is derived from three sets at 1984.80, 1986.76 and 1988.11, is close to the Minster-Jordan AM0-2 plate motion of 53mm/y and is larger than recent results of SL7.1 [NASA GSFC 1987] as  $-26 \pm 5$ mm/y, Murata's result of  $-32 \pm 11$ mm/y and also the previous SPORT result of  $-31$ mm/y. However the semi-long arc result of HYDRANGEA seems smaller than the early result of Tapley *et al.* [1985] as  $-64 \pm 9$ mm/y and the result of the "BEST" as  $-61 \pm 25$ mm/y [Christodoulidis *et al.* 1985]. The change of the same baseline length derived by four year VLBI observation [Ma *et al.* 1989] for the duration from mid-1983 to mid-1987 is  $-29.6 \pm 5.6$ mm/y.

The results of five-day-arcs derived by the HYDRANGEA and several other results are given for comparison in Table IV-23. The table shows a little bit large difference from the AM0-2 model of Minster-Jordan for the baselines of Simosato-Wetzell, Simosato-Matera, Hawaii-Wetzell and Hawaii-Matera. But other changes of arc lengths almost coincide with the motion derived from the AM0-2 model.

The coincidence of changes of arc lengths given by the author with the AM0-2 model except Simosato and Hawaii, is not self-evident in spite of the assumption that the fixed stations are slightly shifted according to the AM0-2 model. Because there are many freely solved stations in this procedure and only a little influence for positioning of the many solved-for stations is caused directly from the positional relation of the fixed stations. This point should be emphasized. The coincidence of results of this paper with the AM0-2 model are rather lead from the fact that natural plate motions agree well with the AM0-2 model as given by the following NASA results [e.g. NASA GSFC SL-7 solution].

According to a private communication [Bosworth 1988] a recent NASA results show that the position of Simosato has been approaching to Europe by 38mm/y in spite of being believed that the both locations are within the Eurasian plate. A paper read by N. Douglas and C. Harrison [1988] at the NASA Crustal Dynamics Project 15th Principal Investigators Meeting held at Munich in October 1988 strongly suggests that Simosato is moving to the azimuth of  $-44$  degrees by 4cm/y according to their SLR analysis. These subjects support the result given by the HYDRANGEA this time as baselines from Simosato to Wetzell or Matera are decreasing by 31mm/y. For the result of Murata [1988] as he describes in his paper, he fixed the latitude of Simosato and the latitude and longitude of the Goddard station at Maryland and solved other station coordinates in a 3.3year long arc first. So, the position of Simosato was adjusted for only the longitude element. Next, in order to estimate the change of baseline lengths he also fixed the latitude of Simosato as same as the latitude of Goddard and longitude of Yaragadee fixed. Therefore if there is contraction of baseline length toward the direction of  $-45$  degrees of azimuth which directs to Europe on the globe of the earth, the north-south component of the

Table IV-23. JHD SLR DERIVED PLATE MOTIONS 1 (JHDPMTN-1)  
from 1984.80 to 1988.11

				JHD	M/J	SL7, 1(1987)	Murata(1988)
				⟨HYDRANGEA⟩			
				mm/y	mm/y	mm/y mm/y	mm/y mm/y
Simost	[EURA]	— Quincy	[NOAM]	-11	-19	-28 ± 14	-25 ± 18
Simost	[EURA]	— Mon. Pk	[PCFC]	-57	-64	-52 ± 17	-46 ± 17
Simost	[EURA]	— Hawaii	[PCFC]	-119	-99	-87 ± 13	-94 ± 19
Simost	[EURA]	— Yargde	[INDI]	-62	-77	-72 ± 9	-69 ± 15
Simost	[EURA]	— Wetzel	[EURA]	-31	0	—	-19 ± 25
Simost	[EURA]	— Matera	[EURA]	-31	0	—	-4 ± 29
Hawaii	[PCFC]	— Quincy	[NOAM]	+6	+8	0 ± 5	-7 ± 15
Hawaii	[PCFC]	— Mon. Pk	[PCFC]	+13	0	+4 ± 3	+1 ± 16
Hawaii	[PCFC]	— Yargde	[INDI]	-109	-103	-96 ± 7	-77 ± 11
Hawaii	[PCFC]	— Wetzel	[EURA]	-70	-40	—	-33 ± 33
Hawaii	[PCFC]	— Matera	[EURA]	-73	-43	—	-3 ± 27
Mon. Pk	[PCFC]	— Quincy	[NOAM]	-49	-53	-26 ± 5	-32 ± 11
Mon. Pk	[PCFC]	— Yargde	[INDI]	-96	-103	-91 ± 7	-43 ± 5
Mon. Pk	[PCFC]	— Wetzel	[EURA]	0	+1	—	+1 ± 45
Mon. Pk	[PCFC]	— Matera	[EURA]	+3	+5	—	-20 ± 42

change of position of Simosato referring to latitude of Goddard still might be suppressed. The resultant contraction rates of  $-19\text{mm/y}$  for the baseline of Simosato-Wettzell and  $-4\text{mm/y}$  for the Simosato-Matera derived by Murata might be too much smaller than the result of  $-31\text{mm/y}$  of this paper.

The results of the author show there exists a contraction of baseline length between Simosato and Europe in the rate of  $3\text{cm/y}$ . The baseline arc from Simosato to Wettzell or Matera goes northwest through the north part of China, Lake Baikal, Ural mountain range, northern from Moscow and south edge of Balt Sea as shown in Figure IV-15. So, there might be specific contraction zones between Simosato and Europe. There may be many microplates on the line from Simosato to Europe and it is considered that simple plate model can not be applied, especially on land usually. However roughly saying, according to Seno [1989] and Molnar [1988], the northward penetration of India on the Indian plate toward Siberia causes thrust faulting at Himalaya and Tien Shan, and strike-slip faulting, primarily left-lateral, on faults emanating from Tibet and cross Mongolia. The effect thrusts the crust of North China eastward. In this sense the baseline arc length should be rather expanded than contraction because there seems no specific contraction zone of microplate in the north part of Europe on the line of arc from Simosato to Europe. Next considering that the motion of the Philippine Sea plate referring to the Eurasian plate is a level of several centimeters of the direction to almost the northwest, the contraction may be caused by the force of the Philippine Sea plate underthrusting toward northwest direction.

Generally speaking, the northwest-ward motion of Simosato area being underthrusting by the Philippine Sea plate can be certified from the accumulation of contraction after the release of stress energy by a big earthquake. The effective area of stress beyond a subduction zone being underthrusting is estimated as the area within  $300\text{km}$  to  $500\text{km}$ , or  $1000\text{km}$  at most from the edge of the plate facing to the next plate, in general [Seno 1986]. Simosato is located at around  $100\text{km}$  northwest from Nankai



Figure IV -15. Simosato centered location of SLR stations projected on the globe.

Trough and sometimes neighboring point near subduction zone may be withdrawn with a sinking plate but Simosato is sufficiently far from the subduction zone in this sense. Seno [1986] considers that there is no reason for the existence of the stress to the direction of eastwest-ward in the Southwest Japan because of the direction of the motion of Philippine Sea plate is toward westnorthwest or northwest. According to Seno [1977], the Philippine Sea plate moves to northwest in the rate of 4.4cm per year referring to the Eurasian plate near Simosato.

The discussion above shows that there is no specific contraction between Simosato and Europe. Therefore the major reason of the contraction of baseline arc of Simosato-Europe may be caused by the stress induced by the Philippine Sea plate underthrusting at the area of southeast of Simosato toward northwest direction.

As for the change of baseline length of Hawaii-Wetzell and Hawaii-Matera, if there is a slip by 40mm to north direction at Hawaii station because of a little bit larger error estimate of z-component for the year 1988 than others, the deflection from AM0-2 model can be explained. There is a possibility

that the result on Hawaii-Europe baseline can be narrowly explained.

## V. SUMMARY AND CONCLUSIONS

After a new era in satellite geodesy in mid-1970s, developments of Satellite Laser Ranging (SLR) systems and the Japanese Geodetic Satellite advanced in Japan. An experimental system of SLR was installed at the Kanozan Geodetic Observatory of the Geographical Survey Institute of Japan (GSI) under cooperation with the Hydrographic Department of Japan (JHD) and GSI. A fixed SLR system was installed at the Simosato Hydrographic Observatory of JHD in 1982 and SLR observation has been continued since then. In 1986 the Japanese Geodetic Satellite, AJISAI, was launched successfully on a circular orbit of 1500km altitude. AJISAI has been tracked by worldwide SLR stations, especially in the precision of a centimeter level at some high precision SLR stations. In early-1988 a transportable SLR station, named HTLRS, was completed, and the field work using the station has been continued since then. The author has been deeply involved in these plannings, developments and other subjects above since mid-1970's in Japan.

The development of an orbital processor/analyzer to treat SLR data for geodynamic purposes has also been continued since 1981, and it has been almost completed recently and named **HYDROGRAPHIC DEPARTMENT RANGE DATA ANALYZER (HYDRANGEA)**. The HYDRANGEA is based on the linear estimation theory and a numerical integration technique. The dynamical systems adopted were almost based on the MERIT Standards [Melbourne *et al.* 1983]. Derivation of a number of formulas of partial derivatives, expression of forces and almost every programing including formation of the processor/analyzer were made independently by the author. The estimable geodynamical parameters are the geocentric constant of gravitation ( $GM$ ), the dynamical form factor of the earth ( $J_2$ ), a ballistic coefficient of a satellite concerned, a reflectivity coefficient of the satellite, along track acceleration of the satellite, the pole position of the earth, the excess rotation per day (minus sign of the excess length of day), and arbitrary number of three dimensional station coordinates. The description on the development of the orbital processor has been given in Chapter III.

The processor/analyzer, HYDRANGEA, was applied to a specific short arc technique named SPORT (**S**uccessive **P**asses **O**rbit **R**evising **T**echnique). The SLR data of two successive passes simultaneously obtained at a few nearby SLR stations are used to estimate baseline lengths between the stations in high precision.

To estimate validation of the SPORT at first, the SLR data of 65 sets for LAGEOS successive passes observed simultaneously both at Quincy and Monument Peak around 883.6Km apart crossing San Andreas Fault, California, from August 1984 to July 1987 were used. In average, around a thousand of range data are included in a data set. The estimated straight baseline lengths are around 883602.21m in August 1984 and 883602.12m in July 1987 and so on as given in Figure IV-2. The plotted points show a linear baseline change of which slope is  $-31\text{mm/year}$ .

The SPORT is applied to the AJISAI SLR data obtained in early 1988 by the fixed SLR station at Simosato and the transportable SLR station, HTLRS, located at Titi Sima in Ogasawara Islands. The SPORT is also applied to AJISAI and LAGEOS SLR data obtained by the fixed SLR station at Simosato and the HTLRS located at Minamitori Sima in early 1989. The estimated baseline lengths are  $937665.041 \pm 0.004\text{m}$  for Simosato-Titi Sima and  $2024874.042 \pm 0.007\text{m}$  for Simosato-Minamitori Sima. It has been verified that the specific short arc technique, SPORT, is very effective technique to determine baselines

between nearby SLR stations, especially for the data of low altitude satellites as AJISAI. It is supposed that the powerful efficiency of the SPORT comes from rather geometrical effect among the satellite orbit, geocenter, earth rotation axis and station location.

Next, the HYDRANGEA is applied to semi-long arcs (8 five-day-arcs) of LAGEOS SLR data obtained at worldwide SLR stations in late September to early November in 1984. The derived results of the geophysical parameters using GEM-T1 geopotential are as follows :

$$GM = 398600.4453 \pm 0.0003 \text{Km}^3/\text{s}^2,$$

$$J_2 \text{ (which does not include the tidal permanent deformation)} = (1082.571 \pm 0.015) \times 10^{-6},$$

$$\text{solar reflectivity coefficient of LAGEOS} = 1.111 \pm 0.008,$$

$$\text{mean along-track acceleration} = (-2.5 \pm 3.7) \times 10^{-12} \text{m/s}^2.$$

In the developed orbital processor/analyzer, HYDRANGEA, the earth rotation parameters are not estimated directly, but only the smaller differences of  $x$  and  $y$  components with reference earth rotation parameters in each arc are estimated. Therefore pole positions are treated as if moving with reference pole motion with a small constant differences which are to be estimated. The earth rotation parameters in the MERIT Campaign from September 1983 to October 1984 are also estimated by using LAGEOS SLR data. The LAGEOS normal point data used are 49,576 of 85 five-day-arcs. The gravity field used is GEM-L2. The reference station coordinates adopted is SSC (CSR : Center for Space Research, the University of Texas at Austin) 85L07 [Tapley *et al.* 1985]. The resulting mean range residual for all the normal point data is 9.77cm, and most of the internal errors for the derived pole positions and excess rotation per day are less than 0.5 milliarcseconds (mas). The resultant values are given in Table IV-11 and Figure IV-3. The comparison of the derived results with BIH (Bureau International de l'Heure) and CSR results is made. The BIH results have a systematic difference of the expression compared with the derived results. by  $(dx_p, dy_p) = (-8.7\text{mas}, -1.8\text{mas})$  with the standard deviation of  $(4.1\text{mas}, 2.3\text{mas})$ . The derived results coincide well with CSR results as the systematic difference of  $(-0.56\text{mas}, -0.13\text{mas})$  and the standard deviation of  $(1.1\text{mas}, 1.4\text{mas})$ . This means that the accuracy of coincidence of the derived results with CSR results is 3 - 4cm level for each five-day-arc.

The results of the excess rotation per day (minus sign of excess length of day) are also shown in Figure IV-4. The results well coincide with change of angular velocity of the earth rotation mainly caused by the atmospheric wind effect estimated by Naito and Yokoyama [1985] and the fluctuation of the derived results seems a little smaller than a results derived from the difference of UTI of ERP (CSR) 85L07 given by Tapley *et al.* [1985, 1987].

The pole position is also solved by using worldwide AJISAI SLR data of three day arcs. 136369 range data in 35 three-day-arcs from mid-August to late November in 1986 are used. The gravity field used is full model of GEM-T1. The results are given in Table IV-12 and Figure IV-5. The fluctuation of the pole position derived from AJISAI SLR data seems a few times larger than LAGEOS results.

The estimation of the station coordinates and determination of the baseline arc lengths have been made. The three dimensional station coordinates are determined coinciding the origin with the center of mass of the earth whereas the VLBI technique, for instance, can not make any positional relation between observation stations and the geocenter.

The positions of observation stations are also solved simultaneously with geophysical parameters and the earth rotation parameters. For the same case of 8 five-day-arcs of LAGEOS SLR data from late September to early November 1984, described in the paragraph of geophysical parameter estimation, 61 unknowns including three dimensional coordinates of 16 stations are solved. The mean range

residual for each normal point data is 7.1cm. Since the station coordinates are solved with pole position and excess rotation per day of the earth, the following parameters of the earth rotation phase (UTI) at an initial time, the longitude of one station and the latitudes of two SLR stations, (of which longitudes are expected to be different by 90 degrees for a good geometrical separation of station location and pole position,) should be fixed numerically in principle in the procedure for each five-day-arc. However such numerically fixed and defining stations which produce sufficient amount of SLR data for determination of unknown parameters in every five-day-arcs can not be selected from the station file because no station can obtain ideally sufficient SLR data owing to weather-and operational conditions in every short arcs. Therefore several but sufficient station coordinates should be fixed in advance in this kind of semi-long arc method. As the a priori fixed coordinate set, several station coordinate values of SSC(CSR) 85L07 are adopted. The derived station coordinates are given in Table IV-15. The mean internal error of the three dimensional station coordinates from 14 freely determined stations except a station (Metsahovi, Finland) with large residuals and another station (Platteville, Colorado) of very few SLR data is (2.6cm, 2.4cm, 2.9cm), and the comparison with the coordinates of the same stations include in SSC(CSR) 85L07 gives good coincidence as (3.4cm, 3.1cm, 5.1cm) for the mean individual difference (r.m.s). The internal error for the results solved freely in a partial frame of SSC (CSR) 85L07 in 8 five-day-arcs is very small and mean external difference is only a little larger than the internal error. The facts show that the average of multi semi-long arc results is powerful method to determine the dynamical parameters and station coordinates well because there is no large integrated dynamical error owing to short duration of integration as five days, and mean range residual is kept small as 7.1cm in this case and other cases given below as 5.3cm for the data of 1986 and 4.7cm for 1988 whereas range residuals for one-month-arcs or longer arcs are usually 10cm level [Tapley 1986].

The similar procedures have been made for other 8 five-day-arcs of LAGEOS at the mean epoch of 1986.76 and 9 five-day-arcs of LAGEOS at 1988.11. The mean range residuals for two data sets are 5.3cm and 4.7cm, respectively. The resultant station coordinates are given in Table IV-17 and IV-18. The treatment of the a priori fixed station for these cases is the same for the previous case of 1984 but the positions are slightly shifted from the values of SSC (CSR) 85L07 by using the plante motion model of AM0-2 given by Minster and Jordan [1978].

In order to estimate plate motions in horizontal plane on the surface of the earth, the change of arc lengths on the surface of a reference ellipsoid has been considered. The baseline arc lengths for each epoch of 1984.80, 1986.76 and 1988.11 between two of freely determined SLR stations, Simosato, Hawaii and Monument Peak, and between one of freely determined stations and one of the fixed stations of Yaragadee, Quincy, Wettzell and Matera, are evaluated, and the changes of arc lengths for the same baselines at three epochs are estimated. The estimated results are tabulated in Table IV-21 and are shown in Figures IV-6, IV-7 and IV-8 with Minster-Jordan AM0-2 results. The derived worldwide plate motions are also given on a map in Figure IV-9.

The coincidence of changes of arc lengths given by the author with the AM0-2 model except Simosato, is not self-evident in spite of the assumption that the fixed stations are slightly shifted according to the AM0-2 model. Because, there are many freely solved stations in this procedure and only a little influence for positioning of the many solved-for stations is caused directly from the positional relation of the fixed stations. This point should be emphasized. The coincidence of the results of this paper with the AM0-2 model is rather lead from the fact that natural plate motions agree well with the AM0-2 model as given by some NASA results.

The results of HYDRANGEA show that the baseline between Simosato and Europe seems to be contracted in the rate of 3.1cm per year whereas Simosato is believed on the edge of the Eurasian plate as same as Europe.

According to Douglas and Harrison [1988] and a worldwide SLR analysis made by NASA [Bosworth 1988], the major SLR stations except Simosato seem to move on the plate motions of the AM0-2 model and Simosato seems to be moving to the direction of 44 degrees of azimuth in the rate of 4cm/year. The author's result almost coincides with this value.

The northward penetration of the Indian plate toward Siberia causes thrust faulting at Himalaya and Tien Shan area, and strike-slip faulting, primarily left-lateral, on faults emanating from Tibet and across Mongolia. The effect thrusts the crust of North China eastward. In this sense the baseline are length between Simosato and Europe should be rather expanded.

The motion of the Philippine Sea plate referring to the Eurasian plate is around 4cm level to northwest [Seno 1977] and Simosato is located at around 100Km northwest from Nankai Trough which is belived as the subduction zone of the Philippine Sea plate. Therefore the contraction of arc length between Simosato and Europe seems to be caused by the stress of the Philippine Sea plate underthrusting Simosato area toward northwest.

As a future prospect of SLR, it seems advancing today. A Soviet SLR satellite, named ETALON with a diameter of 1.3m and weight of 1400kg was launched in early 1989 in an extremaly high orbit of altitude of 19000km. ETALON is really expected to be used for the geodynamic purpose because of its high altitude.

The European Remote Sensing satellite, ERS-1, with a major purpose for altimetry will be launched in early 1991 [Ganako 1989]. The satellite is equipped with a set of laser reflectors for precise orbit determination and calibration of the altimeter. The NASA altimeter satellite, TOPEX/POSEIDON, will also be launched in an orbit of 1300km altitude in 1992 [Segawa 1989]. The worldwide SLR stations will track ERS-1 and TOPEX/POSEIDON satellites. The SLR tracking will contribute much to researches of the gravity field of the earth, the effect of ocean to the earth rotation, estimation of earth's interia, tidal effects and the ocean circulation of the current in the both satellite altimetry projects. The second LAGEOS will be launched in cooperation with Italy and NASA in the future and also the plan of the third LAGEOS has been investigated.

For these laser ranging satellite projects, NASA has started the development of an advanced multi-color SLR system of which precision will reach a level of a few millimeters. The spaceborne laser ranging project named the Geoscience Laser Ranging System, GLRS, is also planned in NASA. The SLR system is not based on the ground but based on a spacecraft and many laser retroreflectors are distributed on the ground. The changes of the baseline lengths between retroreflectors are to be detected in the precision of less than one centimeter.

As has been described, in order to elucidate the dynamics of the earth, the efficiency of the SLR technique at present has been proved to be excellent and the future prospect of the technique is very promising.

#### ACKNOWLEDGMENTS

The author wishes to thank Prof. J. Segawa for his encouragement and advice during the preparation of this paper. He also expresses his gratitude to Dr. Y. Ganeko for his long time support and



encouragement to the author for this work. The author thanks so much Mr. A. Sengoko for having discussions on many subjects in this work. He also appreciates help of Mr. T. Kawai for computer operation. Dr. Y. Kubo, Mr. K. Inoue, Mr. T. Kanazawa and Dr. T. Fukushima contributed to many useful discussions and comments on this work. This work is also indebted to the discussions and suggestions given by Dr. E. C. Silverberg, Prof. B. D. Tapley and Prof. B. E. Schutz while the author was stayed in the University of Texas at Austin in early 1980s. He finally expresses his gratitude to many observers at Simosato and other SLR stations in the world of which SLR data were used in this work.

This paper is the author's dissertation submitted to the University of Tokyo as a fulfilment of the requirements for the doctorate of science.

#### REFERENCES

- Abshire, J.B. : Plan for investigating atmospheric errors in satellite laser ranging systems. NASA Rep. (1989), 11pp.
- Aoki, S., B. Guinot, G. H. Kaplan, H. Kinoshita, D. D. McCarthy and P. K. Seidelmann : The new definition of Universal Time. *Astron. Astrophysics*, 105, (1982), 359-361.
- BIH : Circular D, (1983-1984).
- Campbell, J. W., W. Carter, N. Kawajiri, B. Ronnang, S. Ye : IRIS Bulletin A, No.40, June, (1987).
- Christodoulidis, D. C. and D. E. Smith : Prospects for TLRs baseline accuracies in the western USA using LAGEOS. NASA Tech. Memo., TM 82133, April (1981).
- Christodoulidis, D. C., D. E. Smith, R. Kolenkiewicz, S. M. Klosko, M. H. Torrence and P. J. Dunn : Observing tectonic plate motions and deformations from satellite laser ranging. *J. Geophys. Res.*, 90, (1985), 9294-9263.
- Cohen, S. C. and D. E. Smith : LAGEOS scientific results, Introduction. *J. Geophys. Res.*, 90, (1985), 9217-9220.
- Decker, W. M. : Summary of laser quick-look data-Nov. 1988. Monthly Rep. Goddard Laser Tracking Network, GSFC. Greenbelt, Feb. (1989).
- Fehlberg, E. : Classical fifth-, sixth-, seventh-, and eighth-order Runge-Kutta formulas with stepsize control. NASA TR-R-287, (1968), 82pp.
- Ganeko, Y. : An astrogeodetic geoid of Japan. *J. Geophys. Res.*, 82, (1977), 2490-2500.
- Ganeko, Y. : European Remote Sensing Satellite ; ERS-1. Gekkan Chikyu (The earth monthly), Vol.11, No.8, (1989), 454-461, (in Japanese).
- Gaposchkin, E. M. and K. Lambeck, (eds.) : 1969 Smithsonian Standard Earth (II). *SAO Special Rep.* 315, SAO, (1970), 93pp.
- Gilbert, F. and A. M. Dziewonski : An application of normal mode theory to the retrieval of structural parameters and source mechanism from seismic spectra. *Phil. Trans. R. Soc. London, Ser. A.* 278, (1975), 187-269.
- Goad, C. C. : Gravimetric tidal loading computed from integrated Green's functions. *J. Geophys. Res.*, 86, (1980), 2679-2683.
- Hashimoto, H. : private communication, (1986).
- Herring, T. A., C. R. Gwinn and I. I. Shapiro : Geodesy by radio interferometry : Studies of the forced nutations of the earth, 1. Data analysis., *J. Geophys. Res.*, 91, (1986), 4745-4754.

- Hosono, T. : Satellite ranging by the Kanozan laser tracker. Prog. of Symposium on Space Techniques in positional astronomy, A. Tsuchiya (ed.), Tsukuba, (1983) 19-26, (in Japanese).
- Jaccia, L. G. : Revised static models of the thermosphere and exosphere with empirical temperature profiles, *SAO Spec. Rep.*, (1971), 322pp.
- JHD : *Japanese Ephemeris for 1983, for 1984, for 1985 and for 1988.* (1982), (1983), (1984), (1987).
- Kanazawa, T., A. Sengoku and M. Nagaoka : Satellite laser ranging observations in 1987. *Data Rept. Hydrogr. Obs. Series of Satellite Geodesy*, JHD, No.2, (1989), 1-27.
- Kinoshita, H. : Third order solution of an artificial satellite theory. *Rep. Center for Astrophys. Preprint Series*, Harvard College Obs. and SAO, 594, (1976).
- Kozai, Y. : Second order solution of artificial satellite theory without air drag. *Astron. J.*, 67, (1962), 446-461.
- Kozai, Y. : Correction to geodetic coordinates in Japan. *J. Geod. Soc. Japan*, 26, (1981), 267-269.
- Kozai, Y., A. Tsuchiya, K. Tomita, T. Kanda, H. Sato, N. Kobayashi and Y. Torii : Satellite laser ranging instruments operated at Tokyo Astronomical Observatory. *Tokyo Astronomical Bulletin*, TAO, 223, (1973), 2597-2605.
- Kubo, Y. : Friction in the rotation of the earth and the nutation. Japanese Sympo. on Earth Rotation, Astrometry and Geodesy, M. Miyamoto (ed.), Tokyo, Jan. (1989), 59-66.
- Lerch, F. J., S. M. Klosko, G. B. Patel and C. A. Wagner : A gravity model for Crustal Dynamics (GEM-L2). *J. Geophys. Res.*, 90, (1985), 9301-9311.
- Leroy, C. F. : The impact of GRS 80 on DMA products. Defense Mapping Agency Report, (1982).
- Liebelt, P. B. : *An introduction to optimal estimation*, Addison-Wesley, Reading, Mass., (1967), 273pp.
- Lieske, J. H., T. Lederle, W. Fricke and B. Morando : Expressions for the precession quantities based upon the IAU (1976) system of astronomical constants. *Astron. Astrophys.*, 58, (1977), 1-16.
- Lundquist, C. A. (ed.) : Geodetic satellite results during 1967. *SAO Special Rep.* SAO, 264, (1967), 344pp.
- Lundquist, C. A. and G. Veis (eds.) : Geodetic parameters for a 1966 Smithsonian Institution Standard Earth. *SAO Special Rep.* SAO, 200, Vol. I, II and III, (1966), 690pp.
- Ma, C, J. W. Ryan and D. Caprette : Crustal Dynamics Project Data Analysis-1988, VLBI geodetic results 1979-87. NASA technical Memorandum 100723, (1989).
- Marini, J. W. and C. W. Murray, Jr. : Correction of laser range tracking data for atmospheric refraction at elevation above 10 degrees. NASA Report, X-591-73-351, GSFC, (1973), 39pp.
- Marsh, J. G., F. J. Lerch, B. H. Putney, D. C. Chistodoulidis, T. L. Felsentreger, B. V. Sanchez, D. E. Smith, S. M. Klosko, T. V. Martin, E. C. Pavlis, J. W. Robbins, R. G. Williamson, O. L. Colombo, N. L. Chandler, K. E. Rachlin, G. B. Patel, S. Bhati and D. S. Chinn : An improved model of the earth's gravitational field ; GEM-T1. NASA Technical Memorandum 4019, NASA GSFC, Greenbelt, MD, (1987), 354pp.
- Marsh, J. G., F. J. Lerch and R. G. Williamson : Precision geodesy and geophysics using STARLETTE laser ranging. *J. Geophys. Res.*, 90, (1985), 9335-9345.
- Martin, T. V., I. H. Oh, W. F. Eddy and J. A. Kogut : Geodyn system description, EG&G/Washington Analytical Center, Inc., Maryland, (1976).
- Matsushima, K., T. Shiho, M. Murata and S. Takeuchi : Space trajectory and mission analysis program "STANPS". Technical Memorandum of National Aerospace Laboratory, TM-359, National Aerospace Laboratory, Tokyo, (1978), 106pp.

- McCarthy, D., C. Boucher, T. Fukushima, T. Herring, J. Lieske, C. Ma, H. Montag, P. Paquet, C. Reigber, B. Schutz, E. Standish, C. Veillet and J. Wahr : International Earth Rotation Service Standards, Dec. 1988, (private communication). (1989).
- McMillan, J. D. : Mathematical Specifications of the University of Texas orbit processor and application to the laser observations of the BEACON EXPLORER-C satellite. Univ. of Texas Applied Mechanics Research Laboratory Report, 1052, Austin (1973), 77pp.
- Melbourne, W., R. Anderle, P. Bender, M. Feissel, D. McCarthy, P. Shelus, D. Smith, B. Tapley and R. Vicente : Standards for the MERIT campaign-first draft Nov. 1980, (private communication), (1981).
- Melbourne, W., R. Anderle, M. Feissel, R. King, D. McCarthy, D. Smith, B. Tapley and R. Vicente : Project MERIT Standards. Circ. No.167, U. S. Naval Observatory, Washington, D. C., Dec. (1983).
- Mister, J. B. : Subroutine ABSMOV. in Chap. 9, IERS Standards, Melbourne *et al.* Dec. 1988, (private communication), (1989).
- Minster, J. B. and T. H. Jordan, Present-day plate motions. *J. Geophys. Res.*, **83**, (1978), 5331-5354.
- Molnar, P. : Continental tectonics in the aftermath of plate tectonics. *Nature*, **335**, (1988), 131-137.
- Mori, T., Y. Ganeko, E. Nishimura and M. Sasaki : Report on the study for development of a satellite laser ranging system. Research Coordination Bureau, Science and Technology Agency, Tokyo, May (1977), 43-75, (in Japanese).
- Murata, M. : Filtering theory applied to near-earth satellite orbit determination. Technical Report of National Aerospace Laboratory, TR-555, National Aerospace Laboratory, Tokyo, (1978), 50pp.
- Murata, M. : Station coordinates, Earth rotation and plate motions from LAGEOS laser ranging : 1983-1986. *J. Geod. Soc. Japan*, **34**, (1988a), 33-57.
- Murata, M. : Preliminary orbital analysis of SLR data of the Geodetic Satellite, AJISAI. Proc. on Earth Rotation, Astrometry and Geodesy. I. Okamoto (ed.), Tokyo, (1988b), 191-195, (in Japanese).
- Naito, I. and K. Yokoyama : A computation of atmospheric excitation functions for the earth's rotation based on JMA global analysis data. Proc. International Conf. on Earth Rotation and Terrestrial Reference Frame, I.I.Mueller (ed.), July 1985, Columbus, Ohio, (1985), 434-439.
- NASA GSFC : SL7 yearly global station coordinate solutions. Crustal Dynamics Data Information Systems, (1987).
- Oon, F : Development of precise time device. *Rep. Hydrogr. Researches*, JHD, No.18, (1983), 121-135, (in Japanese).
- Rubincam, D. P. : Postglacial rebound observed by LAGEOS and the effective viscosity of the lower mantle, *J. Geophys. Res.*, **89**, (1984), 1077-1087.
- Sasaki, M. : Report on the study for basic research of laser reflecting balloon. Research Coordination Bureau, Science and Technology Agency, Tokyo, (1975), (in Japanese).
- Sasaki, M. : An experimental system for satellite laser ranging. *Rep. Hydrogr. Researches*, JHD, No.12, (1977), 95-106.
- Sasaki, M. : Optimum orbit of the Geodetic Satellite GS-1, *Rep. Hydrogr. Researches*, JHD, No.14, (1979), 131-144, (in Japanese).

- Sasaki, M. : Geodetic position of Minami-tori Sima (Marcus) by PAGEOS. *Data Rep. Hydrogr. Obs., Series of Astronomy and Geodesy*, JHD, No.14 (1980), 73-81.
- Sasaki, M. : On a baseline measurement by satellite laser rangings. *J. Geod. Soc. Japan*, 27, (1981), 333-337.
- Sasaki, M. : On a laser ranging system at Simasato Hydrographic Observatory. Proc. General Meeting of IAG, I. Nakagawa (ed.), Tokyo, May, (1982), 173-178.
- Sasaki, M. : On the software of the satellite laser ranging system. *Technical Bull. on Hydrography*, JHD, No.1, (1983), 42-45, (in Japanese).
- Sasaki, M. : Algorithm for determination of satellite orbit and geodetic parameters by using laser ranging data and preliminary results of its application. *Rep. Hydrogr. Researches*, No.19, (1984a), 107-133.
- Sasaki, M. : Satellite laser ranging at the Simosato Hydrographic Observatory and its preliminary results. *J. Geod. Soc. Japan*, 30, (1984b), 29-40
- Sasaki, M. : Completion of the Japanese Geodetic Satellite, GS-1. *Technical Bull. on Hydrography*, JHD, No.4, (1986), 1-4, (in Japanese).
- Sasaki, M. : Japanese Geodetic Satellite "AJISAI" launched in August 1986. Proc. Sixth International Workshop on Laser Ranging Instrumentation, Sept. 1986, Antibes, J. Gaignebet and F. Baumont (eds.), (1986), 527-546.
- Sasaki, M. : Japanese Geodetic Satellite for expansion of marine control. *Proc. International Symp. on Marine Positioning, INSMAP86*, Oct. 1986, Reston, Va., M. Kumar and G. A. Maul (eds.), D. Reidel, Dordrecht, (1987), 77-85.
- Sasaki, M. : Completion of a transportable laser ranging station (HTLRS). *Data Rep. Hydrogr. Obs., Series of Satellite Geodesy*, JHD, No.1 (1988a), 59-69.
- Sasaki, M. : Algorithm for determination of the earth rotation parameters and geodetic coordinates by using satellite laser ranging data. *Rep. Hydrogr. Researches*, No.24, (1988b), 59-64.
- Sasaki, M. and H. Hashimoto : Launch and observation program of the Experimental Geodetic Satellite of Japan. *IEEE Transactions on Geoscience and Remote Sensing*, GE-25, (1987), 526-533.
- Sasaki, M. and M. Nagaoka : Satellite laser ranging observations in 1982. *Data Rep. Hydrogr. Obs., Series of Astronomy and Geodesy*, JHD, No.18, (1984), 55-67.
- Sasaki, M., Y. Ganeko and Y. Harada : Satellite laser ranging system at Simosato Hydrographic Observatory. *Data Rep. Hydrogr. Obs., Series of Astronomy and Geodesy*, JHD, No. 17, (1983), 49-60.
- Sasaki, M., A. Sengoku, Y. Kubo and T. Kanazawa : Baseline determination by a short arc satellite laser ranging technique. *J. Geod. Soc. Japan*, 35, (1989), 117-126.
- Sasaki, M. and Y. Suzaki : Satellite laser ranging system at the Simosato Hydrographic Observatory and the transportable system, HTLRS. Proc. Sixth International Workshop on Laser Ranging Instrumentation, Sept. 1986, Antibes, J. Gaignebet and F. Baumont (eds.), (1986), 45-58.
- Sasao, T., S. Okubo and M. Saito : A simple theory on the dynamical effects of a stratified fluid core upon nutational motion of the earth. Proc. IAU Sympo. No.78, Kiev. May, (1977), 165-183.
- Sasao, T. and I. Kikuchi : private communication, (1982).

- Segawa, J. : An outline of the Japan Geodetic TOPEX/POSEIDON plan. *Gekkan Chikyu* (The earth monthly), Vol.11, No.8, (1989), 449-453, (in Japanese).
- Sengoku, A. : Collocation observation between two SLR stations at the Simosato Hydrographic Observatory in 1987. *Data Rep. Hydrogr. Obs., Series of Satellite Geodesy*, JHD, No.2, (1989), 28-49.
- Sengoku, A. and Y. Kubo : Simulations on SLR translocation method. *Proc. Japanese Symposium on Earth Rotation, Astrometry and Geodesy*, Dec. 1986, Tokyo, I. Okamoto and T. Hara (eds.), (1986), 19-24, (in Japanese).
- Sengoku, A., M. Sasaki and T. Kawai : Detection of the plate motion using satellite laser ranging, *Proc. Japanese Sympo. on Earth Rotation, Astrometry and Geodesy*, I. Okamoto (ed.), (1988), 115-118, (in Japanese).
- Sengoku, A., M. Sasaki and T. Kanazawa : Determination of the baseline length between Minamitori Sima and Simosato by satellite laser ranging. *71th Meeting Program and Abstracts*, May (1989), 59, (in Japanese).
- Seno, T. : The instantaneous rotation vector of the Philippine Sea plate relative to the Eurasian plate. *Tectonophysics*, 42, (1977), 209-226.
- Seno, T. : Middle Pleistocene of Japan Islands : What happened at 0.5 Mega d'annees?. *Gekkan Chikyu* (The earth monthly), Vol.8, No.12, (1986), 708-715, (in Japanese).
- Seno, T. : private communication, (1989).
- Schutz, B. E. : Analysis of LAGEOS laser ranging data : full rate data analysis, from Jane-May. CSR, Univ. Texas at Austin, (1985).
- Schutz, B. E. : Analysis of LAGEOS laser ranging data, from May-Aug., CSR, Univ. Texas at Austin, (1987).
- Schwiderski, E. W. : Global ocean tides, part I, A detailed hydrodynamical model, Rep. TR-3866, U.S. Naval Surface Weapons Center, Dahlgren, (1978).
- Shen, P. Y. and L. Mansinha : Oscillation, nutation and wobble of an elliptical rotating earth with liquid outer core. *Geophys. J. Roy. Astr. Soc.*, 46, (1976), 467-496.
- Tajima, M. and K. Komaki : *Theory of least square method and its applications*. Toyo Publishing (Shoten), Tokyo, (1986), 477pp., (in Japanese).
- Takemura, T. : Positions of geodetic and astronomical reference points at Simosato Hydrographic Observatory. *Data Rep. Hydrogr. Obs., Series of Astronomy and Geodesy*, JHD, No. 17, (1983), 44-48, (in Japanese).
- Takemura, T. : Satellite Doppler positioning of off-lying islands in 1983. *Data Rep. Hydrogr. Obs., Series of Astronomy and Geodesy*, JHD, No.19, (1985), 85-98, (in Japanese).
- Takemura, T. : Satellite Doppler Positioning of off-lying islands in 1984. *Data Rep. Hydrogr. Obs., Series of Astronomy and Geodesy*, JHD, No.20, (1986), 72-85, (in Japanese).
- Takemura, T. and T. Kanazawa : Satellite Doppler positioning of off-lying islands in 1980-1981. *Data Rep. Hydrogr. Obs., Series of Astronomy and Geodesy*, JHD, No.17, (1983), 61-87, (in Japanese).
- Takemura, T. and T. Kanazawa : Satellite Doppler Positioning of off-lying islands in 1982. *Data Rep. Hydrogr. Obs., Series of Astronomy and Geodesy*, JHD, No.18, (1984), 42-54, (in Japanese).
- Tapley, B. D. : Statistical orbit determination theory. *Recent Advances in Dynamical Astronomy*, B. D.

- Tapley and V. G. Szebehely (eds.), D. Reidel, Dordrecht, (1973), 396-425.
- Tapley, B. D. : private communication, (1987).
- Tapley, B. D., R. J. Eanes and B. E. Schutz : Earth rotation from laser ranging to LAGEOS : ERP (CSR) 85L07. Rept. MERIT-COTES Campaign on Earth Rotation and Reference Systems, Part III, M. Feissel (ed.), IHB, Paris (1986), B67-B73.
- Tapley, B. D. and B. E. Schutz : A comparison of estimation methods for the reduction of laser range observations. Proc. Sympo. Earth's Gravitational Field & Secular Variations in Position, R. S. Mather and P. V. Angus-Leppan (eds.), Univ. New South Wales, Sydney, (1973), 489-508.
- Tapley, B. D., B. E. Schutz and R. J. Eanes : Station coordinates, baselines and earth rotation from LAGEOS laser ranging ; 1976-1984. *J. Geophys. Res.* 90, (1985), 9235-9248.
- Van Gelder, B. H. W. : (private communication), (1988).
- Veis, G. (ed.) : *The use of artificial satellites for geodesy, Vol. II.* National Technical University, Athens, Greece, (1967), 647pp.
- Wahr, J. M. : The tidal motion of a rotating, elliptical, elastic and oceanless earth. Ph. D. thesis, Univ. Colorado, Colorado, (1979). 216pp.
- Yamazaki, A. : Determination of relative geodetic position from simultaneous observations of artificial satellites. *Rep. Hydrogr. Researches*, JHD, No.7, (1971), 1-22.
- Yamazaki, A. and T. Mori : Marine Geodetic Controls around Japan, *Marine Geodesy*, 7, (1983), 331-344.
- Yamazaki, A., T. Mori and T. Takemura : Geodetic positions of Tori Sima by the Echo-II. *Rep. Hydrogr. Researches*, JHD, No.3, (1967), 49-56.
- Yamazaki, A., T. Mori and Y. Ganeko : Geodetic position of Titi Sima. *Researches in Hydrography and Oceanography, in commemoration of the centenary of the Hydrographic Department of Japan*, D. Shoji (ed.), JHD, Tokyo, (1972), 251-269.
- Yoder, C. F., J. G. Williams and M. E. Parke : Tidal variations of earth rotation. *J. Geophys. Res.*, 86, (1981), 881-891.

## 衛星レーザー測距法による地球力学の研究 (要旨)

佐々木 稔

1970年代中期以降、日本において3台の衛星レーザー測距 (SLR) 装置が製作された。1台目は、試作機として水路部と国土地理院とが共同で開発し、国土地理院の測地観測所に設置された。2台目は、下里水路観測所に設置され(固定式)、1982年以来、同装置を用いて衛星レーザー測距観測が続けられている。可搬式レーザー測距装置は、3台目として水路部で開発され、1988年初期から海洋測地の一環として、年に2カ所ずつ離島における観測が同装置を用いて実施されている。初めに、これらの装置についての計画、開発、観測並びにデータ処理について述べた。

線型推定理論に基づく衛星軌道プロセッサ/アナライザの開発を1981年以降行ってきたが、このたび、一応完成させ、これをHYDRANGEAと名づけた。次に、このアルゴリズムについて及びこれを衛星レーザー測距データに適用して求めた地球自転、観測局位置及び局間距離並びに地心重力定数 (GM)、地球形状力学係数 ( $J_2$ ) 等の地球物理パラメーターについての諸成果について述べた。

すなわち、HYDRANGEAにより行ったデータ処理及び解析結果については、まず、レーザー測距局間距離 (基線長) を正確に求めるのに、複数の観測局で同時に、連続したパスについて得たデータのみを用いた短アーク法が、極めて有効であることが示され、下里の固定式観測装置と、可搬式装置により得たLAGEOS、AJISAIの測距値からこの方法を用いて求めた下里-父島間及び下里-南鳥島間の直線距離は、 $937665.041 \pm 0.004\text{m}$ 及び $2024874.042 \pm 0.007\text{m}$ となった。

次にHYDRANGEAを3~5日間の長さのアークに適用した。地球重力場としてGEM-T1を用い、LAGEOSの8つの5日アークの平均から2つの地球物理のパラメーターの値は、

$$GM : 398600.4453 \pm 0.003 \text{km}^3/\text{s}^2 \text{ 及び}$$

$$J_2 : (1082.571 \pm 0.015) \times 10^{-6}$$

と求まった。

地球の極位置 ( $X_p, Y_p$ ) 及び自転角速度過量 ( $\Delta\omega$ ) については、1983年9月から1984年10月までの14カ月の、85個の5日アーク (総データ数49576) から算出した。これらのHYDRANGEAの結果は、テキサス大学オースチン校と宇宙研究センター (CSR) が求めて発表したERP (CSR) 85L07とは、 $(\delta X_p, \delta Y_p, \delta \Delta\omega) = (-0.51 \text{milliarcsecond} (\text{mas} \sim 3 \text{cm}), -0.13 \text{mas}, -0.87 \text{ms/d})$ の系統差及び個々の5日値については、 $(\pm 1.1 \text{mas}, \pm 1.4 \text{mas}, \pm 0.42 \text{ms/d})$ のr. m. sで一致した。このとき、全期間について求めた軌道までの距離と実際の測距値との差の平均値は9.8cmであった。

また、1984.80、1986.76及び1988.11の3つの時期についてのSLR観測局の地心3次元座標をLAGEOSの8~9個の5日アークの平均から求めた。1984.80年について得られた14の観測局の位置の内部誤差は、(2.6cm, 2.4cm, 2.9cm)、LSC85L07との座標系の系統差は、(+0.5cm, +0.5cm, +3.1cm)、LSC85L07の各々の観測局との差の平均は、(3.4cm, 3.1cm, 5.1cm)であった。上記の3つの時期の観測局の位置を地球楕円体に投影した場合の楕円体上の局間距離の差から、下里、ハワイ、モニュメントピーク (カリフォルニア) 他の局間のプレート運動を算出した。結果は、+を伸び、-を縮みとして、

下里-ハワイ :	-11.9cm/年,
下里-モニュメントピーク :	-5.7cm/年,
下里-クインシー (カリフォルニア) :	-1.1cm/年,
下里-ヴェッツェル (西独) :	-3.1cm/年,
下里-ヤラガデ (オーストラリア) :	-6.2cm/年,
ハワイ-モニュメントピーク :	+1.3cm/年,
ハワイ-クインシー :	+0.6cm/年,
ハワイ-ヴェッツェル :	-7.0cm/年,

ハワイ-ヤラガデ:	-10.9cm/年,
モニュメントピーク-ヴェッツェル:	0.0cm/年,
モニュメントピーク-ヤラガデ:	-9.6cm/年,

であった。下里-ヴェッツェル以外は、ミンスター/ジョルダン (1978) AM 0-2 モデルによるプレート運動とほぼ一致する。

下里, ヴェッツェルはともにユーラシアプレート上にあるとされるが, この間の基線長の変化は, 年間3.1 cmの縮小と求められた。これは, 下里の南東方の南海トラフ域においてフィリピン海のプレートが日本列島を北西方に押し上げているために生じたものと考えられる。